UC San Diego

UC San Diego Electronic Theses and Dissertations

Title

Identifying regulatory elements of mRNA stability and translation in the nervous system

Permalink

https://escholarship.org/uc/item/7c79z9kz

Author

Sharifnia, Panid

Publication Date

2015

Peer reviewed|Thesis/dissertation

eScholarship.org Powered by the California Digital Library
University of California

UNIVERSITY OF CALIFORNIA SAN DIEGO

Identifying regulatory elements of mRNA stability and translation in the nervous system

A dissertation submitted in partial satisfaction of requirements for the degree of Doctor of Philosophy

in

Neuroscience

by

Panid Sharifnia

Committee in charge:

Professor Yishi Jin, Chair
Professor Jeffrey Goldberg
Professor Jens Lykke-Anderson
Professor Amy Pasquinelli
Professor Binhai Zheng

2015

Copyright

Panid Sharifnia, 2015

All Rights Reserved

The Dissertation of Panid Sharifnia is approved, and it is acceptable in quality and form for publication on microfilm and electronically.

_____

_____

_____

_____

_____

Chair

University of California, San Diego

2015

Table of Contents

Signature Page……iii

Table of Contents…….. iv

List of Abbreviations……. vi

List of Figures…… vii

List of Tables…….. x

Acknowledgments…… xi

Vita…….. xii

Abstract of the Dissertation…… xiii

Chapter 1 – Abstract …… 1

1.1 – Introduction……..…… 1

1.2 – General Methodology ……..……. 4

1.3 – Regulatory Factors Controlling Alternative Splicing…..……..... 8

1.4 – Regulatory Nuclear Polyadenylation Contributes……..…….... 16

1.5 – Regulation Via 3'UTR and Small RNA Pathways in Olfaction…… 18

1.6 – MiRNA in Development Plasticity…….……...… 22

1.7 – MiRNA in Dauer Formation……..…….…….. 23

1.8 – MiRNA in Synaptic Transmission…….……... 24

1.9 – Roles of MiRNA and MRNA Regulation in Axon Regeneration..... 25

1.10 – Conclusions and Perspectives……..……..... 27

Chapter 2 – *Cis* Element Dissection of *CEBP-1* 3'UTR……..…….. 28

2.1 – Analysis Using Single-Copy Genomic Integrated Reporters…….. 29

2.2 – *Cis* Element of 339-438 Contains a Unique Stem-Loop..……... 38

2.3 – *Cis* Elements, 230-358BP and 388-418BP, are Regulated……... 44

2.4 – 3'UTR Elements are Important for *CEBP-1* Function……..…... 49

2.5 – Discussion……... 56

2.6 – Materials and Methods……..……... 59

Chapter 3 – Introduction to *TRANS* Factors Regulating *CEBP-1* MRNA……... 70

3.1 – Introduction to TIA-1/TIAR FAMILY Regulating *CEBP-1* MRNA... 70

3.2 – *TIAR-2* Allele *TM2923* is a Loss of Function Allele…...……... 71

3.3 – The RRM Protein TIAR-2 Regulates *CEBP-1* MRNA VIA 3'UTR.. 76

3.4 – *TIAR-2* is Expressed in Cytoplasm and Inhibits Regeneration…... 82

3.5 – TIAR-2 Role in Synaptic Development……..……..89

3.6 – *TIAR-2* Regulated by *RPM-1* and *DLK-1* Pathway……..……....90

3.7 – *NIPI-3* Regulates *CEBP-1*, Possibly in Other Tissues……....96

3.8 – Discussion……... 99

3.9 – Materials and Methods……..……. 102

References…….. 108

LIST OF ABBREVIATIONS

mRNA – messenger Ribonucleic acid

RBP – RNA binding protein

5'UTR – 5'Untranslated Region

3'UTR – 3'Untranslated region

RRM – RNA recognition motif

PAS - polyadenylation and cleavage sites

miRISC - miRNA induced silencing complex

HITS-CLIP – High-throughput sequencing – cross-linking immunoprecipitation

PCR – polymerase chain reaction

RT-PCR – real time poymerase chain reaction

qRT-PCR – quantitative real time polymerase chain reaction

ALM/PLM – anterior and posterior lateral microtubule neuron

GFP – green fluorescent protein

DsGFP – destabilized green fluoresecent protein

kb – kilobase

LIST OF FIGURES

Figure 1.1: Splicing reporters characterize cell specific isoform expression….. 7

Figure 1.2: Alternative splicing and polyadenylation signals can produce multiple different 3'UTR isofroms of the same gene……..17

Figure 1.3: Olfactory adaptiaon assay used in *C. elegans*…… 19

Figure 2.1: *cebp-1* 3'UTR sequence determined by cDNA analysis…… 31

Figure 2.2: Sequence alignment of *cebp-1*'s 3'UTR with its homologs……... 32

Figure 2.3: Diagram of *cebp-1* 3'UTR reporter for transgenic *cis* dissection…. 33

Figure 2.4: Deletion constructs and results of GFP intensity from ventral nerve cord…… 34

Figure 2.5: Dissection of baseline mRNA stability *cis* elements of *cebp-1* 3'UTR using single copy insertion reporter…….. 36

Figure 2.6: Quantification of GFP fluorescence and mRNA levels using single copy reporters……... 37

Figure 2.7: Model of stem-loop prediction in *cebp-1* 3'UTR…….. 40

Figure 2.8: Prediction of changes to secondary RNA structure after mutating resides in stem of stem-loop #2. Stem mutated from actgg to ttaat…… 41

Figure 2.9: Stem-loop regulates expression of *cebp-1* 3'UTR reporter…….. 42

Figure 2.10: α-amanitin drug treatment on animals with 3'UTR reporters..…... 43

Figure 2.11 Single copy *cebp-1* 3'UTR reporter shows more cells expressing GFP fluorescence in *rpm-1(lf)* background compared to wild type control…... 46

Figure 2.12: Quantification of GFP fluorescence of single copy 3'UTR reporters in wildtype and *rpm-1(lf)* backgrounds…….. 47

Figure 2.13: Single cell resolution of *rpm-1* regulation of *cebp-1* 3'UTR through stem-loop……... 48

Figure 2.14: Single-copy constructs of GFP-tagged CEBP-1 with various 3'UTRs……... 52

Figure 2.15: Single-copy rescue of CEBP-1 function in axon regeneration…... 53

Figure 2.16: Different levels of rescue of *rpm-1; cebp-1* suppression with single copy constructs……. 54

Figure 2.17: Single-copy constructs show no phenotype in *cebp-1(lf)* background in PLM…….. 55

Figure 2.18: qRT-PCR for *cebp-1* in *rpm-1(lf); cebp-1(lf)* background with single-copy CEBP-1 constructs……. 56

Figure 3.1: Protein cladogram with homolgous proteins in different species for TIAR family…… 73

Figure 3.2: Protein alignnment with Human and Mouse TIA-2/TIAR…….. 74

Figure 3.3: *tiar-2(tm2923)* is a probably loss of function allele……. 76

Figure 3.4: *cebp-1* mRNA is upregulated in *tiar-2(tm2923)* mutant……. 77

Figure 3.5: *tiar-2* regulates *cebp-1* through its 3'UTR…… 79

Figure 3.6: *tiar-2* may interact with *cebp-1* mRNA through stem-loop structure 80

Figure 3.7: *tiar-2(tm2923)* regulates *cebp-1* 3'UTR *cis* elements 339-438bp in nerve ring…….. 81

Figure 3.8: Genetic locus and transcriptional and translational construct reporters for *tiar-2*…… 84

Figure 3.9: *tiar-2* is expressed cytosolically in different tissues…… 85

Figure 3.10: *tiar-2(tm2923)* enhances PLM regeneration……. 86

Figure 3.11: *tiar-2* is expressed cytosolically in the ALM and PLM……..... 87

Figure 3.12: *tiar-2* changes localization after injury…… 88

Figure 3.13: *tiar-2* affects motor neuron synaptic development……... 91

Figure 3.14: *tiar-2* does not have a *rpm-1*- like phenotype in the PLM …….. 92

Figure 3.15: *tiar-2*'s posterior extension developmental phenotype in PLM..... 93

Figure 3.16: *rpm-1* positively regulates *tiar-2* transcriptionally ……..... 94

Figure 3.17: *dlk-1* acts downstream of *tiar-2*'s regulation of *cebp-1* through *cebp-1*'s 3'UTR in the PLM…….. 95

Figure 3.18: *nipi-3(fr4)* does not display a presynaptic phenotype…….. 97

Figure 3.19: *nipi-3(fr4)* does not have a developmental PLM phenotype…….... 98

LIST OF TABLES

Table 1.1: RBPs conserved from *C. elegans* to mammals…….. 3

Table 2.1: List of strains, genotypes, and transgenes for Chapter 2..…….... 59

Table 2.2: List of plasmids for Chapter 2 …… 66

Table 2.3: List of primers and sequences used for Chapter 2…….. 68

Table 3.1: List of strains with genotypes and transgenes for Chapter 3…….... 102

Table 3.2: Plasmid construct numbers and descriptions for Chapter 3…… 105

Table 3.3: List of primers and sequences used for Chapter 3…… 107

ACKNOWLEDGMENTS

Chapter 1 is slightly modified from a review. Sharifnia P and Jin Y (2015) Regulatory roles of RNA binding proteins in the nervous system of *C. elegans*. *Front. Mol. Neurosci*. 7:100. The dissertation author was the primary investigator and author of the paper.

Chapter 2 is based off a paper in preparation. Sharifnia P, Kim K, Wu Z, and Jin Y**.** *Cis* elements mediating regulation of *cebp-1* mRNA stability and translation. The dissertation author was the primary investigator and author of the paper.

Chapter 3 of this dissertation is from a paper in preparation. Sharifnia P, Andrusiak M, Wu Z, Jin Y. The role of *tiar-2* in the nervous system. The dissertation author was the primary investigator and author of the paper.

VITA

2008	Bachelor of Arts, University of California, Berkeley
2008-2017	MD/PhD Dual Degree Program, University of California, San Diego
2015	Doctor of Philosophy, University of California, San Diego

ABSTRACT OF THE DISSERTATION

Identifying regulatory elements of mRNA stability and translation in the nervous system

by

Panid Sharifnia

Doctor of Philosophy in Neuroscience

University of California, San Diego, 2015

Professor Yishi Jin, Chair

The mechanism from gene to protein, also known as the central dogma, has been one of the fundamental principles of biology (1). From the start of transcription, to the production of a mature RNA transcript, and to the translation of RNA into protein, regulatory steps control the entire process. Studies have

revealed many layers of quality control, especially in regards to mRNA stability, decay, localization and translation (2, 3)

In the nervous system, the idea of mRNA regulation is tempting in regards to certain events, such as those that require quick responses to stimuli. Key experiments have identified ribosomes in dendrites of neurons (4). RNA binding proteins (RBPs) that localize cytoplasmically and sequences within the untranslated regions of mRNA that mediate binding of these RBPs that regulate its localization and stability (5)

It has become apparent that both *cis* and *trans* elements contribute to this tightly controlled network of biology but few studies have examined this interaction in the nervous system of *C. elegans*. In the following chapters I will describe my studies using the model organism *C. elegans* to examine RBPs in the nervous system with specific regard to a transcription factor, *cebp-1*, whose 3'UTR has important roles in controlling its expression during development and adult stages, and two *trans* factors that may regulate *cebp-1* through *cebp-1*'s 3'UTR.

CHAPTER 1 - ABSTRACT

Neurons have evolved to employ many factors involved in the regulation of RNA processing due to their complex cellular compartments. RNA binding proteins (RBPs) are key regulators in transcription, translation, and RNA degradation. Increasing studies have shown that regulatory RNA processing is critical for the establishment, functionality, and maintenance of neural circuits. Recent advances in high-throughput transcriptomics have rapidly expanded our knowledge of the landscape of RNA regulation, but also raised the challenge for mechanistic dissection of the specific roles of RBPs in complex tissues such as the nervous system. The *C. elegans* genome encodes many RBPs conserved throughout evolution. The rich analytic tools in molecular genetics and simple neural anatomy of *C. elegans* offer advantages to define functions of genes *in vivo* at the level of a single cell. Notably, the discovery of microRNAs has had transformative effects to the understanding of neuronal development, circuit plasticity, and neurological diseases. Here we review recent studies unraveling diverse roles of RBPs in the development, function, and plasticity of *C. elegans* nervous system. We first summarize the general technologies for studying RBPs in *C. elegans*. We then focus on the roles of several RBPs that control gene- and cell-type specific production of neuronal transcripts.

CHAPTER 1.1 – INTRODUCTION

Precise regulation of RNA, including mRNAs and small RNAs, is essential for controlling gene expression in a spatial and temporal manner. Research has identified critical roles of RBPs in neuronal development and synaptic transmission, which when disrupted through mutations, can cause neurological diseases. The *C. elegans*' genome encodes approximately 500 RBPs, defined by having an RNA binding domain such as the RNA recognition motif (RRM) and K Homology Domain (KH)(6). Many of these genes are conserved from nematode to mammals, such as the PUF family of RBPs, whose name is derived from the homologs identified in *Drosophila* (Pumilio) and *C. elegans* (Fem-3)(Table 1)(7-12). Studies of RNA and RBPs in non-neuronal tissues of *C. elegans* have made pioneering discoveries for RNA interference and microRNAs (13-16). In *C. elegans* neurons, the studies on the miRNA *lys-6* have led to a deep understanding of the complex regulatory network in neuronal fate diversification (17, 18). Comparatively, the investigation for the function of RBPs in other aspects of the nervous system is just at the beginning. Recent studies by genetic screens using elegant splicing reporters in the nervous system, combined with genomic studies, have hinted at the multiple roles RBPs play in neurons, including behavior and synaptic plasticity. Here, we first review the technologies used to study RBPs in the nervous system in *C. elegans*. We then discuss several studies that have identified roles for RBPs in mRNA processing and splicing in the nervous system via mechanisms dependent on 3'-untranslated region (3'UTR) and small RNAs

Table 1.1: RBPs conserved from *C. elegans* to mammals. Listed are the gene names for RBPs in *C. elegans,* definition of the gene name, known targets for RBPs in the nervous system, mammaliam homologues of *C. elegan* RBPs, and known functions

C. elegans gene name	Definition	Target genes in neurons	Mammalian homologue	Function
alg-1	Argonaute like gene-1	*lin-41*	Argonautes	silencing, splicing, and transcriptional regulation[4]
ess-2	ES2 similar-2	*dlk-1*	ES2/DGCR14	splicing[49]
exc-7	Excretory canal abnormal-7	*unc-16*	ELAV-like family	splicing, decay, translation, polyadenylation, transport[2]
fbf-1	Fem-3 mRNA binding factor-1	*egl-4*	PUF family	translational regulator, localization[7]
grld-1	Glutamate receptor level decreased-1	*glr-1*	Split Ends Protein (SPEN)	Splicing in C. elegans[45]
mbl-1	Muscleblind splicing regulator homolog-1	Unknown	Muscleblind	splicing, localization, translation[5]
mec-8	Mechanosensory abnormality-8	*mec-2*	RNA binding protein with multiple splicing (RBPMS)	Splicing in C. elegans[27-29], unclear in mammals
msi-1	Musashi family-1	*arx-1,-2, -3*	Musashi	translational regulator[6]
syd-9	Synapse defective-9	Unknown	Zinc-Finger Protein (ZFP)	splicing in C. elegans[56]
sydn-1	Synaptic defective enhancer-1	Unknown	Unknown	polyadenylation regulator in C. elegans[57]
unc-75	Uncoordinated-75	*unc-16, unc-32, unc-64*	CELF/BrunoL	splicing, decay, translation[3]

CHAPTER 1.2 – GENERAL METHODOLOGY

A major technological advance in studying RNA regulation in the past decade is deep-sequencing of transcriptomes. In *C. elegans*, comprehensive transcriptome analyses for several developmental stages by the modEncode Consortium have provided valuable information for validating gene structures as well as revealing many new alternative splice junctions (19). An independent study that combined RNA-seq and microarray strategies also identified similar cohorts of alternative splicing transcripts as well as new isoforms of transcripts (20). Using multiple techniques, including 3'RACE and RNA-seq, two independent studies reported global analyses of 3'UTRs in *C. elegans*, both of which revealed multiple polyadenylation and cleavage sites (PASs) in mRNA, as well as many previously unannotated 3'UTRs (21, 22). Use of multiple PAS sites may be a way to impart tissue and cell specificity of transcripts due to different possible isoforms

In addition to transcriptomics, genome wide analyses of downstream targets of RBPs have been instrumental to understanding mechanisms of regulation involving RBPs, such as the miRNA induced silencing complex (miRISC). miRNAs, as part of the miRISC, guide the miRISC to specific mRNA targets. Two key components of the miRISC are the Argonautes *alg-1* and *alg-2*, which are critical for miRNA biogenesis and miRISC gene-silencing activity (23, 24). Zisoulis *et al* used the high throughput sequencing and UV cross-linking and immunoprecipitation (HITS-CLIP) method to determine the binding sites of ALG-1 (25). While this study confirmed the binding sites for many previously

established targets of microRNAs such as *lin-41*(26), they also found that *alg-1* can bind along the entire mRNA transcript, with a higher percentage of occupancy towards the 3' end of mRNA (25). Interestingly, the authors found ALG-1 bound to several components of microRNA machinery, implying auto-regulation in the microRNA pathway (25).

As the *C. elegans* adult hermaphrodite has 302 neurons and the major tissues are non-neuronal cells, a technical hindrance in defining transcriptomes of neurons is that neuronal mRNAs are often poorly represented in samples prepared using whole animals. Thus, a clever method, developed by Kudlow *et al* allows tissue-specific CLIP in the intestine and muscle by using specific promoters tagged to the protein of interest (27). Than *et al* adapted this approach to the nervous system by using a pan-neuronal promoter to express an epitope tagged GW182 protein AIN-2 (28), one of a family of proteins that bind to the miRISC and are essential for microRNA induced silencing (28, 29). In addition to *ain-2*, *C. elegans* has another GW182 protein, AIN-1 that is also a miRISC component (30). A majority of the mRISC bound microRNA neuronal transcripts enriched in the AIN-2 CLIP assay confirmed a previous study that observed neuronal expression with these microRNAs' promoter fusion reporters (31).

Traditional genetic screening in *C. elegans* remains a powerful way to identify functionally relevant genes. Several RBPs that act in neurons were originally identified serendipitously in genetic screens for mutants disrupting specific behaviors, touch sensitivity, protein trafficking, and synapse

development. Recently, the use of tissue- and cell-specific splicing reporters has also shown promise to dissect the precise regulation of neuron-type specific transcripts by RBPs at the single-cell resolution (Figure 1.1A). Together with the transcriptome-wide methods examining RNA regulation, genetic screens in *C. elegans* have expanded our knowledge of RBPs in the nervous system.

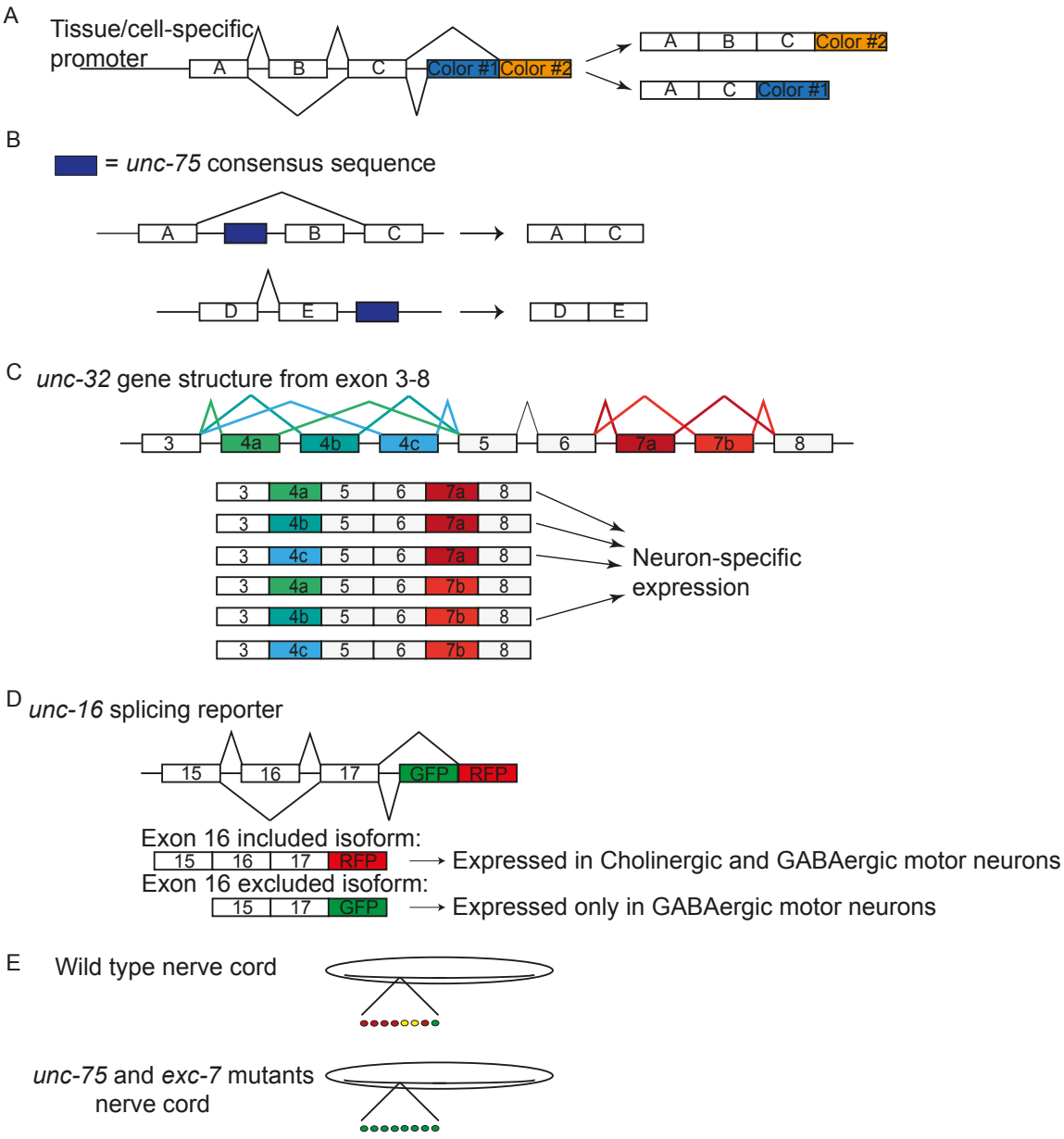


Figure 1.1: Splicing reporters characterize cell specific isoform expression. A) General design of splicing reporters that change the fluorescent protein depending on the exon included/excluded B) *unc-75* consensus sequence correlates with exon exclusion when upstream of exon and exon inclusion when downstream of exon (32) C) *unc-32* gene structure displaying alternative splicing of exons 4 and 7. There are 3 alternative exons for exon 4 and 2 for exon 7. The 6 possible isoforms are shown below the gene model. D) *unc-16* splicing reporter used by Norris *et al* (33) to examine expression in nervous system E) patterns of *unc-16* expression motorneurons in wild type and *unc-75* and *exc-7* mutants in nerve cord (33)

CHAPTER 1.3 – REGULATORY FACTORS CONTROLLING ALTERNATIVE SPLICING OF NEURONAL GENES

Regulatory factors controlling alternative splicing of neuronal genes

Proteins involved in mRNA splicing play critical roles in regulating the maturation of transcripts. It is thought that certain neuronal diseases result from abnormal regulation of the mRNA splicing, such as in spinal muscular atrophy (SMA). One hypothesis for the mechanism of SMA is the loss of the survival motor neuron 1 protein (SMN1), which can assemble pre-mRNA splicing machinery, resulting in abnormal mRNA splicing in neurons(34).

One of the first RBPs reported to function in the nervous system of *C. elegans* was identified based on the behavioral phenotype of genetic mutants. In *C. elegans*, touch sensitivity is controlled by the mechanosensory neurons. Chalfie and Sulston carried out a forward genetic screen after random mutagenesis to find mutants displaying touch insensitivity, and identified *mec-8* (35). Fifteen years later, Lundquist *et al* cloned the *mec-8* gene and found that it contained two RRM domains (36). MEC-8 is broadly expressed in nervous system and epidermis. Interestingly, *mec-8(lf)* mutations genetically enhance less severe loss of function mutations of *unc-52,* which, through alternative splicing, produces multiple isoforms of perlecan, an extracellular matrix heparan sulfate proteoglycan (HSPG) conserved to humans (36, 37). *unc-52(lf)* shows lethality at the 2-fold embryo state and appears paralyzed but certain alleles of *unc-52* are viable and fertile (38). In combination with *mec-8(lf)*, these viable alleles of *unc-52* mimic the lethal and paralyzed phenotype (39). Furthermore,

Lundquist and colleagues found that *mec-8(lf)* results in differential expression of specific isoforms of *unc-52* by RT-PCR and immunofluorescence compared to wild type, supporting the notion MEC-8 may act as a splicing factor of *unc-52* mRNA in the epidermis (36). In touch neurons, Calixto *et al* found *mec-8* necessary for the alternative splicing of a specific isoform of *mec-2*, a component of a degenerin/epithelial sodium channel (DEG/ENaC) involved in mechanosensation (40, 41). These studies illustrate a single factor *mec-8* can mediate mRNA splicing of different genes in a tissue type specific manner.

The CELF/BrunoL proteins are defined by 3 RRM motifs and are conserved from *C. elegans* to humans (8). *In vitro* studies have shown that these proteins act mainly as splice factors (8). A *C. elegans* CELF protein, *unc-75*, was identified first based on locomotion behavior and later shown to affect the axonal morphology of GABAergic motor neurons (42). UNC-75 protein is localized in the nucleus, exhibiting speckles, resembling other proteins involved in mRNA splicing(42). *unc-75*'s locomotion phenotype suggests defects in neurotransmission. In *C. elegans*, presynaptic and postsynaptic phenotypes can be examined through two assays, the aldicarb and levamisole tests (43). The *unc-75* mutant displayed defects in the aldicarb assay but normal behavior in the presence of levamisole, suggesting a presynaptic neurotransmission role for *unc-75* (42). Importantly, this study showed that expressing vertebrate CELF4 can rescue some defects of *unc-75* mutants, supporting evolutional conservation in function (42). While the authors did not determine *unc-75*'s splicing targets,

they proposed *unc-75* might act to control synaptic neurotransmission by regulating mRNA splicing in the nervous system.

Several groups have recently taken advantage of new tools to identify the targets of *unc-75* in the nervous system. Through deep sequencing analysis of RNA in both wild type and *unc-75* mutants, Kuroyanagi *et al* reported 24 targets of *unc-75*. They also determined a binding motif (G/U)UGUUGUG shared among these targets and confirmed UNC-75 could bind this sequence, which is similar to other studies that identified G/U-rich motifs for the CELF proteins (8, 32). Additionally, these sequences are present upstream of excluded exons, while downstream of included exons of transcripts (Figure 1.1B) suggesting the location of the *unc-75* binding site could regulate exclusion and inclusion of an exon. In parallel, this group performed a forward genetic screen looking for regulators of isoform specific expression from the gene *unc-32*, which encodes a subunit of vacuolar –type H^+ ATPases (44, 45). The *unc-32* gene structure contains two sets of exons alternatively spliced, exon 4 and 7. Exon 4 has 3 possible isoforms - exon 4a, 4b, or 4c - while exon 7 has 2 – exon 7a or 7b (Figure 1.1C). These options for exon 4 and 7 lead to 6 possible transcripts (Figure 1.1C). mRNAs containing exon 4b and 7a were exclusively expressed in the nervous system, which required *unc-75* (44). An *unc-32* mutation that removes the splice site in the exon 4b shows an uncoordinated behavioral phenotype (45). Interestingly, loss of function in *unc-75* suppressed the movement defects of this *unc-32* mutant (44). The authors suggest *unc-75(lf)* suppressed the behavioral phenotype of this *unc-32* allele by allowing

expression of the other isoforms of *unc-32* in the nervous system to compensate for the loss of exon 4b isoform. Thus, these data provide functional evidence for *unc-75*'s regulation of this specific exon in the nervous system (44).

An independent study by Norris *et al* has further expanded the list of targets for *unc-75* (33). They developed a strategy to generate reporters for alternatively spliced exons in genes previously known to be expressed in the nervous system, such as *mod-1*, a chloride channel, and *dyn-1*, dynamin, and *unc-16*, JIP3 (33). A reporter for *unc-16/*JIP3 showed specific expression in the GABAergic motorneurons that depended on the exclusion of exon 16 (Figure 1.1D). Using this reporter, they performed a forward genetic screen, and identified *unc-75,* as well as another RBP *exc-7* such that in these mutants, the GABAergic specific isoform became ubiquitously expressed in the motor neurons (Figure 1.1E). They further performed RNA-seq analysis on wild type and *unc-75* mutants and generated gene network predictions for new genes. Among them, they reported that *unc-64*/syntaxin, a protein essential in synaptic vesicle release, is an *unc-75* target (33). *unc-64* has two isoforms that differ by the inclusion or exclusion of an exon, and only one of the isoforms can completely rescue *unc-64*'s neuronal phenotypes, suggesting *unc-64*'s splicing must be tightly regulated to ensure proper neuronal function (33).

Combinatory interactions of RBPs can allow more complex regulation of mRNA splicing. The *C. elegans* homolog of the ELAV/Hu proteins, *exc-7*, has been found to act in a parallel pathway for mRNA splicing to *unc-75* (33, 42). The ELAV family was first documented in *Drosophila* and named due to the

mutant phenotype of embryonic lethal, abnormal visual system (46). In humans, the homolog of this family was reported as an antigen in an autoimmune disease and named after the patient whose serum was used, Hu (47). Studies characterized Hu as an RBP homologous to *elav* (48), which led to the name of ELAV/Hu family of RBPs. While *unc-75* and *exc-7* have non-overlapping targets based on RNA-seq analysis, they were also found to bind over 40 of the same transcripts, including *unc-16*/JIP3 (33). As the *unc-16* isoform excluding exon 16 is expressed specifically in the GABAergic motor neurons, the isoform including exon 16 is expressed in both cholinergic and GABAergic motor neurons (Figure 1.1D). *unc-75* and *exc-7* are both expressed in the cholinergic neurons, while only *unc-75* is expressed the GABAergic neurons (42). Due to these expression patterns in the motor neurons, they were suggested to act together to ensure proper expression of the *unc-16* isoform in cholinergic motor while *unc-75* by itself regulates *unc-16* expression in the GABAergic motor neurons (33). Thus, multiple RBPs may act in concert to direct isoform expression from same gene in a cell-specific manner.

AMPA-type glutamate receptors mediate rapid excitatory neurotransmission from worm to human (49). In *C. elegans*, *glr-1* and *glr-2* encode AMPA-type glutamate receptors expressed postsynaptic to motor and inter-neurons, including the command interneurons responsible for regulating the locomotor circuit (50-52). To examine the expression pattern and regulation of the AMPA receptor in the AVE interneurons, Wang *et al* designed a genomic fusion reporter for *glr-1* and performed a forward genetic screen to isolate

mutations that disrupted the localization of receptor (53). They identified *grld-1(lf)* mutants as they showed decreased fluorescence intensity of the *glr-1* reporter and a reduction in a response to a nose-touch assay, a behavioral test dependent on the AVE interneuron (53). *grld-1* encodes a homolog of the Spen RBP family. Wang *et al* found overexpression of a *glr-1* cDNA construct, lacking introns, could rescue the fluorescence intensity of the *glr-1* reporter and partially rescue the nose-touch phenotype(53). Additionally, *glr-1* constructs lacking the first two introns partially rescued the fluorescent intensity. Given this data, the authors suggest *grld-1* controls *glr-1* mRNA splicing specifically at introns 1 and 2 (53).

The muscleblind-like family (MBNL) consists of RBPs, named after the discovery of the gene in *Drosophila* required in both the muscles and visual system, known to associate with mRNA and regulate splicing (54, 55). In myotonic dystrophy (DM), MBNLs are prevented from binding their targets due to expansions in two genes - dystrophia myotonica protein kinase gene for DM type 1 or CCHC-type zinc finger nucleic acid binding protein gene for DM type 2 - that sequester MBNLs in the nucleus (54). The muscleblind genes are widely expressed in many tissues, yet there has been a focus on their function in the muscles due to the phenotype of myotonic dystrophy. In a screen for regulators of a synapse formation in the *C. elegans* DA9 motorneuron, Spilker *et al* identified a role for a homolog of the muscleblind family genes, *mbl-1*. The DA9 motorneurons form synapses in the dorsal nerve cord, visualized by a fluorescent-tagged synaptic vesicle marker RAB-3 (56). They found MBL-1

localized to nuclei in the ventral nerve cord. In the *mbl-1* mutant, presynaptic proteins localization was spatially unrestricted in both the dorsal and ventral nerve cords, but the postsynaptic muscle remained normal (56). Interestingly, a *mbl-1* genomic construct expressed in the DA9 neurons could rescue this synaptic phenotype while muscle expression failed to rescue thus suggesting a neuronal role for this RBP(56).

A context-dependent regulation of neuronal transcripts was recently reported by Noma *et al* (57). Loss of function mutants of a conserved E3 ubiquitn ligase, *rpm-1*, display an abnormal synaptic phenotype consisting of fewer and disorganized synapses (58, 59). A well-studied downstream target of *rpm-1* is *dlk-1*, a conserved MAP3K (60). In a suppressor screen for *rpm-1(lf)*, *ess-2,* related to the mammalian ES2/DGCR14 protein, was found to regulate *dlk-1* mRNA when splicing junction was altered. ES2/DGRC14 is a component of the splicesome complex(61). *ess-2(lf)* mutants, by themselves, do not show obvious effects on splicing, but reduce the levels of *dlk-1* mRNA expression in a mutant in which the splice site in the third intron of *dlk-1* was mutated. *ess-2(lf)* was also found to act similarly on an allele of *dpy-10*, a cuticle collagen, which changes a splice acceptor site leading to unspliced and spliced transcripts (62). These data suggest *ess-2* functions in splicing in certain contexts, such as when there are non-canonical or mutated splice sites.

The power of forward genetic screening also resides in the discovery of new genes. From a mutant isolated in a screen for genes functioning in GABAergic neuron synapse formation (63), Wang *et al* reported the

identification of *syd-9* (64). SYD-9 protein contains C2H2 zinc-finger domains and has a nuclear speckle-like expression in muscles and neurons, similar to other splicing factors. C2H2 zinc-finger proteins are generally known to bind DNA but have also been found to interact with RNA (65). In the *syd-9* mutant, several presynaptic proteins, including synaptobrevin, were disorganized and animals exhibited abnormal electrophysiological recordings, suggesting impairment in synaptic vesicle release (64). Additionally, the authors observed specific genetic interactions of *syd-9* with sets of genes involved in synaptic vesicle (SV) endocytosis, such as synaptojanin and endophilin. Consistent with a model that the abnormal neurotransmission may results from problems in endocytosis, Wang and colleagues found through electron microscopy decreased number of SVs, altered distribution of SVs away from the active zone, and vesicle accumulations in the presynaptic terminal (64). The authors suggest that *syd-9* can regulate mRNA processing of these endocytosis genes. The conservation of the C2H2 domains of SYD-9 extends to its homologs in humans (66, 67). Interestingly, these human proteins, Glis2 and ZNF74, also display similar nuclear speckle-like localization (66, 67), which suggests functional conservation for this newly discovered gene in higher animals.

CHAPTER 1.4 – REGULATORY NUCLEAR POLYADENYLATION CONTRIBUTES TO SPECIFIC PATHWAYS IN NERVOUS SYSTEM DEVELOPMENT

In the nucleus, a key step in parallel to pre-mRNA splicing is 3'-end processing, which leads to formation of 3'UTR and addition of polyadenylates. Production of the 3'UTR from a pre-mRNA transcript is a multi-step process that includes cleavage at the end, followed by the addition of a polyA tail by the polyA adenylation complex. Nuclear processing of transcripts may result in mRNAs with several 3'UTRs that impart tissue and other types of specificity (Figure 1.2). In *C. elegans*, the polyadenylation pathway was identified to also affect neuronal development. In a genetic screen for regulators of synapse formation by Van Epps *et al*, the gene *sydn-1* was found to regulate synapse and axon development such that *sydn-1(lf)* mutants displayed abnormal synapses and ectopic axon branches (68). SYDN-1 protein appears to be specific among nematodes and is localized to the nucleus. Through a suppressor screen the authors further identified members of the polyadenylation machinery downstream of *sydn-1*, suggesting *sydn-1* inhibits nuclear polyadenylation in the nervous system for proper development (68). Polyadenylation factors can have temporal and tissue specific regulation of transcripts. In fact, not all of the components of the PolyA complex suppressed *sydn-1(lf)*, which implies specific roles for certain members of this machinery in the nervous system(68). Thus it appears that *sydn-1* negatively regulates specific RBPs to ensure proper development of the nervous system.

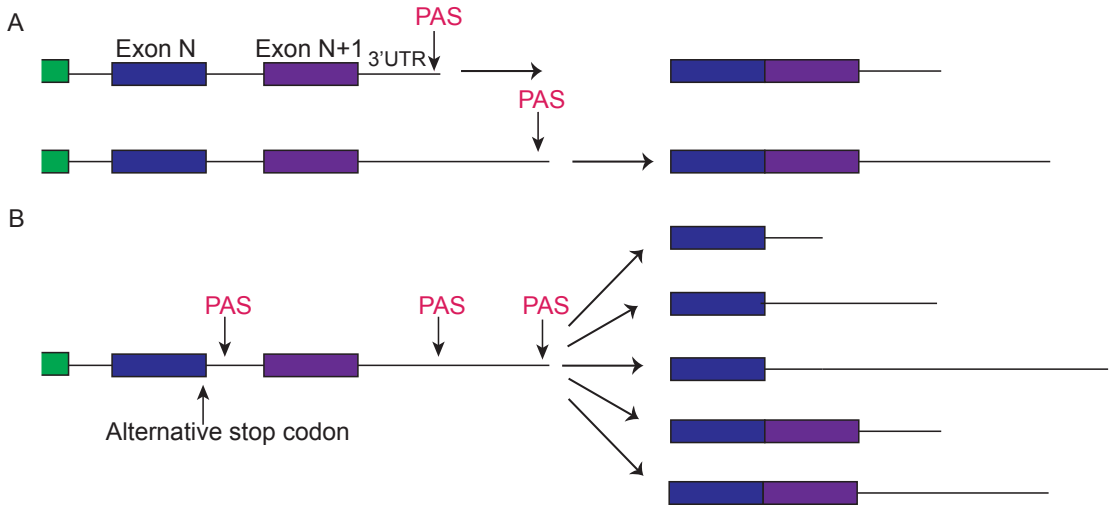


Figure 1.2: Alternative splicing and polyadenylation signals can produce multiple different 3'UTR isoforms of the same gene. A) Two different PAS sites in the 3'UTR create two different isoforms of transcript, one with a short 3'UTR and one with a longer 3'UTR. B) Alternative splicing of a gene, paired with alternative polyadenylation can create different 3'UTRs that may include the sequence of an exon

CHAPTER 1.5 – REGULATION VIA 3'UTR AND SMALL RNA PATHWAYS IN OLFACTION

The interaction of RBPs with the 3'UTR of mRNA can serve many functions, such as regulating mRNA's localization, stability and/or translation. microRNAs, bound to argonautes, can directly bind to downstream targets through the targets' 3'UTRs. Studies have discovered that the 3'UTR regulation also extends to the nervous system, including in *C. elegans*. These types of mechanisms can provide tight temporal and spatial control for synaptic plasticity, development and regeneration.

A classic assay in *C. elegans* is olfactory adaptation that is a form of synaptic plasticity allowing the nervous system to strengthen or weaken synapses in response to stimuli, which is thought to underlie memory formation. In this assay animals are tested for their preference for an odor after exposure to the same order (Figure 1.3A). Wild type animals, after odor exposure, will display avoidance for the trained odor, which fades over time and can be quantified by a chemotaxis index (Figure 1.3A,B). This behavior depends on the AWC sensory neuron (69). A series of studies have identified a cGMP-dependent protein kinase, *egl-4* that is expressed in the AWC neuron, to be required in this type of synaptic plasticity and further revealed a regulatory mechanism involving *egl-4'*s 3'UTR (70). L'Etoile *et al* isolated *egl-4* mutants through a forward genetic screen for suppressors of a dauer phenotype, a specific state the animals enter under starvation or particular stressful conditions, associated with impaired chemotaxis. Interestingly, among alleles of

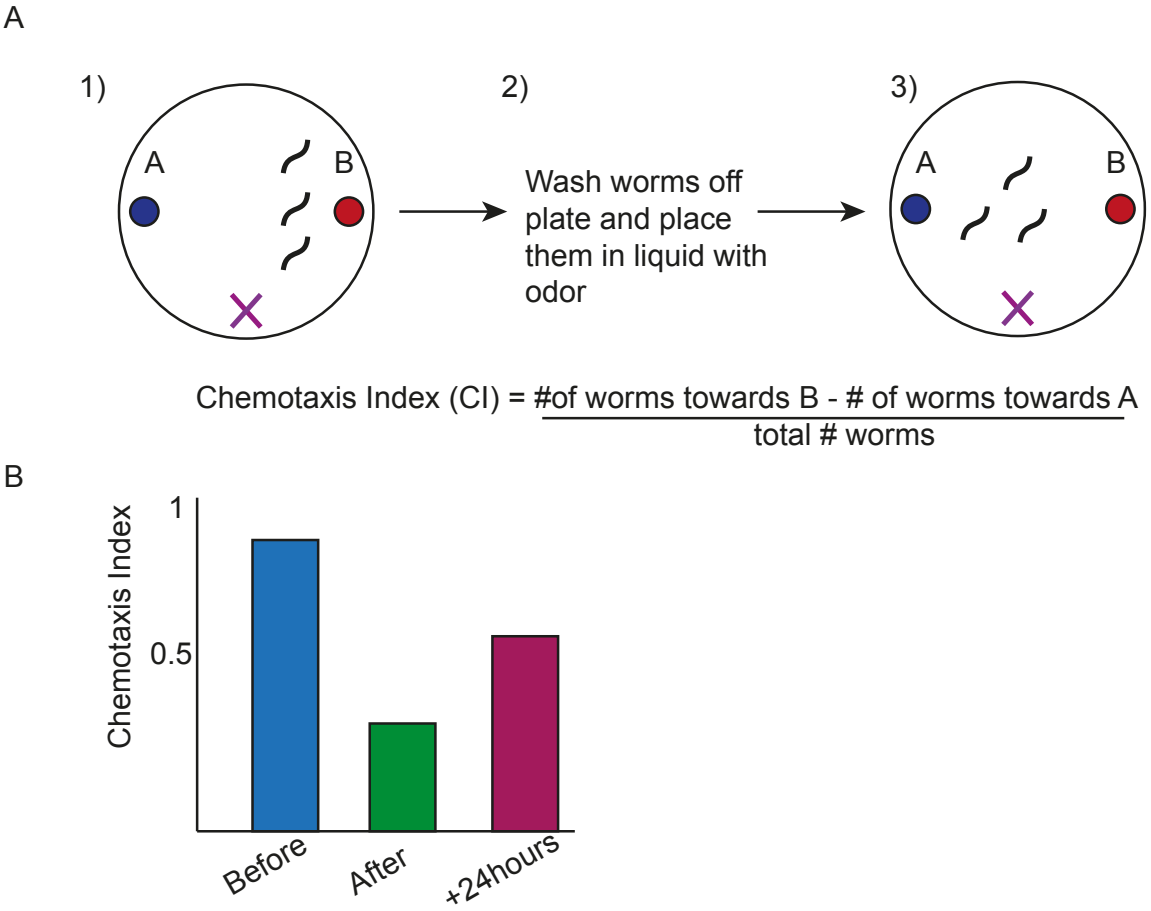


Figure 1.3: Olfactory adaptation used in *C. elegans*. A) (1)Animals are placed inbetween two odors (denoted by X), one which they are attracted to (labeled B). (2) Worms are exposed to odor B while starved (3) Animals are placed back onto plates with the same design as in (1). Movement towards the order is measured by a chemotaxis index (CI). The formula is shown. B) Representative graph of chemotaxis index of wild type animals after before, after, and 24 hours after olfactory adaptation assay.

egl-4, they found several mutations within *egl-4*'s 3'UTR, suggesting this 3'UTR was important for adaptation. Through 3'UTR sequence analysis of these point mutations, Kaye *et al* identified sequences similar to the Nanos Response element within these nucleotides (71). The Nanos Response Element (NRE) is defined based on studies in *Drosophila* embryo where NRE elements are bound by members of the PUF family of RBPs for the proper patterning of the embryo (72). Kaye *et al* therefore tested the worm homologs of the PUF family in olfactory adaptation and found that a member of this family, *fbf-1*, was necessary for olfactory adaption to several odors. To address the possibility that *fbf-1* regulated translation of *egl-4* through its 3'UTR, they used a photoconvertible reporter tagged to *egl-4*'s 3'UTR expressed in the AWC neuron. In wild-type animals, new protein synthesis could be visualized after photoconversion in the AWC. This protein translation was absent in *fbf-1(lf)* mutants indicating *fbf-1* promoted translation of the reporter through *egl-4*'s 3'UTR (71). Furthermore, Kaye and colleagues showed that this new protein synthesis correlated with olfactory adaptation: animals with increased protein synthesis of the reporter after the olfactory adaptation assay displayed decreased chemotaxis towards the odor. This pattern of protein synthesis was absent in a reporter with the NRE sequence mutated, suggesting this correlation depended on *fbf*-1's binding site in the 3'UTR. While the PUF family of proteins usually repress translation based on studies in *S. cerevisiae*, *Drosophila* and *C. elegans* (73), in this context it appears *fbf-1* promotes translation of *egl-4* for olfactory adaptation.

In addition to the PUF family of RBPs, the small RNA pathways have been identified to have roles in olfactory adaptation. Juang *et al* found components of the small endogenous nuclear RNAi pathway that mediate this response (74). Loss of function mutations in multiple genes, such as Argonaute, Dicer, and siRNA 3'-5' exonuclease, fail to adapt to odors (74). It was previously shown that the gene *odr-1* is guanyl cyclase specifically expressed in a subset of chemosensory neurons (69, 75, 76). In this study, they observed that the *odr-1* locus can produce small RNAs known as 22GRNAs and found these 22GRNAs were transcribed from the *odr-1* locus after adaptation. 22GRNAs are small RNAs transcribed from the locus of genes that function in silencing of DNA such as transposons (77). This upregulation of *odr-1* derived 22GRNAs depended on the siRNA 3'-5' exonuclease, *mut-7* (74). Given the observation *odr-1* mRNA levels decreased after adaptation, one possibility is the 22GRNAs inhibit *odr-1* transcription. *hpl-1* and *hpl-2* are the *C. elegans* homologs of the heterochromatin proteins that recognize and bind to specific chromatin marks and repress transcription (78). Juang and colleagues found increased *hpl-2* occupancy at the *odr-1* locus after adaptation that depended on the presence of *mut-7*, providing a mechanism for decreased *odr-1* mRNA after adaptation. Thus, the authors suggest that this small endogenous RNAi pathway can mediate the local regulation of genes for odor adaptation.

Along with the formation of the olfactory memory, a recent study suggests mechanisms involving the 3'UTR of mRNAs can mediate memory loss. Hadziselimovic *et al* examined, through a candidate screen, roles for genes

interacting with the cytoskeleton for formation and retention of memory (79). Using the olfactory adaptation assay, they found the RBP Musashi, *msi-1*, was necessary for memory loss after odor adaptation (79). Musashi proteins consist of two RRMs and are known to be translational repressors (80). Hadziselimovic and colleagues demonstrated that *msi-1* can downregulate the translation of members of the Arp2/3 Complex, a protein structure involved in actin branching, by observing increased fluorescence in reporters for the 3'UTR of certain Arp2/3 components (*arx-1, -2, -3)* in the *msi-1(lf)* (79). Furthermore, the authors showed a direct interaction between Musashi and the 3'UTRs of the Arp2/3 Complex through immunoprecipitation of MSI-1 and the *arx* mRNAs (79). They suggest a model in which Musashi regulates part of the actin capping and branching process through the 3'UTR of members of the Arp2/3 Complex to modulate memory retention.

CHAPTER 1.6 – MIRNA IN DEVELOPMENT PLASTICITY

In *C. elegans* larval development, a group of motor neurons, called the DD neurons, undergo synaptic remodeling. They form synapses first on the ventral muscles, which are removed and reformed onto the dorsal muscles after the first-stage larval(L1) (81). This process is important for the nematodes' locomotion as it establishes a circuit of excitation and inhibition of the body wall muscles to allow the movement in a sinusoidal pattern.

A variety of factors, including microRNAs, transcription factors and synaptic activity, influence DD remodeling (82, 83). The timing to initiate DD

remodeling depends on a heterochronic gene, *lin-14*, as *lin-14(lf)* mutants displayed precocious synaptic remodeling (82). *lin-14* was already known as a target of the microRNA *lin-4* (84, 85), and this modulation of *lin-14* would provide a tight temporal control of its expression. An additional study implicated another target of the microRNA pathway in DD remodeling. Thompson-Peer *et al* demonstrated that the C2H2 zinc finger transcription factor *hbl-1*, the *C. elegans* homolog of hunchback, is important for this remodeling process (83). *Hbl-1* mutants delayed DD remodeling while the microRNA *mir-84*, remodeled precociously compared to wildtype. The *mir-84* developmental phenotype was suppressed by the *hbl-1* mutation, suggesting this microRNA pathway controls synaptic remodeling by negatively regulating *hbl-1* (83). By examining a reporter for *hbl-1*'s 3'UTR, Thompson-Peer and colleagues observed increased fluorescence in the *mir-84* mutant, hinting *mir-84* down-regulated *hbl-1* through its 3'UTR (83). Thus, this study identified *hbl-1* as a microRNA target for synaptic remodeling.

CHAPTER 1.7 – MIRNA IN DAUER FORMATION

MicroRNAs can affect other developmental processes in the nervous system as well, such as dauer formation. For example, Than *et al* found roles for neuronal microRNAs in dauer formation (28). The authors found that neuronally enriched microRNAs, *mir-81/82*, *mir-234*, and *mir-124* loss of function mutants enhanced dauer development with *unc-3(lf)* (28). UNC-3 is a *C. elegans* homolog of the Collier/Olf-1/Early B-cell Factor (COE) transcription factor family

shown to inhibit dauer formation (86). This dauer formation was enhanced when *unc-3(lf)* was paired with the GW182 homolog, *ain-1(lf)*, suggesting microRNA involvement. However, the individual mutants of the microRNAs and *unc*-3*(lf)* could not completely recapitulate the percentage of dauer formation observed in *unc-3; ain-1*, suggesting that multiple microRNAs contribute to the dauer phenotype (28). With further improvement, such efforts will aid the studies of cell-specific expression of microRNAs acting by themselves and combinatorially with other microRNAs.

CHAPTER 1.8 – MIRNA IN SYNAPTIC TRANSMISSION

The microRNA pathway has also been implicated in synaptic transmission. In *C. elegans*, the conserved *mir-1* family of microRNAs has been useful to study, as mutations are viable, whereas in other organisms mutations are lethal. While *C. elegans miR-1* is expressed in the muscles and not in the nervous system, Simon *et al* found *mir-1* regulated a signal passed from the muscle to neuron to modulate synaptic transmission (87). The authors identified MEF-2, a transcription factor, as a target of *mir-1* in the muscle and suggest a model where MEF-2's transcriptional targets affect the presynaptic terminals of neurons at the neuromuscular junction (NMJ) by inhibiting neurotransmitter release (87). In another paper looking at possible targets of *mir-1* in synaptic transmission, two synaptic adhesion proteins, neurexin and neuroligin were examined. Both genes were found to suppress *mir-1*'s phenotype of decreased

acetylcholine release, suggesting these two adhesion proteins transmit the retrograde signal to decrease neurotransmission (88).

CHAPTER 1.9 – ROLES OF MIRNA AND MRNA IN AXON REGENERATION

In the adult nervous system, the ability to quickly respond to stimuli such as an injured neuron is quite essential. 3'UTRs are known to mediate mRNA localization and translation in dendrites and axons and may provide a rapid response to axon injury(89). Recent studies have shown axon regeneration after injury can depend on mRNA 3'UTRs and RBPs.

MicroRNAs are important mediators of mRNA regulation in several species for axon regeneration (76, 90-92). In the nervous system, there is an age-dependent decline in regeneration across all species studied and which several groups have tried to address. Zou *et al* demonstrated in the *C. elegans* AVM neuron that this decline could be mediated by microRNA processing pathway and its targets (92). Animals mutant for the argonaute gene *alg-1* showed enhanced regeneration in older animals compared to wild type controls. Since Argonautes are guided to their targets by microRNAs, the authors used RT-PCR over the larval and adult stages to determine which microRNAs could mediate this phenotype. The microRNA *let-7* increased in expression as the animal aged and its loss of function mutant also showed enhanced regeneration (92). The study followed up by examining known targets of *let-7* and found a member of the TRIM family proteins, *lin-41*, as a downstream target in axon regeneration. Using a reporter tagged to *lin-41*'s 3'UTR, the group showed

decreased intensity of the reporter in aged animals, which correlated with *let-7*'s increased expression (92). In addition, immuoprecipitation showed a direct interaction between LIN-41 and ALG-1 (92). Thus, increased *let-7* expression in aged animals could decrease nerve regeneration by binding and down-regulating LIN-41 through *lin-41*'s 3'UTR. Interestingly, in a different touch neuron, the PLM, *alg-1(lf)* inhibits adult axon regeneration (93), suggesting cell-context and stage-dependent regulation by miRNAs.

In the PLM mechanosensory neurons, Yan *et al* reported the 3'UTR of a transcription factor important for axon regeneration (94). This transcription factor, *cebp-1*, is the homolog of the CCAAT/Enhancer Binding Protein family (C/EBP) and found to be necessary for axon regeneration (94). *cebp-1* was identified through a suppressor screen for downstream targets of the conserved ubiquitn E3 ligase, *rpm-1*, which also was found to negatively regulate *cebp-1* mRNA levels (94). Two key pieces of data implicated the 3'UTR of *cebp-1* as important for its regulation. First, transgenes expressing *cebp-1* without its 3'UTR partially mimicked *rpm-1(lf)*'s phenotype, suggesting *rpm-1* negatively regulated *cebp-1* through its 3'UTR (94). Second, using a photoconvertible protein tagged to *cebp-1*'s 3'UTR, they showed upregulation of protein synthesis in the distal axon 2 hours after axotomy. When examining a similar reporter tagged to a control 3'UTR this increase in fluorescence in the distal axon was absent. Taken together, these data suggest upregulation of *cebp-1* through its 3'UTR after injury is important for the regenerative response, illustrating a function for the 3'UTR in the adult nervous system. Though so far there are few

studies of RBPs and microRNAs in *C. elegans* in axon regeneration, they all implicate roles for RBPs and microRNAs in controlling local responses to injury and regeneration.

CHAPTER 1.10 – CONCLUSIONS AND PERSPECTIVES

The complexity of the nervous system poses many questions about how it develops, grows and maintains its connections. Studying RNA regulation will identify key mechanisms that can address these questions. *C. elegans* has helped advance the field by providing genetic tools to dissect RNA pathways, specifically in the nervous. Since many RBPs are conserved, their function and mechanism of regulation in *C. elegans* may likely be the same in humans. Additionally, *in vivo* studies in *C. elegans* have displayed the importance of RBPs in mRNA splicing, mRNA 3'-end processing and microRNA pathway, and their resulting effects on synaptic plasticity, synapse formation and axon regeneration. These studies have allowed single-neuron and global dissection of these interactions to highlight the complexity of the nervous system. Future studies of mRNA in the nervous system of *C. elegans* will continue to build a deeper understanding of the complex regulations by RBPs.

Chapter 1 is slightly modified from a review. Sharifnia P and Jin Y (2015) Regulatory roles of RNA binding proteins in the nervous system of *C. elegans*. *Front. Mol. Neurosci*. 7:100. The dissertation author was the primary investigator and author of the paper.

CHAPTER 2 – *CIS* ELEMENT DISSECTION OF *CEBP-1* 3'UTR

The ability to respond quickly to signals is crucial for maintaining normal biological function, especially in the nervous system. Regulation of RNA provides the nervous system with a mechanism to tightly control responses to stimuli, such as during synapse formation, plasticity, or injury. It is well established that *cis* and *trans* elements can regulate mRNA stability, splicing, transport, translation and localization and studies have suggested this regulation can exist in neurons (95). Analysis of *cis* elements, such as those in the 3'-untranslated regions (3'UTRs), have shown roles for sequence motifs for *trans* factors, including RNA secondary structures that can serve as scaffolds for proteins (96). In the nervous system, the importance of these *cis* elements have been shown by affecting various behaviors such as olfactory adaptation in *C. elegans* and synaptic localization in *Aplysia* (71, 95). Signaling pathways are crucial to regulate the spatial and temporal responses of neurons, and we previously showed that the mRNA stability and translation of a transcription factor, *cebp-1*, important during development and axon regeneration, was regulated by a conserved E3 ubiquitin ligase and p38 MAP kinase cascade through *cebp-1*'s 3'UTR(94). In this chapter we address the mechanism regulating *cebp-1* mRNA in the nervous system by dissecting the *cis* elements within *cebp-1*'s 3'UTR as well as the effects on CEBP-1 function in the nervous system.

CHAPTER 2.1 – ANALYSIS USING SINGLE-COPY GENOMIC INTEGRATED REPORTERS IDENTIFIES *CIS* ELEMENTS REGULATING *CEBP-1* MRNA EXPRESSION LEVELS

To gain clues for *cis* elements that regulate *cebp-1* mRNA, we firstmpared the *C. elegans cebp-1* 3'UTR sequence, determined by previous cDNA analysis(94) (Figure 2.1), to those in other nematode species and in mouse C/EBPδ (Figure 2.2). We focused on C/EBPδ for two reasons: first, it is the closest to *cebp-1* based on protein homology and second, studies have indicated a p38 MAP Kinase cascade can affect its mRNA through its 3'UTR(97). We found conserved regions near the middle and end of the 3'UTR (Figure 2.2). We also ran several miRNA prediction programs, all of which predicted miRNA seed sequences within nucleotides 79-98. To assess the roles of these putative elements in regulating *cebp-1* transcripts, we generated a series of 3'UTR deletions and placed them downstream of a destabilized GFP reporter, which has been shown to provide a sensitive readout for dynamic expression (98, 99) (Figure 2.3A, B). We initially analyzed transgenic lines generated as high-copy extrachromosomal arrays using standard methods (Table 2.1). Multiple lines for the same constructs, if available, were analyzed by visual comparison of fluorescent intensity in the nerve cord. We examined if a known regulator of *cebp-1*'s 3'UTR, a conserved E3 ubiquitin ligase *rpm-1*, could affect this reporter and observed an increase in GFP expression in the ventral cord (Figure 2.3 B). While our analyses suggested three regions that appear to affect DsGFP expression level (Figure 2.4), we also encountered problems of

the variable expression among different lines of the same construct, due to caveat inherent to the extrachromosomal arrays. Additionally, these constructs also contained another gene's 3'UTR after the end of *cebp-1*'s 3'UTR due to the vector back bone design, which could possibly complicate our results. To precisely compare the levels of expression by specific sequence elements, we next employed MosSci methodology to generate stably integrate single-copy transgenes on chromosome II (*ttTi5605)* (100). To facilitate visual assessment in this series of reporters, we used standard GFP as a reporter (Figure 2.5A). Our reporter uses the genomic sequence for *cebp-1*'s 3'UTR, shown on the genomic locus diagram (Figure 2.5A). This reporter also differs from the extra-chromosomal arrays as it does not contain an additional *unc-54* 3'UTR at the end of *cebp-1*'s 3'UTR.

cctgcagcttcatcaattaaccaatcaataatttagacacctaggatcctcatatttattccacggcattctcccccc
atcattccagtgacccccccccccccccccccttcattgatcccaatctagtctcccagtgtaaaacaagcatca
aaccgtacataattctattccatctctctcccttccccccaaagctgagctttcatctgttccccccgtttacttgctgg
caagttatttttgttacttagttgtgaaacttgaaatttcctatattttgagagttgctcgcagagcctcttgcgcttcaaa
gtccaataactcgaaattggctggaaaattttccttaacttcctttcaacaccacgtagcaaaaaaccagatcctc
ttccaatccctacaccactggtaatgtttccccttccagtcaactagtgcatttttttgtctgaaaacctatccccccctg
aacatgtgttaactaattttgccttgataatttcaaattcgctttattatttttgccttttttctattgtttttttctttttgatcgctg
attttatctaaatagaataaattcatcagtgctcaaaaaa

Figure 2.1: *cebp-1* 3'UTR sequence determined by cDNA analysis. The polyadenylation signal is marked by the green highlighted region starting at the 575bp into the 3'UTR.

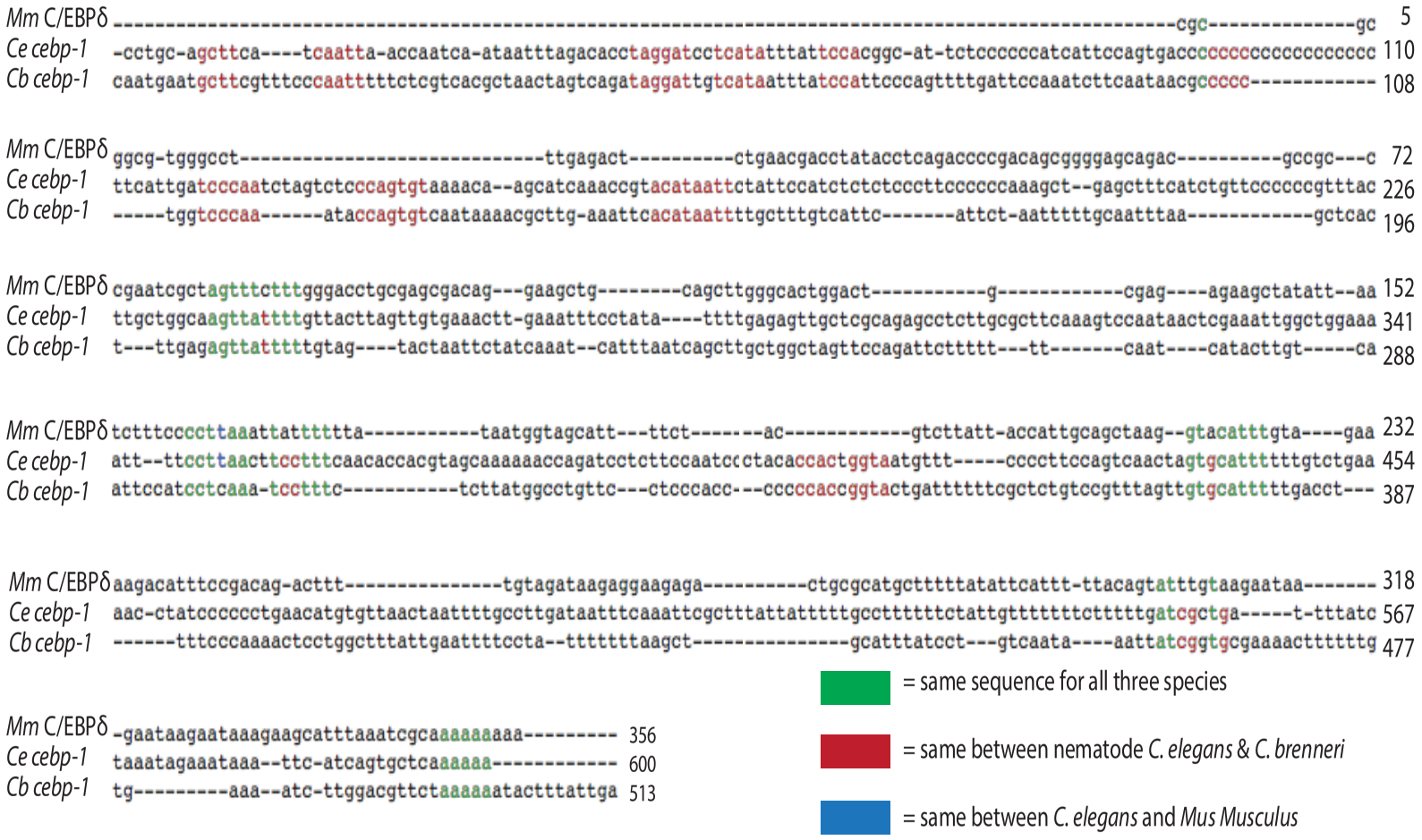


Figure 2.2: Sequence alignment of *cebp-1*'s 3'UTR with its homolog in *C. brenneri* and *M. musculus* (adapted from Clustal Omega). Color legend at bottom right

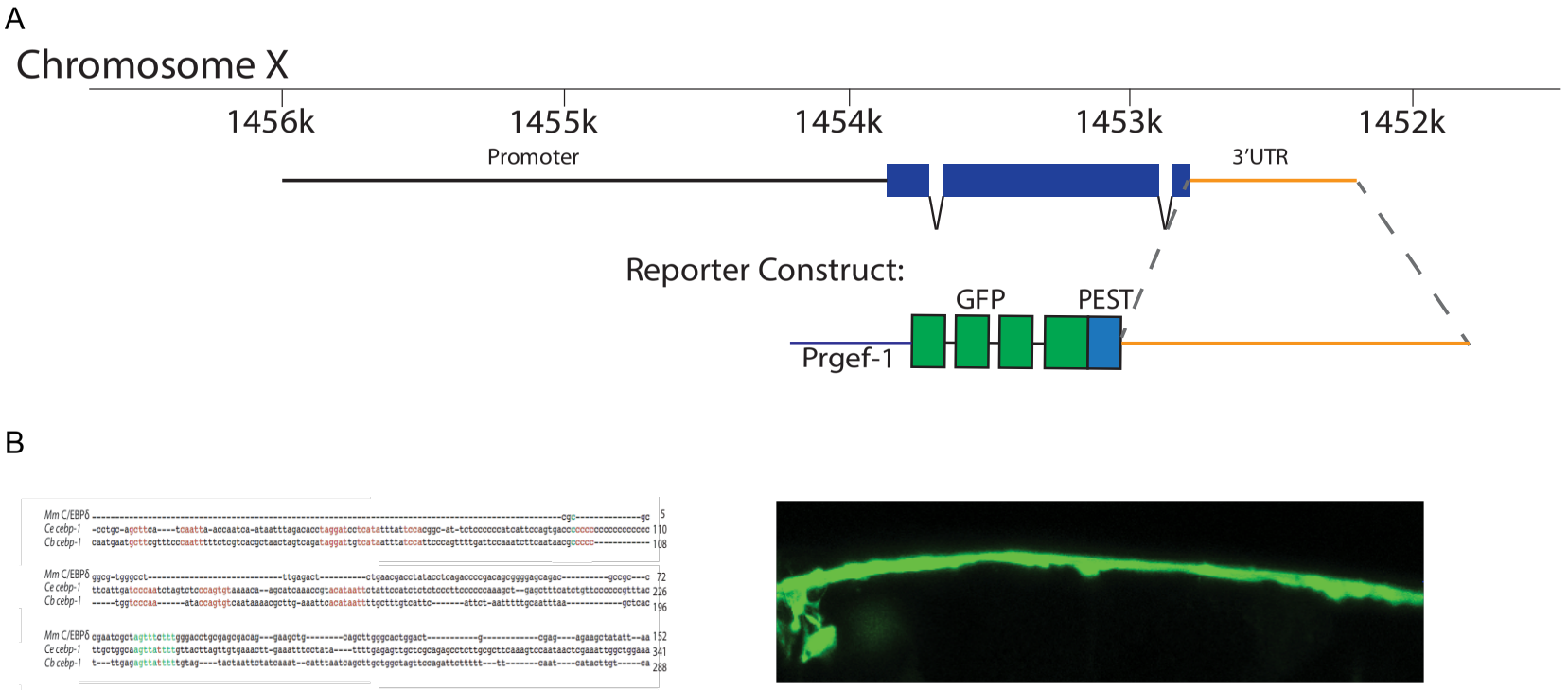
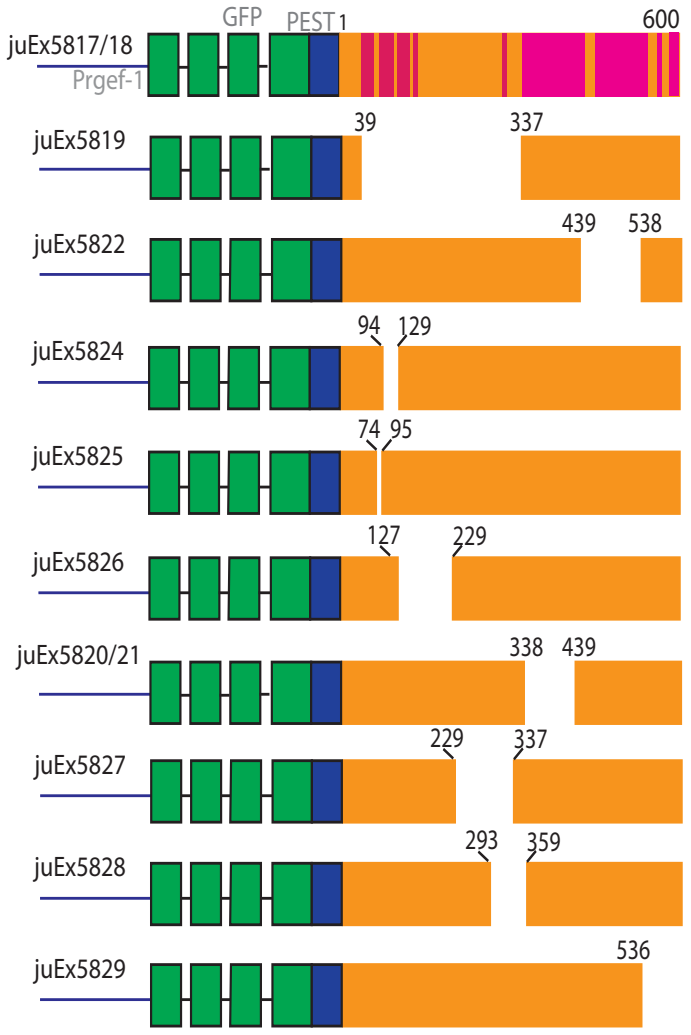


Figure 2.3: Diagram of *cebp-1* 3'UTR reporter for transgenic *cis* dissection A) genomic locus of *cebp-1* shown as well as 3'UTR reporter constructed for genomic 3'UTR of *cebp-1* from nucleotide 1452800 to 1452600. *Cebp-1* is read in the reverse direction as shown by the green arrow marking the promoter start site. 3'UTR reporter consists of pan-neuornal promoter, destabilized GFP, and genomic 3'UTR. The reporter is not drawn to scale. B) Z-stack images of the reporter in the ventral nerve cord of young adult animals in wild type and *rpm-1(lf)* background. Images taken under same conditions.



Baseline compared to full 3'UTR	Increase/decrease in *rpm-1(lf)* vs. N2
	Increase
Same	Increase
Same	Increase
Same	Increase
Same	Increase
Same	Increase
Higher	Decrease
Higher	Decrease
Higher	Decrease
Higher	Decrease

Figure 2.4: Deletion constructs and results of GFP intensity from ventral nerve cord. All constructs were injected at 10ng/ul with Pgcy-8::tagRFP as the co-injection marker. Constructs contain additional *unc-54* 3'UTR in backbone of plasmid. Animals were maintained at 25°C and scored at the young adult stage by measuring the GFP intensity in the ventral nerve cord.

We examined the GFP intensity of each construct in the age-comparable (L4) wild type background. We found that deleting the predicted microRNA seed

element did not affect the baseline expression compared to the full 3'UTR reporter (Figure 2.6A), similar to the observation to overexpression transgenic array reporters (Figure 2.4). We identified two *cis* elements that resulted in increased GFP expression compared to the full 3'UTR reporter (Figure 2.5, 2.6). One element is from nucleotide 439-536, removal of which caused the largest, about 2.5X, increase in expression compared to the full 3'UTR reporter (Figure 2.6A). This region consists of AT rich regions, 69% of the sequence made of A/Ts, slightly higher than the full 3'UTR sequence consisting of 60% A/Ts. Interestingly, this effect was not observed from the overexpression transgenic lines (Figure 2.4), likely due to the variable baseline expression of transgenes using extra-chromosomal arrays or the difference of *unc-54* 3'ends in the extrachromsomal constructs. The other element is 339-438bp that is has a 59% AT content, lower than the percentage in the 439-536bp element.

With the chromosomal integrated single-copy expression of these reporters, which is expressed only in neurons, we next quantitatively measured mRNA produced using qRT-PCR using primers detecting GFP (Table 2.3). Comparing several deletion strains to the full 3'UTR reporter showed that GFP mRNA abundance was not affected in these animals, even in those strains with an upregulation of GFP fluorescence, suggesting these elements may affect translation rather than mRNA stability (Figure 2.6B).

In summary, this analysis reveals that *cebp-1*'s expression is tightly modulated by at least two elements in *cebp-1*'s 3'UTR in the nervous system.

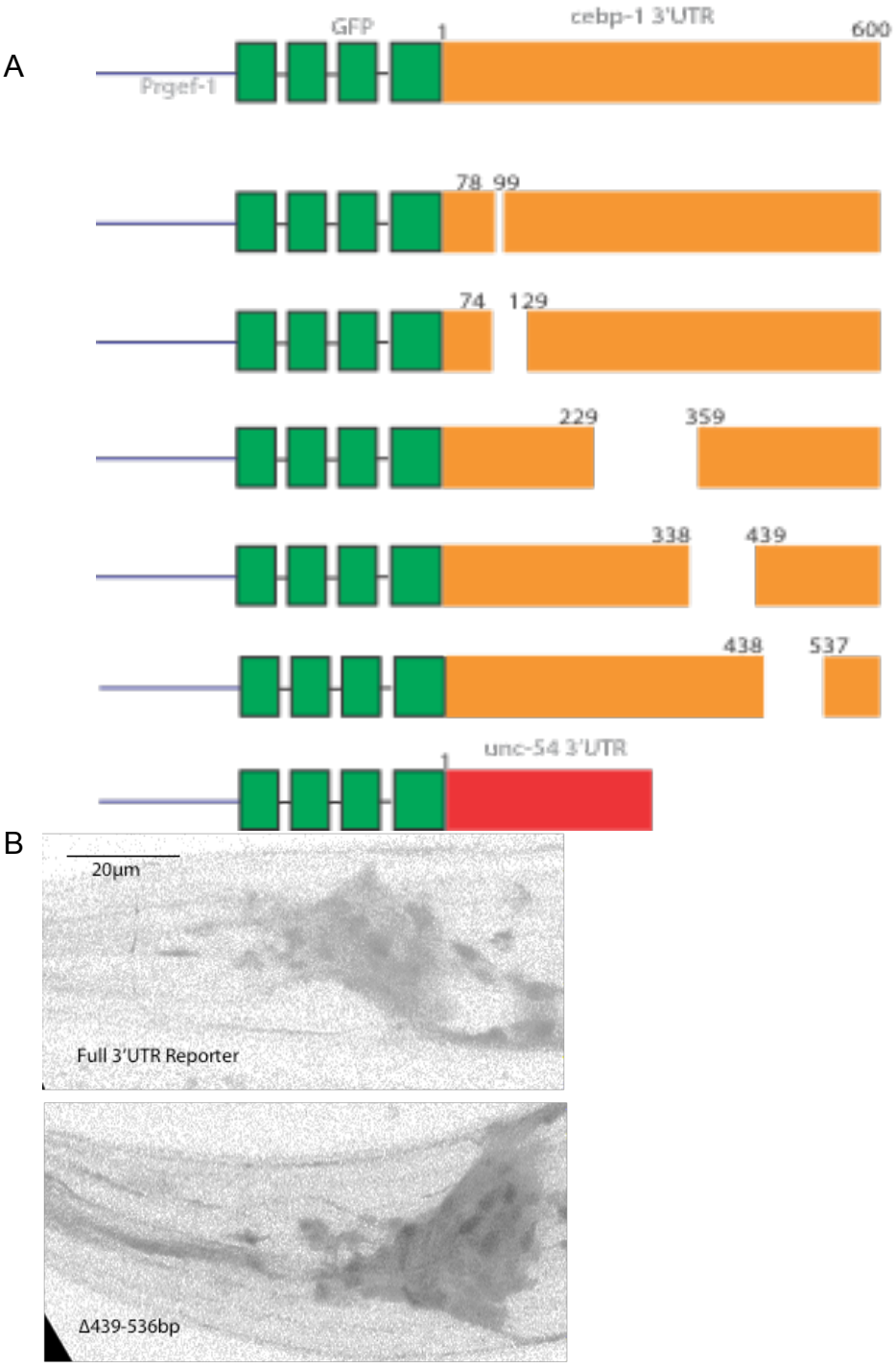


Figure 2.5: Dissection of baseline mRNA stability *cis* elements of *cebp-1* 3'UTR using single copy insertion reporter A) Reporter construct for *cebp-1* 3'UTR and deletion inserted on Chromosome II. These constructs do not have an extra *unc-54* 3'UTR after *cebp-1*'s 3'UTR B) Z-stack images of full 3'UTR and Δ439-536 reporters in wild type background of L4 animals taken at under the same conditions

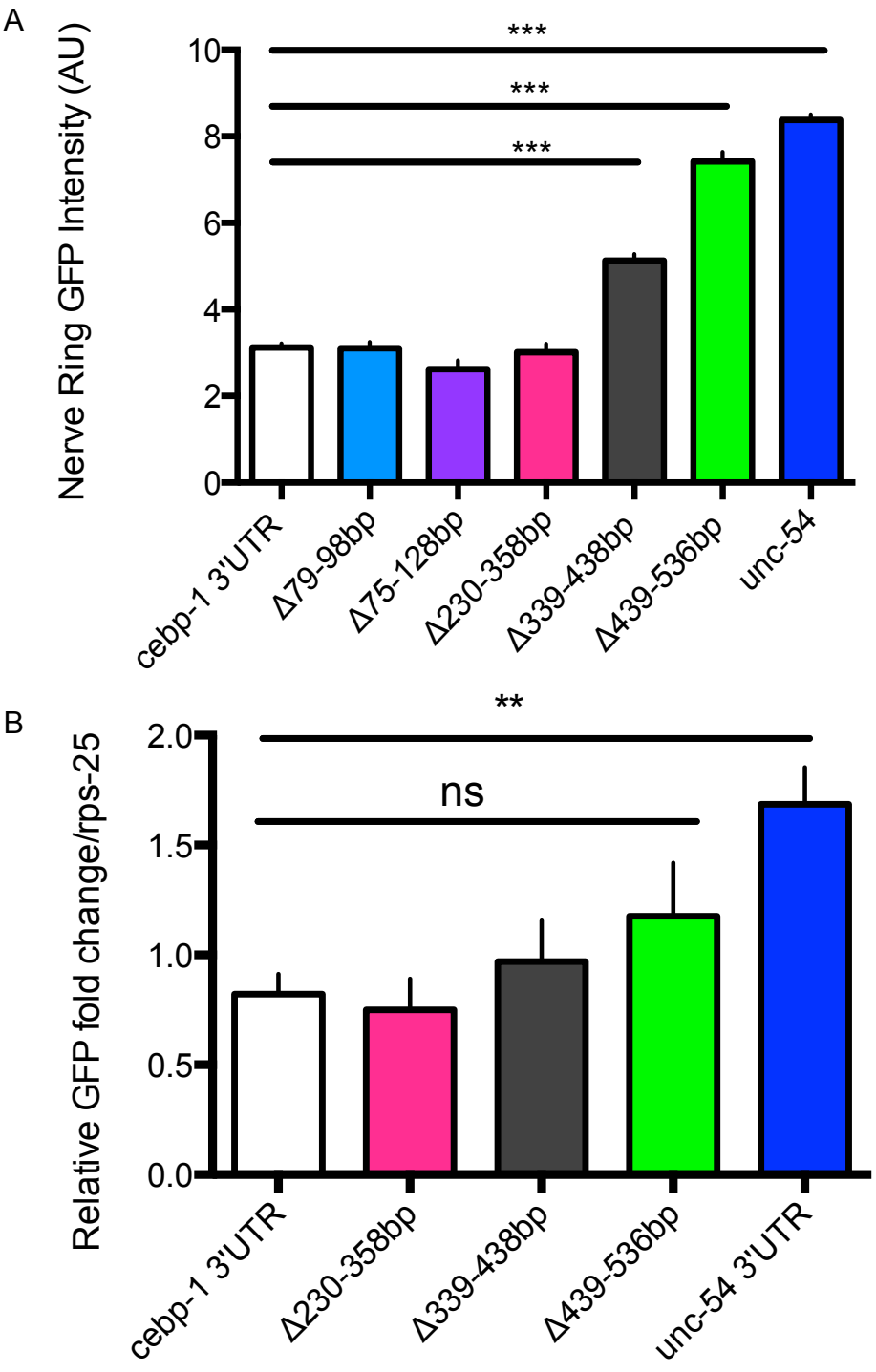


Figure 2.6: Quantification of GFP fluorescence and mRNA levels using single copy reporters A) quantification of GFP fluorescence in nerve ring among different reporters using ImageJ B)qRT-PCR for GFP in different reporter backgrounds. Reference gene is rps-25. Statistical test used is one way ANOVA with the Tukey's multiple comparison test for both intensity and qRT-PCR.

CHAPTER 2.2 – *CIS* ELEMENT OF 339-438 CONTAINS A UNIQUE STEM-LOOP STRUCTURE THAT REPRESSES TRANSLATION

Secondary RNA structure has been implicated in regulating mRNA stability, translation, and interaction with *trans* factors(101). To explore if the *cis*-sequences that affected *cebp-1* baseline mRNA expression might have tendency to form secondary RNA structures we next utilized a computational prediction program, RNApromo(102). This program predicted several stem loop structures within the *cis* element 339-438bp of *cebp-1*'s 3'UTR. Analysis using another program RNAfold(103-105) also shows high probability for this sequence to form two stem-loops (Figure 2.7A). The 439-536bp element also had predictions for secondary structure, but the models were variable depending on the program used, which is why we focused on the 339-438bp element. To test the prediction we created additional deletions that disrupted these RNA hairpins according to computational programs (Figure 2.7B), and generated single-copy expression lines. Analysis of the fluorescence intensity in the wild type background showed that of the deletions 339-387bp and 388-418bp, which would be predicted to prevent different parts of the stem loop structure to form, only the 388-418bp deletion affected GFP intensity (Figure 2.9A) suggesting the second smaller stem-loop structure (stem-loop #2) mediated *cebp-1* reporter baseline stability.

However, with these deletions it is possible that we created new secondary structure that stabilized the expression of the reporter. To test if this stem-loop structure was indeed important for *cebp-1*'s 3'UTR stability we

mutated residues 407-411 of the 3'UTR, to eliminate the stem (Figure 2.8) and tested its effect on the fluorescence intensity. We also found that this stem-loop mutant showed similar upregulation of GFP (Figure 2.9A), suggesting this stem-loop mediated the reporter's baseline expression.

To test if the deletions affected mRNA stability we did qRT-PCR for GFP. We found no difference in GFP mRNA levels among the deletions and mutated stem loop compared to the full length reporter (Figure 2.9B). GFP mRNA levels were also tested in the presence of a transcriptional inhibitor, α-amanitin to further rule out the role of mRNA stability. We found no difference between time match controls of animals incubated with α-amanitin (Figure 2.10), providing more evidence this stem-loop could be affecting translation of the reporter.

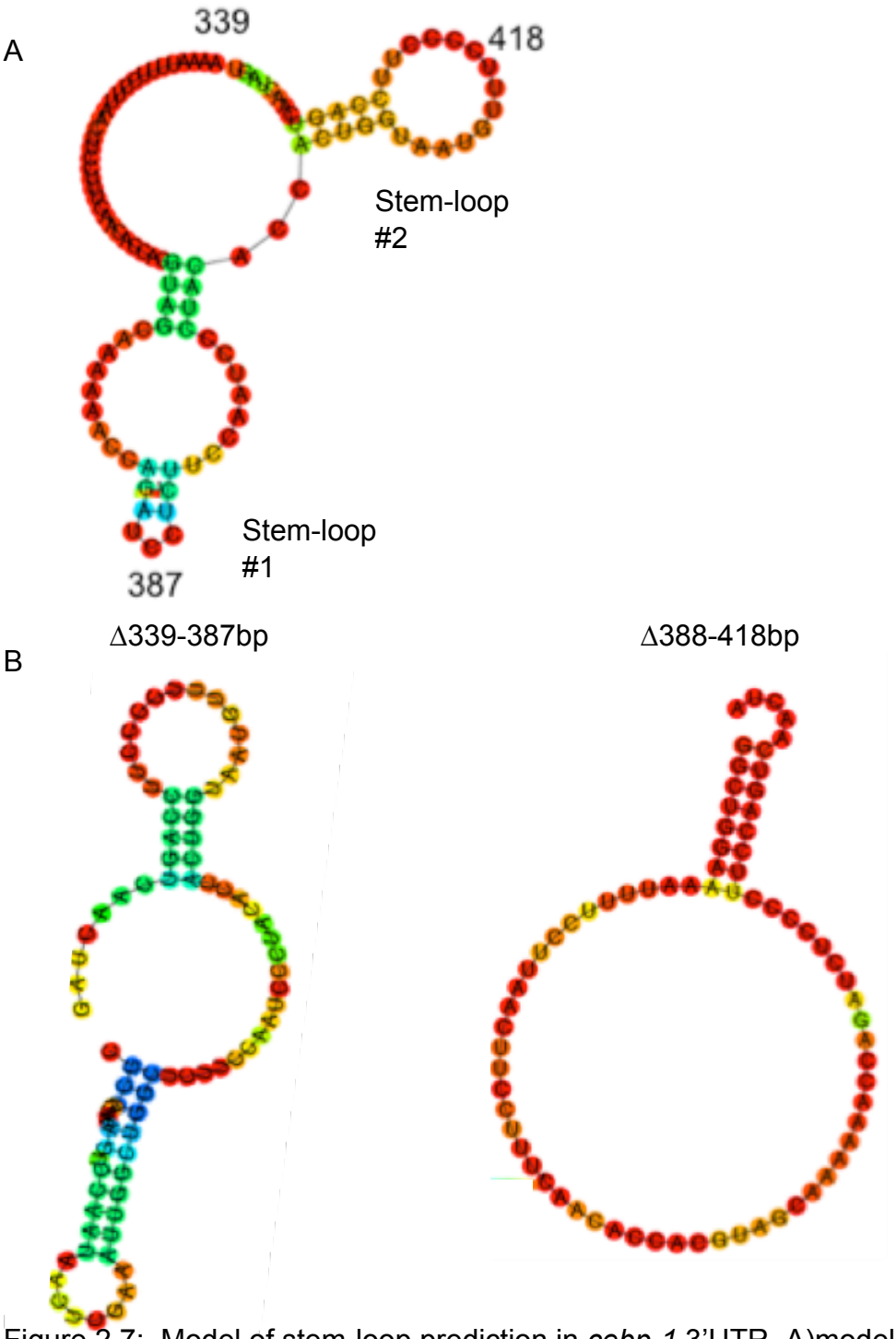


Figure 2.7: Model of stem-loop prediction in *cebp-1* 3'UTR. A)model of stem-loops prediction from 339-436bp. Two stem-loops are labeled in the image, stem loop #1 and stem-loop #2. B) Smaller deletions are predicted to disrupt stem-loops from forming. Δ339-387bp deletion disrupts stem loop #1 while Δ388-418bp délétion disrupts both stem-loops. These predictions are soley based on the 339-436bp sequence, not the whole 3'UTR.

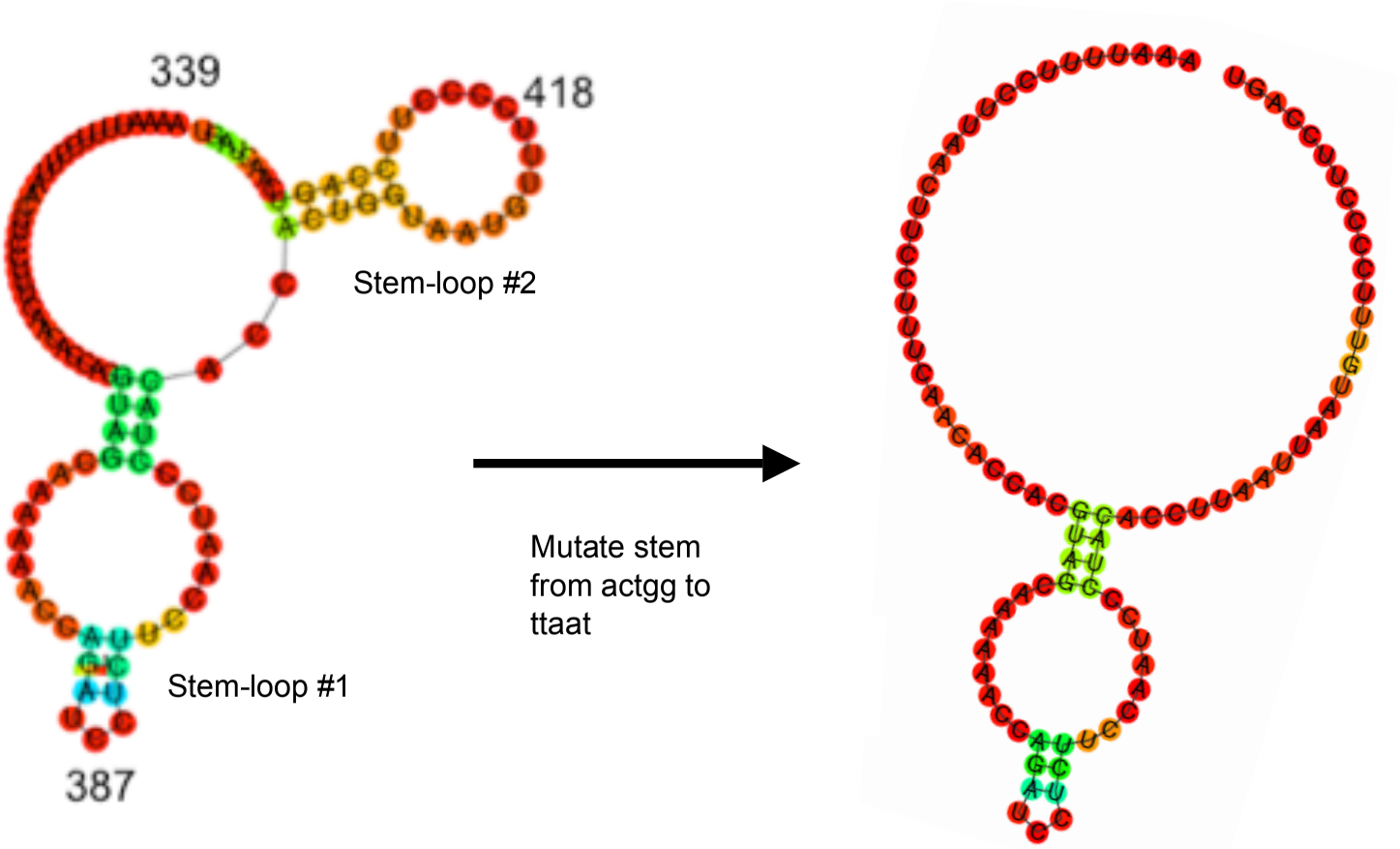
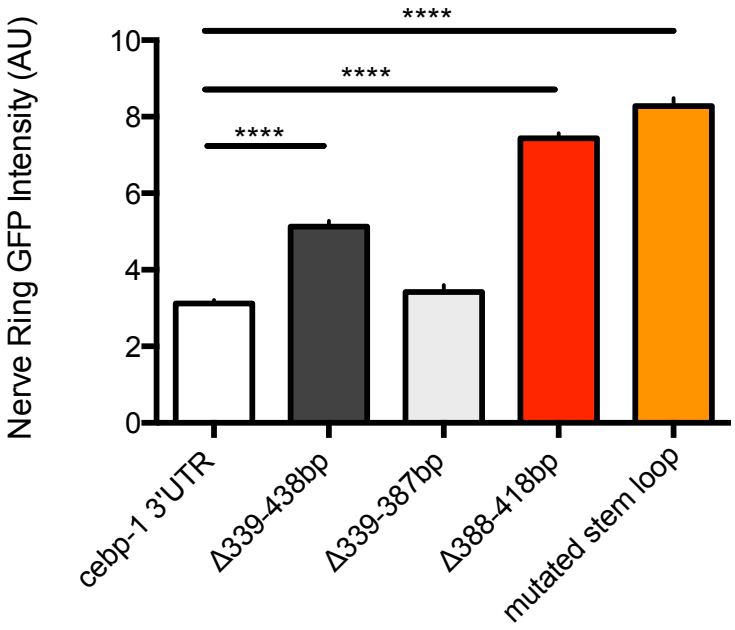


Figure 2.8: Prediction of changes to secondary RNA structure after mutating resides in stem of stem-loop #2. Stem mutated from actgg to ttaat.

A



B

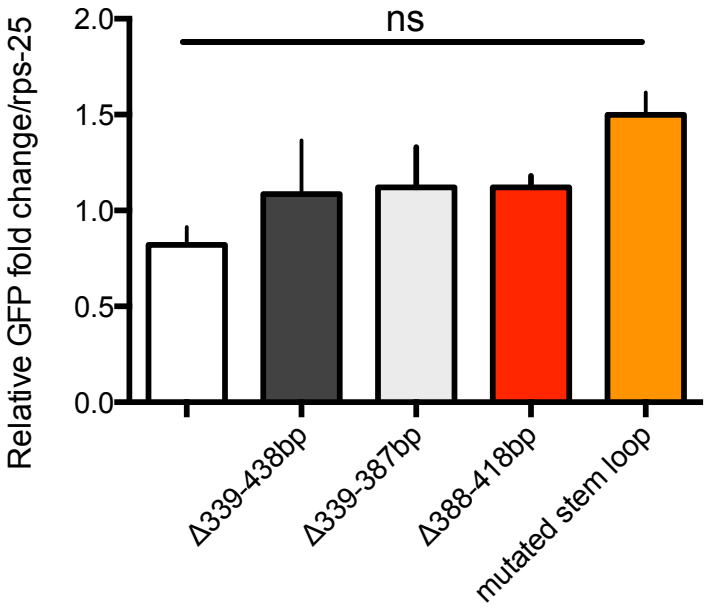


Figure 2.9: Stem-loop regulates expression of *cebp-1* 3'UTR reporter. A) quantification of GFP fluorescence in nerve ring using ImageJ. B)qRT-PCR for GFP in reporter backgrounds. Reference gene is rps-25. Data of cebp-1 3'UTR and Δ339-438bp are the same as used in figure 2.6. Statistical test used is one way ANOVA with the Tukey's multiple comparison test for both intensity and qRT-PCR.

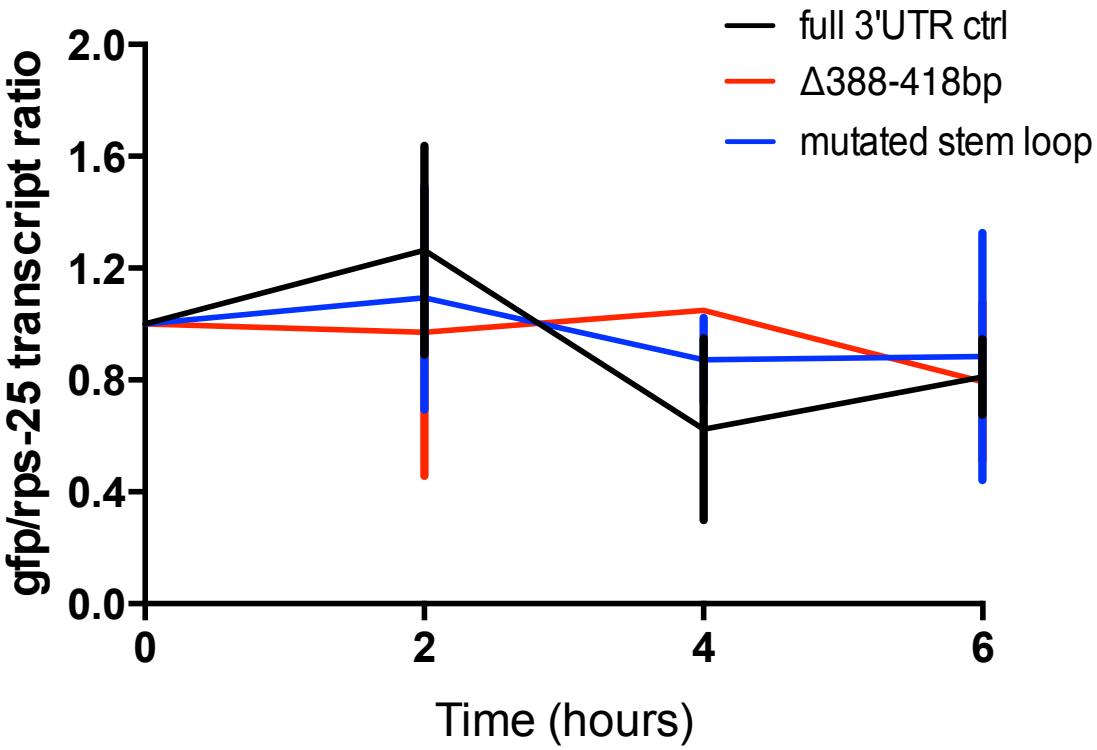


Figure 2.10: α-amanitin drug treatment on animals with 3'UTR reporters does not change GFP mRNA levels compared to time-matched controls.

CHAPTER 2.3 – *CIS* ELEMENTS, 230-358 BP AND 388-418BP, ARE REGULATED BY RPM-1

We examined whether these *cis* elements were also necessary for *rpm-1*'s regulation of *cebp-1*. *rpm-1(lf)* was crossed into these single copy insertion reporters and observed for any fluorescence change. The full 3'UTR reporter showed an increase in GFP both visually and quantitatively by qRT-PCR (Figure 2.11-2.12). As a negative control for *rpm-1* regulation, we tested whether a heterologous 3'UTR, *unc-54*, reporter changed in the *rpm-1(lf)* background. When we compared the reporter in the two backgrounds we found no difference in fluorescence intensity, confirming the specificity of *rpm-1* for *cebp-1*'s 3'UTR (Figure 2.12A). We observed increases in GFP intensity in several reporters in the *rpm-1(lf)* background except for two reporters, Δ230-358bp and Δ339-438bp (Figure 2.12A), which is similar to the studies using extra-chromosmoal arrays (Figure 2.4). The 230-358bp region consists of some repetitive short A/T sequences interspersed among the other nucleotides, but the general A/T percentage content of 63% does not differ particularly from the whole *cebp-1* 3'UTR composition. We also similarly found no change in GFP mRNA levels for these two reporters suggesting these elements were necessary for *rpm-1(lf)*'s increased reporter stability.

Since the putative stem-loop we found in *cebp-1*'s 3'UTR was within the 339-438bp region, we examined if *rpm-1(lf)* also regulated the 3'UTR through this element. Interestingly, while the Δ339-387bp reporter showed an increase in GFP in *rpm-1(lf)* background, the stem-loop deletion, Δ388-418bp, did not have

an increase in GFP in the nerve ring (Figure 2.12A). We additionally looked at the single cell regulation by *rpm-1(lf)* using extra-chromosomal arrays in the PLM and found a similar result (Fig 2.13A,B).

One possible caveat is that the subtle changes in GFP in the *rpm-1(lf)* background might be masked in these reporters due to higher baseline expression. Similar to the extra-chromosomal transgenic reporters, elements towards the end of *cebp-1*'s 3'UTR were required for RPM-1 regulation, including nucleotides 339-438 and 388-418 (Figure 2.12A).

To examine if these *cis* elements regulated by *rpm-1* were through mRNA stability or translation we did qRT-PCR for GFP. While the full 3'UTR reporter displayed an increase in GFP mRNA, the other strains tested did not (Figure 2.12B). From this analysis, it appears there are two different *cis* elements regulated by *rpm-1*. The Δ230-358bp and Δ388-418bp reporters both displayed no difference in GFP fluorescence and mRNA in wild type and *rpm-1(lf)* backgrounds (Fig 2.12A-B), yet the Δ388-418bp reporter has a higher constitutive expression in wild type (Figure 2.12A). This difference may suggest nucleotides 230-358 regulate *rpm-1* dependent *cebp-1* mRNA stability while the stem-loop structure in nucleotides 388-418 regulates *rpm-1* dependent translation. Furthermore, we were able to examine *rpm-1*'s regulation in a cell-specific manner in the PLM by using a mechanosensory neuron specific promoter tagged to DENDRA and *cebp-1*'s 3'UTR. The upregulation of signal in the *rpm-1(lf)* background disappeared in reporters with the 388-418bp deletion suggesting this stem-loop mediates *rpm-1*'s regulation in the PLM (Figure 2.13).

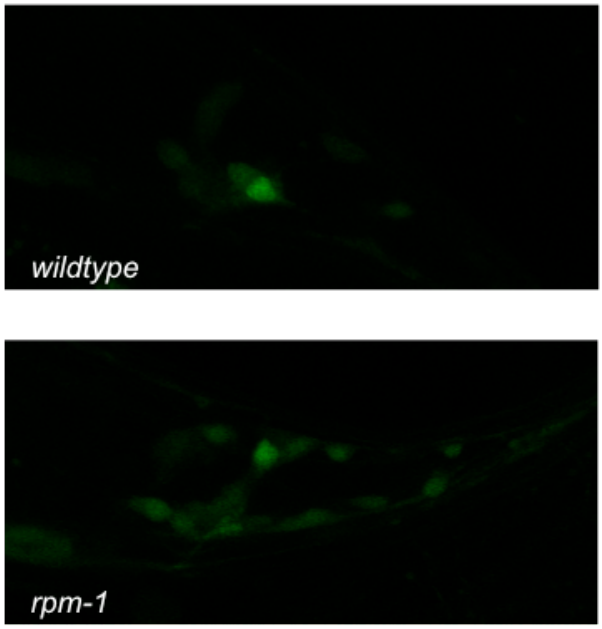
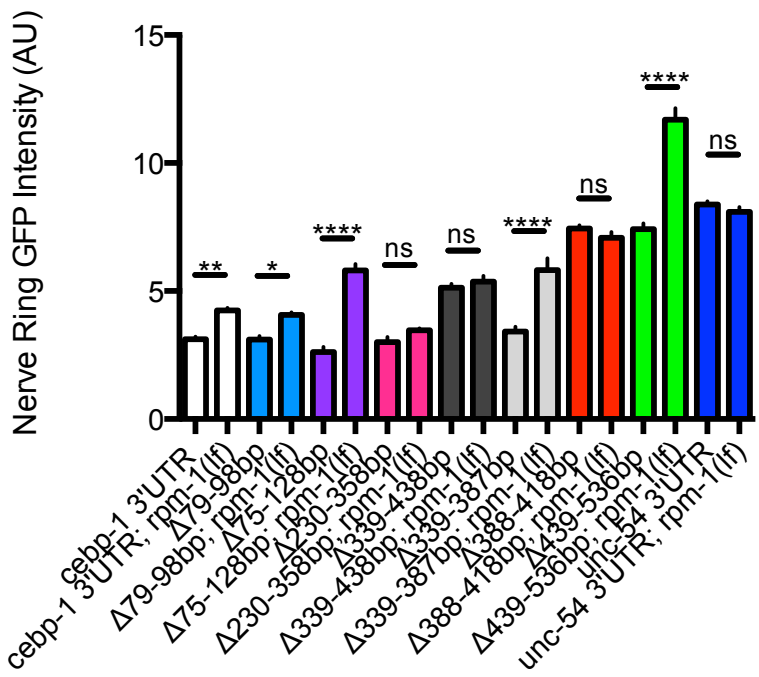


Figure 2.11: Single copy *cebp-1* 3'UTR reporter shows more cells expressing GFP in *rpm-1(lf)* background compared to wild type control. Images from tail of L4 animals taken under the same conditions.

A



B

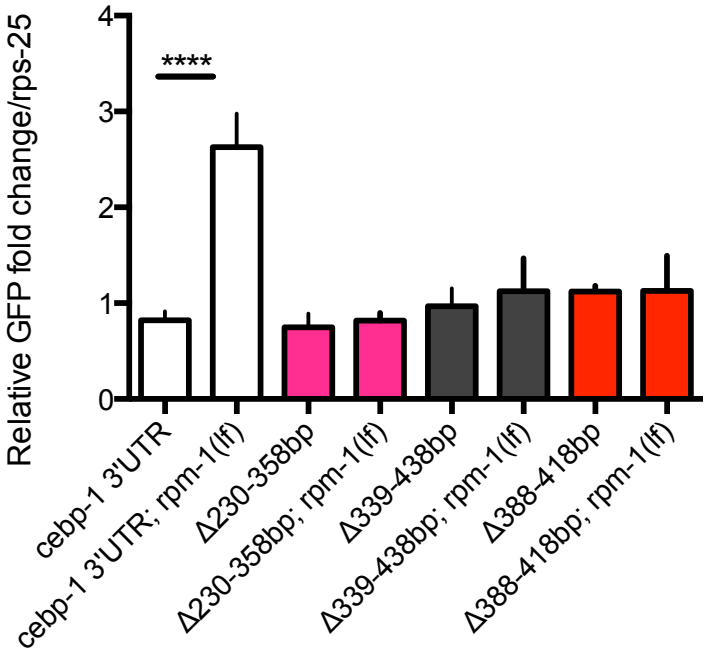


Figure 2.12: Quantification of GFP fluorescence of single copy 3'UTR reporters in wildtype and *rpm-1(lf)* backgrounds. A)quantification of GFP fluorescence in nerve ring of L4 animals using ImageJ B)qRT-PCR for GFP in wildtype and *rpm-1(lf)* backgrounds. Reference gene is rps-25.

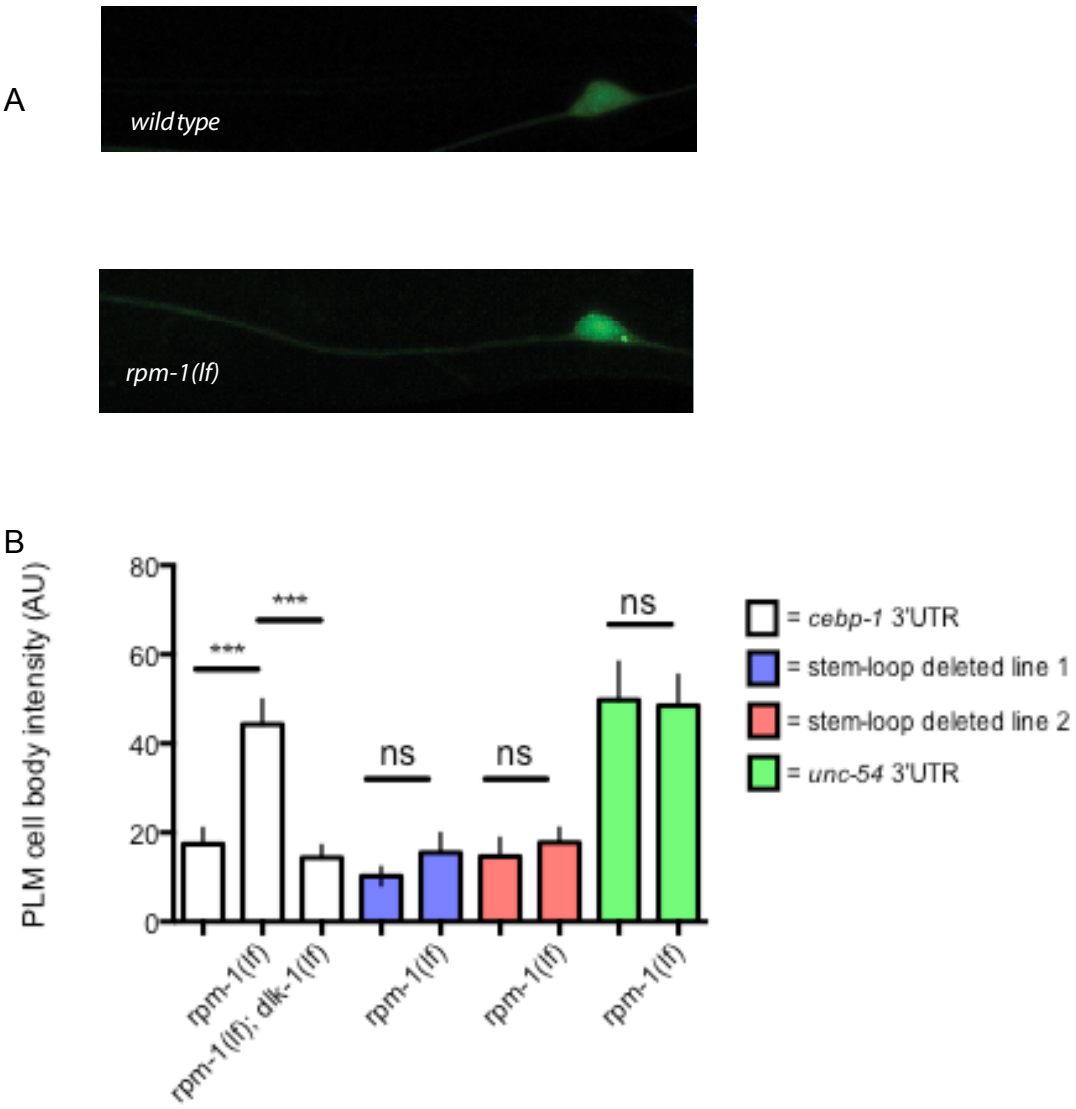


Figure 2.13: Single cell resolution of *rpm-1* regulation of *cebp-1* 3'UTR through stem-loop. A)sample images of mechanosensory *cebp-1* 3'UTR reporter in wildtype and *rpm-1(lf)* background B) quantification of GFP fluorescence in PLM cell body with reporters for full 3'UTR, stem-loop deletion, and unc-54 3'UTR.

CHAPTER 2.4 – 3'UTR ELEMENTS ARE IMPORTANT FOR *CEBP-1* FUNCTION IN THE SUPPRESSION OF *RPM-1* AND REGENERAITON

To examine how these elements affected CEBP-1 function *in vivo*, we undertook rescue experiments of *cebp-1*. We constructed single-copy insertion lines of a pan-neuronal CEBP-1 tagged to GFP and different elements of its 3'UTR. We used single-copy insertion of CEBP-1 tagged to GFP with the *cis* elements 388-418bp and 439-536bp deleted (Figure 2.14A). These two elements were chosen based on the high expression of GFP in the wild type background (Figure 2.6A). The GFP showed nuclear localization in the nerve ring, nerve cord, tail and other neurons (Figure 2.14B). By eye we could not detect significant differences in GFP intensity and localization of CEBP-1 among the different strains (data not shown) despite the increased GFP expression in similar 3'UTR deletion reporters lacking CEBP-1 protein (Figure 2.6A). The addition of CEBP-1 protein to the reporter may allow other factors to affect CEBP-1 levels, masking the 3'UTR regulation previously described or possibly, CEBP-1 protein levels are more tightly regulated by feedback systems that prevent higher expression.

We tested if these transgenes could rescue *cebp-1(lf)*'s function. A single copy construct of *cebp-1* with its full 3'UTR was able to rescue *cebp-1*'s axon regeneration phenotype (Figure 2.15). Constructs expressing CEBP-1 protein with the 388-418bp deletion was also able to rescue, similar to the full 3'UTR (Figure 2.15). A second deletion construct of CEBP-1 protein with 439-536bp deleted of the 3'UTR showed regeneration close to wild type levels, but was still

significantly less than control regrowth (Figure 2.13). This phenotype is similar to the construct with a heterologous 3'UTR, *unc-54* (Figure 2.15).

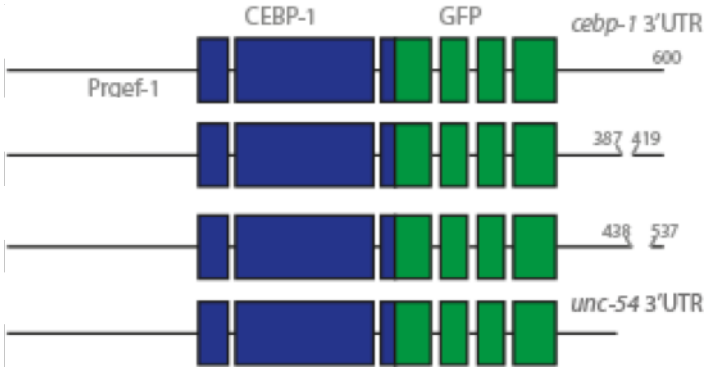
In *rpm-1(lf)* mutants the synaptic branch from the PLM to the nerve cord is lost in about 50% of the animals, which is suppressed by *cebp-1(lf)* (Figure 2.16A-B). We examined if these single copy constructs could rescue *cebp-1*'s suppression of the *rpm-1* phenotype in the PLM. The full length 3'UTR construct was able to rescue the synaptic branch phenotype of *rpm-1(lf)* (Figure 2.16C). Interestingly, the other constructs with the *unc-54* 3'UTR or *cebp-1* 3'UTR deletions could not rescue this phenotype (Figure 2.16C). These results suggest *cebp-1* 3'UTR is essential to regulate the developmental function of CEBP-1 in the PLM. These constructs showed no difference in the *cebp-1(lf)* background (Figure 2.17).

Since there was no obvious difference in GFP levels among these four constructs we examined if *cebp-1* mRNA was changed in these different strains, which have CEBP-1-GFP expressed in the neurons, but *cebp-1(lf)* in other tissues. We found no significant difference, but a trend of increased *cebp-1* mRNA in all the strains with modifications to the 3'UTR of *cebp-1* compared to the full *cebp-1* 3'UTR construct (Figure 2.18). The 388-418bp deleted strain showed the largest increase in *cebp-1* mRNA but there appears to be a general increase the strain with the *unc-54* 3'UTR and 439-536bp deletion, suggesting that these deletions affect *cebp-1* mRNA levels. This difference in *cebp-1* mRNA could explain the failure of these three constructs to rescue the *rpm-1;*

cebp-1 phenotype (Figure 2.16). However, the levels of *cebp-1* may be low enough to rescue axon regeneration (Figure 2.15).

One important aspect of this result is the difference from the qRT-PCR data on the GFP reporters with *cebp-1* 3'UTR deletions in which there was no difference in GFP mRNA levels among the strains (Figure 2.6B, 2.8B). A possible explanation is that *cebp-1* genomic sequence contains elements that are affected by the 3'UTR modifications, where as GFP by itself is not.

A



B

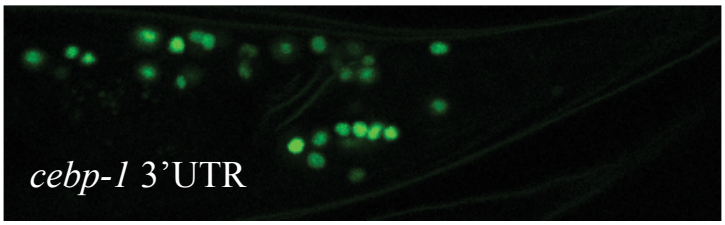


Figure 2.14: Single-copy constructs of GFP-tagged CEBP-1 with various 3'UTRs A) design of pan-neuronal tagged CEBP-1 reporters with various 3'UTRs B) sample image of tail of L4 staged animal with GFP-tagged CEBP-1 with *cebp-1*'s endogenous 3'UTR

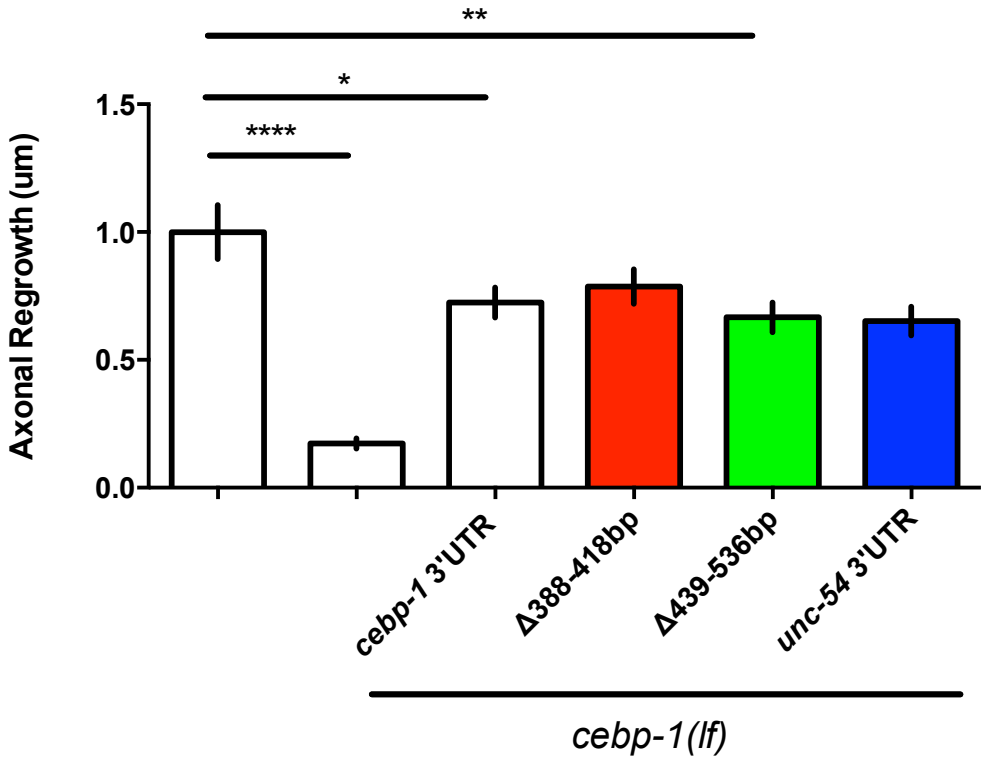
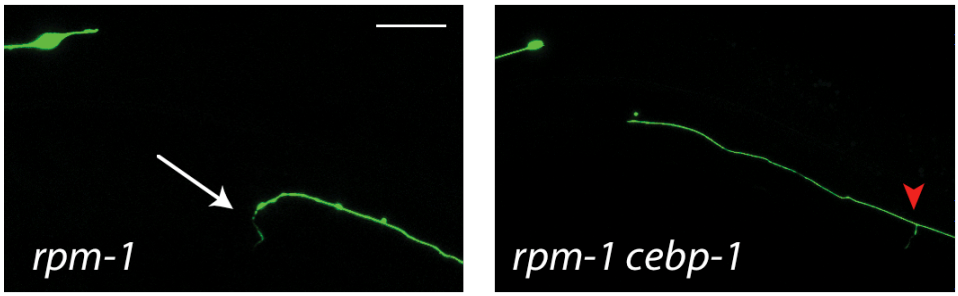


Figure 2.15: Single-copy rescue of CEBP-1 function in axon regeneration. All four constructs rescue the inhibition of regeneration in *cebp-1(lf)*.

A



B

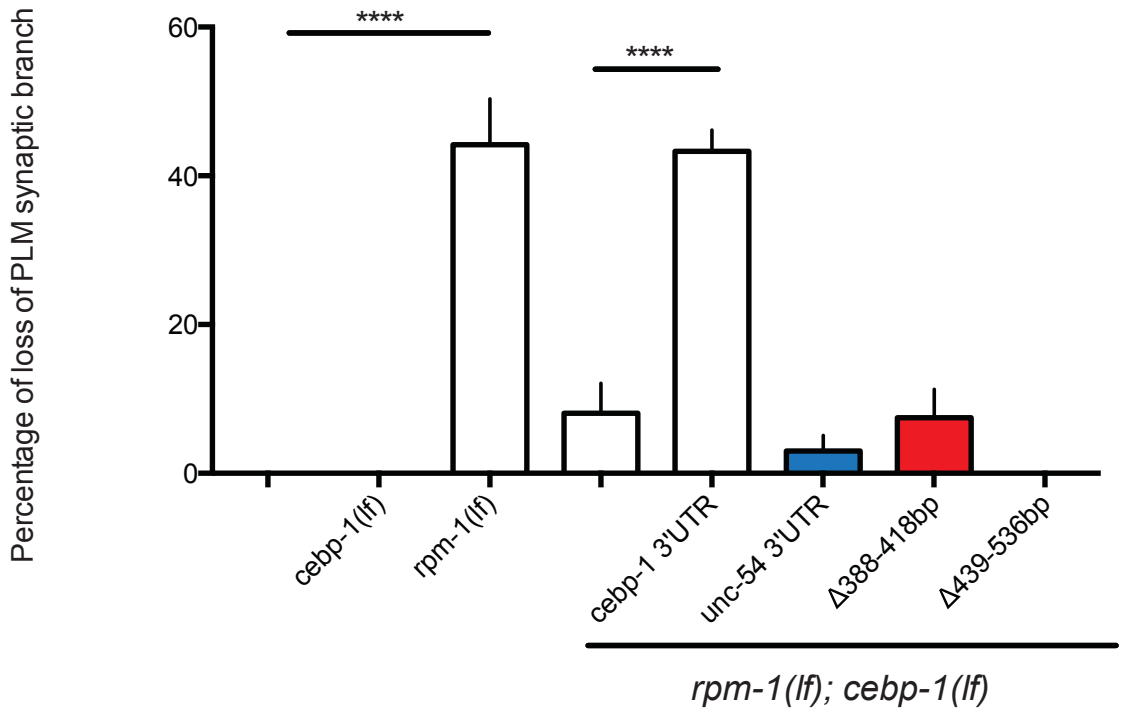


Figure 2.16: Different levels of rescue of *rpm-1; cebp-1* suppression with single copy constructs. A) Sample images illustrating *rpm-1(lf)* phenotype in the PLM. The arrow denotes the abnormal trajectory and arrowhead denotes the synaptic branch. B)quanitifcation of the loss of synaptic branch from the PLM to the nerve cord. Results based on 3 biological replicates with greater than 150 animals for each genotype. One way ANOVA was used for statistical analysis.

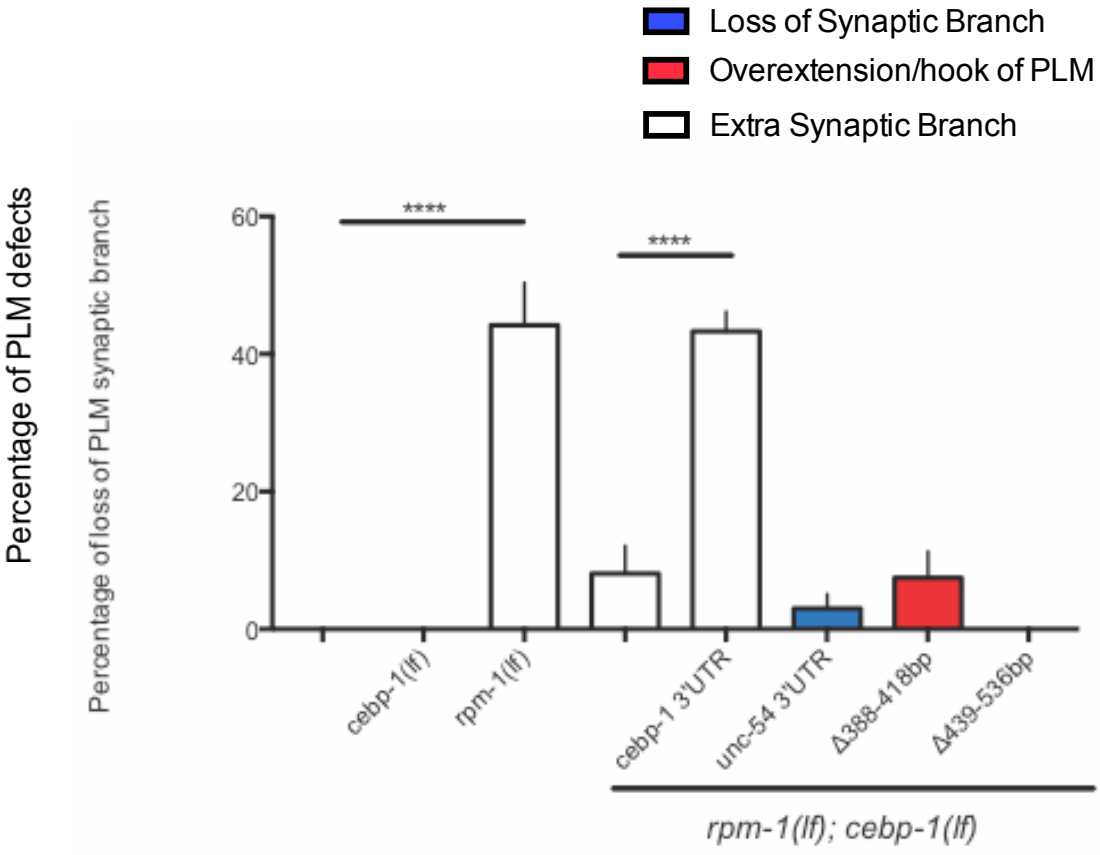


Figure 2.17: Single-copy constructs show no phenotype in *cebp-1(lf)* background in PLM.

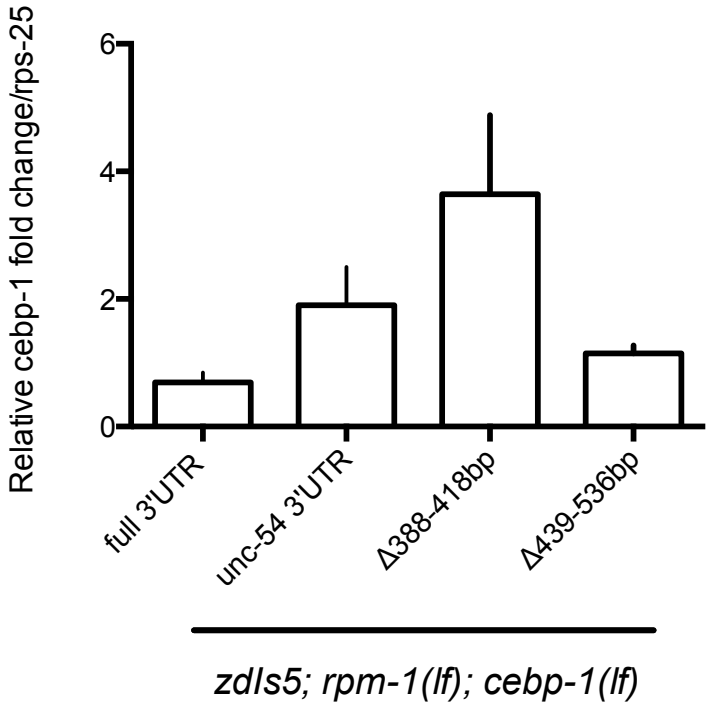


Figure 2.18: qRT-PCR for *cebp-1* in *rpm-1(lf); cebp-1(lf)* background with single-copy CEBP-1 constructs.

CHAPTER 2.5 – DISCUSSION

The C/EBP family of transcription factors have been studied for a variety of roles in different tissues, including the nervous system (106). There are six members of this family and *C. elegans cebp-1* is most similar to C/EBPδ. We first identified *cebp-1* as necessary for axon regeneration and this function has been confirmed in a mammalian model (94, 107). *cebp-1* is regulated post-transcriptionally to ensure proper activity in the nervous system however the *cis*

elements involved in this regulation were not known. We have shown *cebp-1* is regulated through multiple *cis* elements in its 3'UTR by the conserved E3 ubiquitin ligase *rpm-1* in the nervous system and these elements can contribute to both stability and translation.

In our analysis of *cis* elements of *cebp-1*'s 3'UTR we identified two elements mediating baseline expression: 339-438bp and 439-536bp. Within the 339-438 nucleotides, a putative stem-loop structure appears to regulate *cebp-1*'s translation. This stem-loop structure also mediates *rpm-1*'s control over *cebp-1* as several reporters with the deletion of this structure failed to respond to *rpm-1(lf)* (Figure 2.12A, 2.13B). This stem-loop may mediate binding of *trans* factors to *cebp-1* mRNA for *rpm-1*'s regulation of stability and translation as well as control of baseline *cebp-1* activity.

This stem-loop may mediate *cebp-1*'s translation which is especially interesting given evidence *cebp-1* is locally translated after axotomy(94). Future experiments will need to examine if this stem-loop could play a role in translation of *cebp-1* after axotomy.

We identified two elements regulated by *rpm-1* in *cebp-1*'s 3'UTR: 230-358bp and 388-418bp. Our qRT-PCR data suggests these two elements contribute to different roles of *rpm-1* on *cebp-1* mRNA. By examining sequence content, there does not seem to be a difference though the 230-358bp sequences does contain several repeats of A/Ts interspersed among the other nucleotides. Since the 230-358bp deletion showed no difference in GFP fluorescence and mRNA levels, it suggests this element is important for mRNA

stability (Figure 2.12B, C) As the 339-438bp deletion shows an increased level of GFP fluorescence while no change in GFP mRNA levels, this element appears to regulate translation (Figure 2.12B,C). Thus to ensure proper levels of *cebp-1* this pathway allows regulation of both stability and translation of this transcription factor. Interestingly *cebp-1*'s homolog C/EBPδ also has been reported to be post-transcriptionally stabilized by a p38 MAPK cascade in response to ultra-violet radiation (97), suggesting functional conservation of this regulation.

The effect on CEBP-1 protein due to these *cis* elements depended on the scored phenotype. While these *cis* elements had little effect on axon regeneration (Figure 2.13), they appeared to affect development (Figure 2.16B). The full *cebp-1*'s 3'UTR can rescue the synapse defect of the PLM branch (Figure 2.16B). Since the other constructs failed to rescue this synaptic phenotype, it suggests these c*is* elements may be necessary for synaptic formation. These *cis* elements may affect the dosage of CEBP-1 during development and changes to the normal level of CEBP-1, either increase or decreases, may affect CEBP-1 function. This possibility could explain the inability to rescue *cebp-1(lf)*'s phenotype in axon regeneration using extra-chromosomal arrays (data not shown). We examined the effect on *cebp-1* mRNA and found a trend for increased *cebp-1* mRNA in the strains with the modified *cebp-1* 3'UTR compared to the full *cebp-1* 3'UTR (Figure 2.18). This difference in *cebp-1* mRNA levels may explain the difference in rescue ability of the constructs as the proper level of *cebp-1* is controlled through its 3'UTR

during development. However, one important caveat with these single copy constructs is that they do not fully mimic the endogenous regulation of *cebp-1* due to the pan-neuronal promoter, *rgef-1*. Thus this promoter may mask a more significant effect of the *cis* elements on CEBP-1 function.

CHAPTER 2.6 – MATERIALS AND METHODS

We maintained *C. elegans* strains on NGM plates at 20-25°C as previously described (108).The mutations and transgenes we used are listed in Table 2.

Table 2.1: List of strains, genotypes, and transgene numbers used in this study.

Strain Name	Genotype	Transgene #
CZ19271	*Prgef-1::GFP::PEST::3'utr(cebp-1)*	*juEx5817*
CZ20709	*Prgef-1::GFP::PEST::3'utr(cebp-1)*	*juEx6524*
CZ19272	*Prgef-1::GFP::PEST::3'utr(unc-54)*	*juEx5818*
CZ19570	*Prgef-1::GFP::PEST::3'utr(unc-54)*	*juEx5899*
CZ19284	*rpm-1(ju44) V; Prgef-1::GFP::PEST::3'utr(cebp-1)*	*juEx5817*
CZ20710	*rpm-1(ju44) V; Prgef-1::GFP::PEST::3'utr(cebp-1)*	*juEx6524*
CZ19285	*rpm-1(ju44) V; Prgef-1::GFP::PEST::3'utr(unc-54)*	*juEx5818*
CZ19273	*Prgef-1::GFP::PEST::3'utr(cebp-1 with bp 40-336 deleted)*	*juEx5819*
CZ19560	*Prgef-1::GFP::PEST::3'utr(cebp-1 with bp 40-336 deleted)*	*juEx5890*
CZ19571	*Prgef-1::GFP::PEST::3'utr(cebp-1 with bp 40-336 deleted)*	*juEx5900*
CZ19275	*Prgef-1::GFP::PEST::3'utr(cebp-1 with bp 339-438 deleted)*	*juEx5821*

Table 2.1: List of strains, genotypes, and transgene numbers used in this study, Continued.

Strain Name	Genotype	Transgene #
CZ19274	*Prgef-1::GFP::PEST::3'utr(cebp-1 with bp 339-438 deleted)*	*juEx5820*
CZ19572	*Prgef-1::GFP::PEST::3'utr(cebp-1 with bp 339-438 deleted)*	*juEx5901*
CZ19573	*Prgef-1::GFP::PEST::3'utr(cebp-1 with bp 339-438 deleted)*	*juEx5902*
CZ19276	*Prgef-1::GFP::PEST::3'utr(cebp-1 with bp 440-537 deleted)*	*juEx5822*
CZ19277	*Prgef-1::GFP::PEST::3'utr(cebp-1 with bp 75-112 deleted)*	*juEx5823*
CZ19278	*Prgef-1::GFP::PEST::3'utr(cebp-1 with bp 95-128 deleted)*	*juEx5824*
CZ19561	*Prgef-1::GFP::PEST::3'utr(cebp-1 with bp 95-128 deleted)*	*juEx5891*
CZ19562	*Prgef-1::GFP::PEST::3'utr(cebp-1 with bp 95-128 deleted)*	*juEx5892*
CZ19279	*Prgef-1::GFP::PEST::3'utr(cebp-1 with bp 75-94 deleted)*	*juEx5825*
CZ19563	*Prgef-1::GFP::PEST::3'utr(cebp-1 with bp 75-94 deleted)*	*juEx5893*
CZ19280	*Prgef-1::GFP::PEST::3'utr(cebp-1 with bp 128-228 deleted)*	*juEx5826*
CZ19281	*Prgef-1::GFP::PEST::3'utr(cebp-1 with bp 230-336 deleted)*	*juEx5827*
CZ19282	*Prgef-1::GFP::PEST::3'utr(cebp-1 with bp 294-358 deleted)*	*juEx5828*
CZ19574	*Prgef-1::GFP::PEST::3'utr(cebp-1 with bp 294-358 deleted)*	*juEx5903*
CZ19575	*Prgef-1::GFP::PEST::3'utr(cebp-1 with bp 294-358 deleted)*	*juEx5904*
CZ19576	*Prgef-1::GFP::PEST::3'utr(cebp-1 with bp 294-358 deleted)*	*juEx5905*
CZ19283	*Prgef-1::GFP::PEST::3'utr(cebp-1 with bp 537-600 deleted)*	*juEx5829*

Table 2.1: List of strains, genotypes, and transgene numbers used in this study, Continued.

Strain Name	Genotype	Transgene #
CZ19286	*rpm-1(ju44) V; Prgef-1::GFP::PEST::3'utr(cebp-1 with bp 40-336 deleted)*	*juEx5819*
CZ19287	*rpm-1(ju44) V; Prgef-1::GFP::PEST::3'utr(cebp-1 with bp 339-438 deleted)*	*juEx5820*
CZ19288	*rpm-1(ju44) V; Prgef-1::GFP::PEST::3'utr(cebp-1 with bp 339-438 deleted)*	*juEx5821*
CZ19289	*rpm-1(ju44) V; Prgef-1::GFP::PEST::3'utr(cebp-1 with bp 440-537 deleted)*	*juEx5822*
CZ19290	*rpm-1(ju44) V; Prgef-1::GFP::PEST::3'utr(cebp-1 with bp 75-112 deleted)*	*juEx5823*
CZ19291	*rpm-1(ju44) V; Prgef-1::GFP::PEST::3'utr(cebp-1 with bp 95-128 deleted)*	*juEx5824*
CZ19292	*rpm-1(ju44) V;Prgef-1::GFP::PEST::3'utr(cebp-1 with bp 75-94 deleted)*	*juEx5825*
CZ19293	*rpm-1(ju44) V; Prgef-1::GFP::PEST::3'utr(cebp-1 with bp 128-228 deleted)*	*juEx5826*
CZ19294	*rpm-1(ju44) V; Prgef-1::GFP::PEST::3'utr(cebp-1 with bp 230-336 deleted)*	*juEx5827*
CZ19295	*rpm-1(ju44) V; Prgef-1::GFP::PEST::3'utr(cebp-1 with bp 294-358 deleted)*	*juEx5828*
CZ19296	*rpm-1(ju44) V; Prgef-1::GFP::PEST::3'utr(cebp-1 with bp 537-600 deleted)*	*juEx5829*
CZ18841	*Prgef-1::GFP::3'utr(cebp-1) line 1 II; unc-119(ed9) III*	*juSi135*
CZ18842	*Prgef-1::GFP::3'utr(cebp-1) line 2 II; unc-119(ed9) III*	*juSi136*
CZ20711	*Prgef-1::GFP::3'utr(unc-54) II; unc-119(ed9) III*	*juSi176*
CZ18847	*Prgef-1::GFP::3'utr(cebp-1) line 1 II*	*juSi135*
CZ18849	*Prgef-1::GFP::3'utr(cebp-1) line 2 II*	*juSi136*
CZ20712	*Prgef-1::GFP::3'utr(unc-54) II*	*juSi176*
CZ18848	*Prgef-1::GFP::3'utr(cebp-1) line 1 II; rpm-1(ju44) V*	*juSi135*
CZ18850	*Prgef-1::GFP::3'utr(cebp-1) line 2 II; rpm-1(ju44) V*	*juSi136*
CZ20713	*Prgef-1::GFP::3'utr(unc-54) II; unc-119(ed9) III; rpm-1(ju44) V*	*juSi176*

Table 2.1: List of strains, genotypes, and transgene numbers used in this study, Continued.

Strain Name	Genotype	Transgene #
CZ20714	*Prgef-1::GFP::3'utr(unc-54) II; rpm-1(ju44) V*	*juSi176*
CZ20079	*Prgef-1::GFP::3'utr(del 79-98) line 1 II; unc-119(ed3) III*	*juSi154*
CZ20080	*Prgef-1::GFP::3'utr(del 75-128) line 1 II; unc-119(ed3) III*	*juSi155*
CZ20081	*Prgef-1::GFP::3'utr(del 75-128) line 2 II; unc-119(ed3) III*	*juSi156*
CZ20082	*Prgef-1::GFP::3'utr(del 75-128) line 3 II; unc-119(ed3) III*	*juSi157*
CZ20083	*Prgef-1::GFP::3'utr(del 230-358) line 1 II; unc-119(ed3) III*	*juSi158*
CZ20715	*Prgef-1::GFP::3'utr(del 339-438) line 1 II; unc-119(ed3) III*	*juSi177*
CZ20716	*Prgef-1::GFP::3'utr(del 339-438) line 2 II; unc-119(ed3) III*	*juSi178*
CZ20717	*Prgef-1::GFP::3'utr(del 439-536) line 1 II; unc-119(ed3) III*	*juSi182*
CZ20718	*Prgef-1::GFP::3'utr(del 79-98) line 1 II; unc-119(ed3) III; rpm-1(ju44)V*	*juSi154*
CZ20719	*Prgef-1::GFP::3'utr(del 75-128) line 1 II; unc-119(ed3) III; rpm-1(ju44)V*	*juSi155*
CZ20720	*Prgef-1::GFP::3'utr(del 230-358) line 1 II; unc-119(ed3) III; rpm-1(ju44)V*	*juSi158*
CZ20721	*Prgef-1::GFP::3'utr(del 339-438) line 1 II; unc-119(ed3) III; rpm-1(ju44)V*	*juSi177*
CZ20722	*Prgef-1::GFP::3'utr(del 439-536) line 1 II; unc-119(ed3) III; rpm-1(ju44)V*	*juSi182*
CZ19566	*Pmec-4::dendra-3'utr(cebp-1)*	*juEx5896*
CZ19807	*rpm-1(ju23) V; Pmec-4::dendra-3'utr(cebp-1)*	*juEx5896*
CZ19568	*Pmec-4::dendra-3'utr(unc-54)*	*juEx5898*
CZ20726	*rpm-1(ju23) V; Pmec-4::dendra-3'utr(unc-54)*	*juEx5898*
CZ21599	*dlk-1(tm4024) I ; rpm-1(ju23) V; Pmec-4::dendra-3'utr(cebp-1)*	*juEx5896*
CZ21671	*Pmec-4 ::dendra-3'utr(del 388-418bp)*	*juEx6570*
CZ21672	*Pmec-4 ::dendra-3'utr(del 388-418bp)*	*juEx6571*

Table 2.1: List of strains, genotypes, and transgene numbers used in this study, Continued.

CZ21673	*rpm-1(ju44) V ; Pmec-4 ::dendra-3'utr(del 388-418bp)*	*juEx6570*
CZ21674	*rpm-1(ju44) V ; Pmec-4 ::dendra-3'utr(del 388-418bp)*	*juEx6571*
CZ10175	*Pmec-4::GFP I*	*zdIs5*
CZ7097	*Pmec-4 ::GFP I ; rpm-1(ju44) V*	*zdIs5*
CZ22574	*Pmec-4 ::GFP I ; rpm-1(ju44) V ; cebp-1(tm2807) X*	*zdIs5*
CZ18809	*Pmec-4 ::GFP I ; cebp-1(tm2807) X*	*zdIs5*
CZ18807	*Pmec-4 ::GFP I ; Prgef-1 ::CEBP-1 ::GFP ::3'utr(cebp-1) II ; cebp-1(tm2807) X*	*zdIs5* and *juSi127*
CZ18743	*Pmec-4 ::GFP I ; Prgef-1 ::CEBP-1 ::GFP ::3'utr(unc-54) II ; cebp-1(tm2807) X*	*zdIs5* and *juSi126*
CZ21525	*Pmec-4 ::GFP I ; Prgef-1 ::CEBP-1 ::GFP ::3'utr(cebp-1 del 388-418bp) II ; cebp-1(tm2807) X*	*zdIs5* and *juSi220*
CZ21526	*Pmec-4 ::GFP I ; Prgef-1 ::CEBP-1 ::GFP ::3'utr(cebp-1 del 439-536bp) II ; cebp-1(tm2807) X*	*zdIs5* and *juSi222*
CZ20088	*Pmec-4 ::GFP I ; Prgef-1 ::CEBP-1 ::GFP ::3'utr(cebp-1) II ; rpm-1(ju44) V ; cebp-1(tm2807) X*	*zdIs5* and *juSi127*
CZ20089	*Pmec-4 ::GFP I ; Prgef-1 ::CEBP-1 ::GFP ::3'utr(unc-54) II ; rpm-1(ju44) V ; cebp-1(tm2807) X*	*zdIs5* and *juSi126*
CZ22571	*Pmec-4 ::GFP I ; Prgef-1 ::CEBP-1 ::GFP ::3'utr(cebp-1 del 388-418bp) II ; rpm-1(ju44) V ; cebp-1(tm2807) X*	*zdIs5* and *juSi220*
CZ22572	*Pmec-4 ::GFP I ; Prgef-1 ::CEBP-1 ::GFP ::3'utr(cebp-1 del 439-536bp) II ; rpm-1(ju44) V ; cebp-1(tm2807) X*	*zdIs5* and *juSi222*

C. elegans injections

Extrachromosomal transgenes were generated by injecting 10ng/ul of the construct with the co-injection marker Pgcy-8::tagRFP into the *C. elegans* gonad. Lines were formed and analyzed. Single copy insertion reporters were

made by injecting constructs into strains EG4322 and EG6699. These worms were then cultured at 25ºC and checked for rescue of the *unc-119* phenotype. MosSci transgenes were verified with PCR and sequencing to confirm single copy insertion. Plasmids constructed and used are described in Table 2.2.

3'UTR Extrachromosomal Reporter Site directed mutagenesis

Deletions were made using a combination of restriction enzyme digests and site directed mutagenesis. All of these constructs were injected into the *C. elegans* gonad at the same concentration of 10ng/ul with the co-injection marker Pgcy-8::tagRFP.

Fluorescence Microscopy

Fluorescence reporters in live worms were scored using the Zeiss LSM710 microscope. Confocal z-stack images were taken on the LSM710. For quantification of touch neuron morphology (using *zdIs5)* we examined at least 100 one-day old young adult worms, under the Zeiss Axioplan2 Microscope.

Fluorescence intensity was measured using ImageJ (US NIH). Measurements for all images were subtracted for background intensity.

3'UTR Reporter Fluorescence Quantification

All strains were cultured at 25°C. With the extrachromosomal array transgenes, we quantified GFP in the ventral nerve cord, posterior to the vulva. To enable visual comparison, we switched to use standard GFP with the single

copy reporter since the expression of the reporter was low. The MosSci transgene lines were made in strain with a null *unc-119* allele, whch does not affect the expression of our as we compared the full *cebp-1* 3'UTR reporter in the background of the *unc-119* null allele and wild type and found no difference in GFP expression (data not shown) (Table 2.1). We examined GFP expression by measuring the fluorescence intensity in the nerve ring in L4 animals, as well as qRT-PCR for GFP.

mRNA analysis

We isolated total RNA from strains using a combined TRIzol/RNeasy Mini Kit (Invitrogen and Qiagen) protocol. Worms were synchronized by a bleaching protocol, grown in the same conditions and collected at the L4 stage. We used 1-2µg of RNA to reverse transcribe into cDNA using the SuperScript III® First Strand Synthesis System (Invitrogen) with an oligoDT primer. We measured levels of *cebp-1* using two primer sets YJ8984, YJ10370 and YJ10371, YJ8983. GFP levels were measured using primers YJ10372, YJ10373. *rps-25* was used as a control with primers YJ10368, YJ10369. Primer sequences are listed in Table 2.3.

For the α-amanitin experiments, we incubated worms in NaCl with 40µg/ml of the drug with concentrated OP50 for different time periods. We then isolated the animals with Trizol to collect RNA.

Laser Axotomy

PLM axons were cut on anesthetized L4 larvae worms on the near-infrared Ti-Sapphire laser (KMLabs) as previously described (Wu et al.). Worms were placed in 1% 1-phenoxy-2-propanol dissolved in M9, recovered in M9 solution after axotomy and analyzed 24 hours after axotomy for regrowth length.

Statistical Analysis

We used one-way ANOVA with the Tukey test for multiple comparisons and unpaired t-tests in our statistical analysis on the PRISM software.

Table 2.2: List of Plasmid Constructs with pCZGY number and description.

pCZGY	Construct
1083	Prgef-1 ::GFP-PEST ::3'utr(cebp-1)
	Prgef-1 ::GFP-PEST ::3'utr(unc-54)
1082	PCR8 ::GFP-PEST ::3'utr(cebp-1)
2321	PCR8 ::GFP-PEST ::3'utr(cebp-1 with 40-336bp deleted)
2322	PCR8 ::GFP-PEST ::3'utr(cebp-1 with 339-439bp deleted)
2323	PCR8 ::GFP-PEST ::3'utr(cebp-1 with 440-537bp deleted)
2324	PCR8 ::GFP-PEST ::3'utr(cebp-1 with 75-112bp deleted)
2325	PCR8 ::GFP-PEST ::3'utr(cebp-1 with 95-128bp deleted)
2326	PCR8 ::GFP-PEST ::3'utr(cebp-1 with 75-94bp deleted)
2327	PCR8 ::GFP-PEST ::3'utr(cebp-1 with 128-228bp deleted)
2328	PCR8 ::GFP-PEST ::3'utr(cebp-1 with 230-336bp deleted)
2329	PCR8 ::GFP-PEST ::3'utr(cebp-1 with 294-358bp deleted)

Table 2.2: List of Plasmid Constructs with pCZGY number and description, Continued.

pCZGY	Construct
2330	PCR8 ::GFP-PEST ::3'utr(cebp-1 with 537-600bp deleted)
2342	Prgef-1 ::GFP-PEST ::3'utr(cebp-1 with 40-336bp deleted)
2343	Prgef-1 ::GFP-PEST ::3'utr(cebp-1 with 339-438bp deleted)
2344	Prgef-1 ::GFP-PEST ::3'utr(cebp-1 with 440-537bp deleted)
2345	Prgef-1 ::GFP-PEST ::3'utr(cebp-1 with 75-112bp deleted)
2346	Prgef-1 ::GFP-PEST ::3'utr(cebp-1 with 95-128bp deleted)
2347	Prgef-1 ::GFP-PEST ::3'utr(cebp-1 with 75-94bp deleted)
2348	Prgef-1 ::GFP-PEST ::3'utr(cebp-1 with 128-228bp deleted)
2349	Prgef-1 ::GFP-PEST ::3'utr(cebp-1 with 230-336bp deleted)
2350	Prgef-1 ::GFP :-PEST ::3'utr(cebp-1 with 294-358bp deleted)
2351	Prgef-1 ::GFP-PEST ::3'utr(cebp-1 with 537-600bp deleted)
1706	pDONRP4P1 Prgef-1
555	PCR8::GFP(synthetic introns)
2489	pDONRP2P3 3'utr(cebp-1)
	pDONRP2P3 3'utr(unc-54)
2490	pDONRP2P3 3'utr(cebp-1 with 79-98bp deleted)
2491	pDONRP2P3 3'utr(cebp-1 with 75-128bp deleted)
2492	pDONRP2P3 3'utr(cebp-1 with 230-358bp deleted)
2493	pDONRP2P3 3'utr(cebp-1 with 439-536bp deleted)
2494	Prgef-1::GFP::3'utr(cebp-1) MosSci
	Prgef-1::GFP::3'utr(unc-54) MosSci
2495	Prgef-1::GFP::3'utr(cebp-1 with 79-98bp deleted) MosSci
2496	Prgef-1::GFP::3'utr(cebp-1 with 75-128bp deleted) MosSci

Table 2.2: List of Plasmid Constructs with pCZGY number and description, Continued.

pCZGY	Construct
2497	Prgef-1::GFP::3'utr(cebp-1 with 230-358bp deleted) MosSci
2498	Prgef-1::GFP::3'utr(cebp-1 with 439-536bp deleted) MosSci
2524	Prgef-1 ::CEBP-1 ::GFP ::3'utr(cebp-1) MosSci
2525	Prgef-1 ::CEBP-1 ::GFP ::3'utr(unc-54) MosSci
2695	Prgef-1 ::CEBP-1 ::GFP ::3'utr(del 388-418bp cebp-1) MosSci
2696	Prgef-1 ::CEBP-1 ::GFP ::3'utr(del 439-536bp cebp-1) MosSci
762	PCR8::dendra2-3'utr(cebp-1)
766	Pmec-4::dendra2-3'utr(cebp-1)
761	PCR8::dendra-2
765	Pmec-4::dendra2-3'utr(unc-54)
2697	Pmec-4 ::dendra2-3'utr(cebp-1 388-418bp deletion)

Table 2.3: Primers and sequences used in qRT-PCRs

Gene	YJ#	Sequence
cebp-1	8984	R: TCCTTCGCAAGACAAGACTCTCTTA
	10370	L: CGTCAAGATCGTGGAGCAC
cebp-1	10371	R: GCACGACAAGATGAAGAGG
	8983	L: CATCGGGCCTTTATTCCTGAG
GFP	10372	R: CTGTTCCATGGCCAACACTT
	10373	L: ACTTCAGCACGTGTCTTGTAG
rps-25	10368	R: CTCTACAAGGAGGTCATCACC
	10369	L: GACCTGTCCGTGATGATGAACG

Chapter 2 is based off a paper in preparation. Sharifnia P, Kim K, Wu Z, and Jin Y**.** *Cis* elements mediating regulation of *cebp-1* mRNA stability and translation. The dissertation author was the primary investigator and author of the paper.

CHAPTER 3 –INTRODUCTION TO *TRANS* FACTORS REGULATING *CEBP-1* MRNA

cebp-1 appears to be tightly regulated based on the *cis* element analysis – multiple elements control its expression and suggests it is possible to have several *trans* factors contributing to this regulation. *cebp-1* is expressed in tissues outside of the nervous system (data not shown), such as the epidermis, and hints proteins other than *rpm-1* and *dlk-1*, which are exclusively expressed in the nervous system, can regulate *cebp-1* levels. In this chapter we will detail experiments dissecting the role of two *trans* factors we believe to be involved in modulating *cebp-1* expression: *tiar-2* and *nipi-3*.

CHAPTER 3.1 – INTRODUCTION TO TIA-1/TIAR FAMILY REGULATING *CEBP-1* MRNA

Given the importance of *cebp-1* mRNA and its 3'UTR, we hypothesized certain RNA binding proteins interacted with *cebp-1* through the 3'UTR. RNA binding proteins, as discussed before in Chapter 1 of this dissertation, can regulate mRNA through various pathways. Through screening of selective number of RBPs, we identified *tiar-2*, an RNA binding protein that is homologous to the TIA-1 and TIAR proteins in mammals (Figure 3.1). This family has 3 RNA recognition motifs (RRMs) followed by a prion rich domain that is indicative of the TIA-1/TIAR family of proteins (Figure 3.2). Among the three homologs in *C.*

elegans, consisting of *tiar-1, tiar-2,* and *tiar-3*, *tiar-2* shows the most similarity out of the three genes (Figure 3.1).

The TIA-1/TIAR acronym stands for T-cell internal antigen/T-cell internal antigen related. They were first identified in cytotoxic lymphocytes (109, 110) and found to be involved in post-transcriptional gene regulation. They primarily bind AU-rich elements, but can interact other element as well, and regulate mRNA through translational repression and/or mRNA splicing (111-113). However, roles for these proteins have not been described in the nervous system. In this Chapter, I will describe our studies in elucidating *tiar-2*'s regulation of *cebp-1* in the nervous system.

CHAPTER 3.2 – *TIAR-2* ALLELE *TM2923* IS A LOSS OF FUNCITON ALLELE

The *tiar-2* gene spans 5.1 kb and is predicted to have seven exons. We performed reverse transcriptase on cDNA from wild type animals and confirmed the gene structure. The full length TIAR-2 protein is composed of 434 amino acids. The available *tiar-2(tm2923)* allele is a deletion of 334 nucleotides from exon 1 to 3, which would predict to cause a frame-shift and an early stop codon that terminates the protein at 34 amino acids. We examined if this allele was a null mutation of *tiar-2* by cloning cDNA of *tiar-2* in this mutant background. However, there are two possible additional start sites in *tiar-2*. When we amplified transpliced cDNA from the *tm2923* mutant with a SL1 primer that recognizes the beginning of the mRNA and another primer at the end of *tiar-2* we found one major transcript that was about 2kb, which is smaller than the full-

length transcript in wild type (Figure 3.3). Sequencing revealed that this fragment in *tm2923* starts in exon 4 and continues until the end of exon 7 (Figure 3.3). This transcript includes the second and third RRM domains but lacks almost all the first RRM domain. For simplicity, we called this transcript *tiar-2* short (*tiar-2S)*. Next we did qRT-PCR to measure the levels of *tiar-2* in *tiar-2(tm292)* and found very low levels of *tiar-2* transcript compared to wild type control (Figure 3.3). From our analysis we found a lower amount of transcript from the first start site of *tiar-2* in the *tm2923* background compared to wildtype using primers that flanked the deletion site (data not shown). This result suggests that this full length transcript in *tm2923* strain is rapidly degraded or inefficiently transcribed. Overall, this analysis suggests strongly that *tiar-2(tm2923)* is a loss of function allele(Figure 3.3)

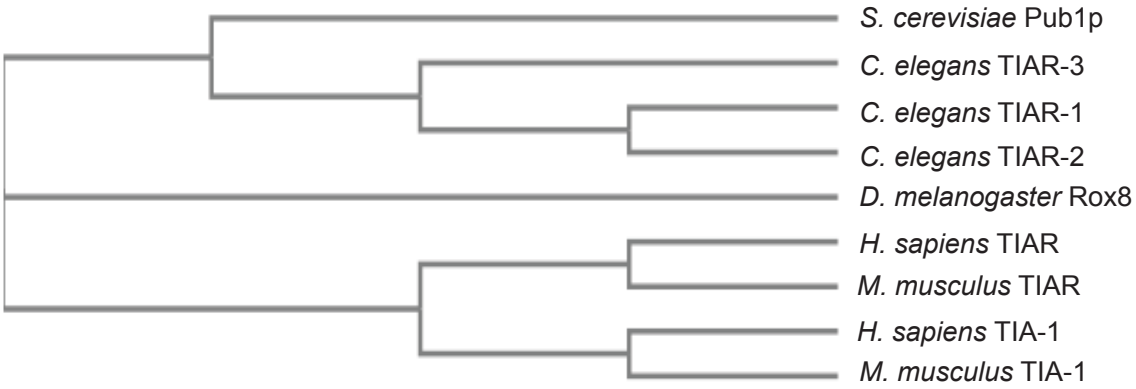


Figure 3.1: Protein cladogram with homolgous proteins in different species for TIAR family (adapted from Clustal W2).

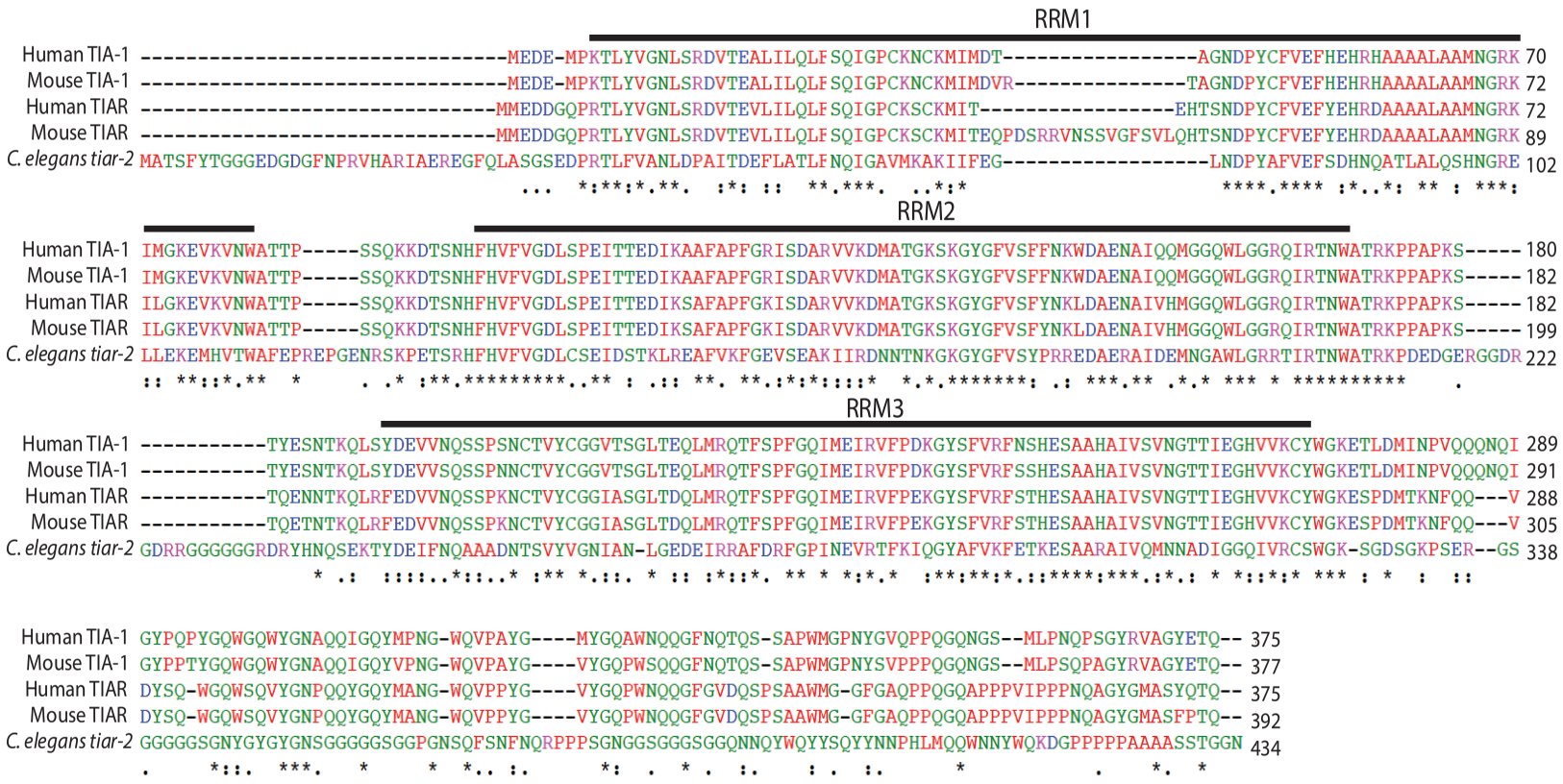


Figure 3.2: Protein alignnment with Human and Mouse TIA-2/TIAR (adapted from ClustalW2).

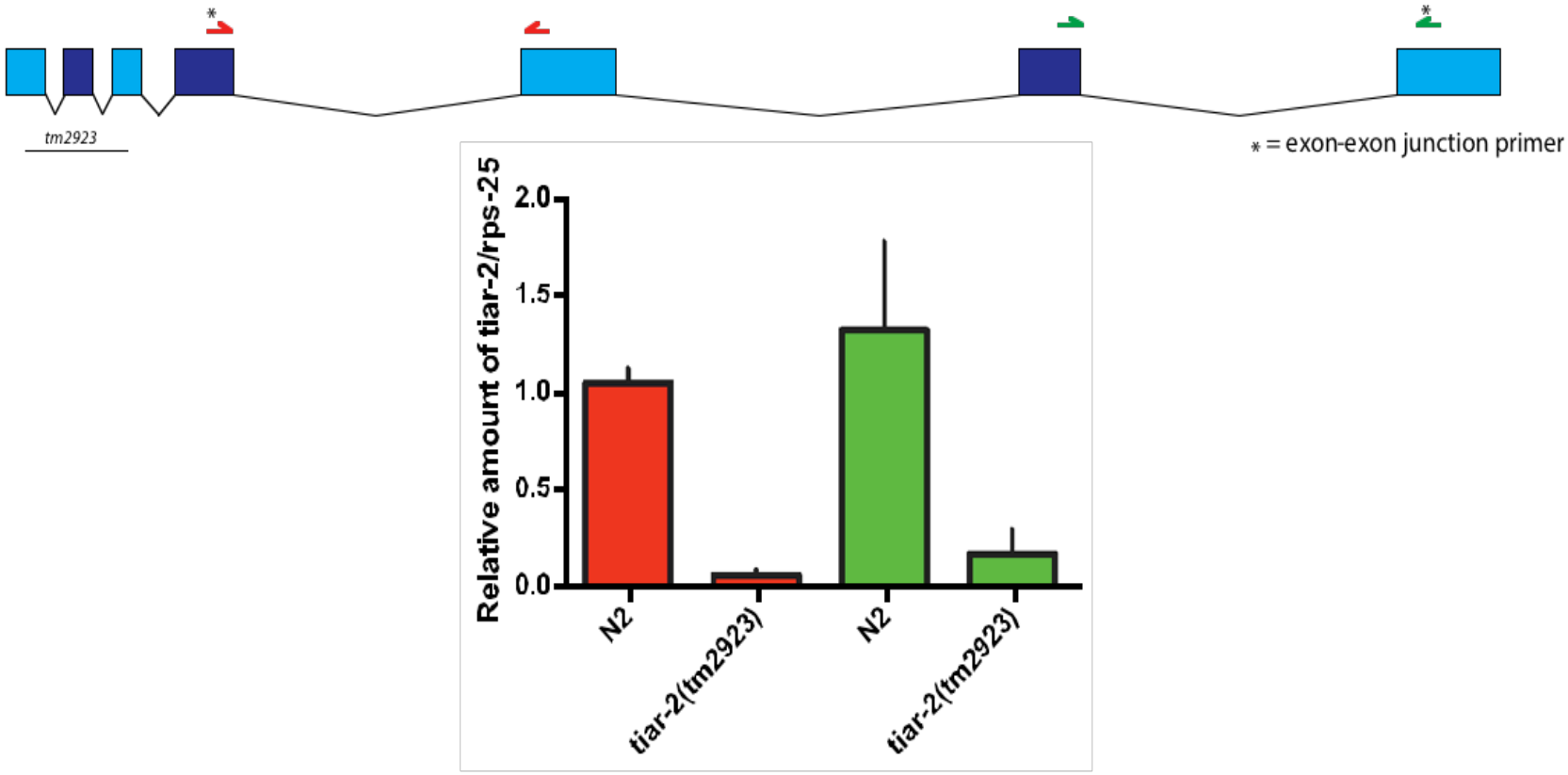


Figure 3.3: *tiar-2(tm2923)* is a probable loss of function allele. Gene structure shown with qRT-PCR primers location. qRT-PCR for *tiar-2* suggests low levels of transcript in *tm2923* mutant background. Location of primers is shown on diagram of gene structure with color coding to indicate which qRT-PCR result corresponds to which

CHAPTER 3.3 – THE RRM PROTEIN TIAR-2 REGULATES *CEBP-1* MRNA VIA 3'UTR

Next, we asked if *tiar-2* could regulate *cebp-1* mRNA by examining the levels of *cebp-1* mRNA in *tiar-2(tm2923)*. Using two primers for *cebp-1*, we found increased *cebp-1* mRNA in *tiar-2(tm2923)* (Figure 3.4), showing *tiar-2* regulates *cebp-1* mRNA.

Since *cebp-1*'s 3'UTR is important for its regulation in other pathways, we wanted to determine if *tiar-2* could regulate *cebp-1*'s 3'UTR, specifically in single neuron. With a reporter for *cebp-1*'s 3'UTR expressed in the posterior lateral microtubule (PLM) neuron, there was an upregulation of signal in the *tiar-2(tm2923)* mutant (Figure 3.5A,B). As a negative control for the fluorescent reporter, we used a similar reporter tagged with the *unc-54* 3'UTR. *tiar-2(tm2923)* did not showed a statistically significant increase of the unc-54 3'UTR reporter, suggesting that *tiar-2* specifically regulates *cebp-1*'s 3'UTR in the PLM (Figure 3.5C). Finally, we show that this up-regulation is rescued by *tiar-2* expression in touch neurons (Figure 3.5C), showing that *tiar-2* acts cell autonomously to regulate *cebp-1*'s 3'UTR.

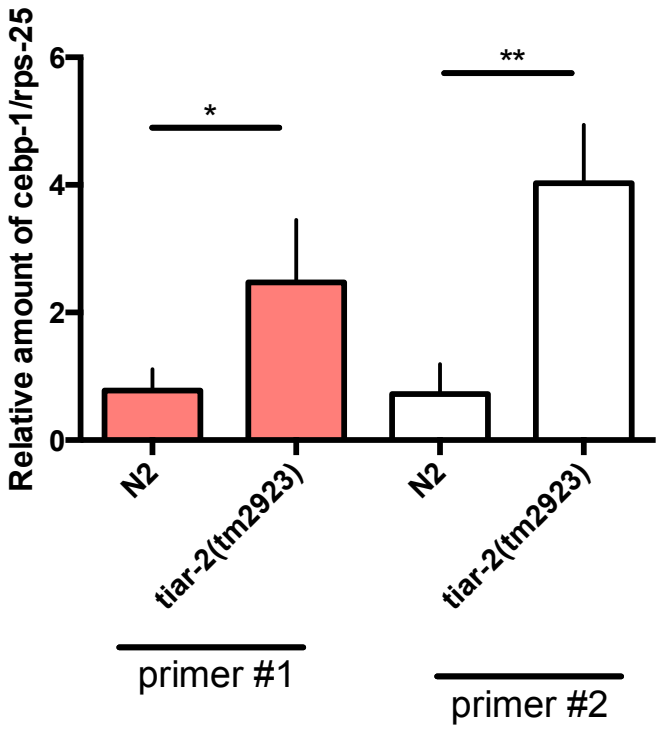


Figure 3.4: *cebp-1* mRNA is upregulated in *tiar-2(tm2923)* mutant using two different primer sets for *cebp-1*. qRT-PCR data is normalized to *rps-25*. Statistical test used is unpaired t test for both sets of data.

Since *tiar-2* is a RNA binding protein, we were interested in the *cis* elements it interacts with *cebp-1*'s 3'UTR. Importantly, we tested if *tiar-2* acts through the stem-loop structure of cebp-1's 3'UTR that was discussed in Chapter 2. We examined *tiar-2(lf)*'s affect on the high copy 388-418bp deleted stem-loop report in the mechanosensory neurons (Figure 3.7A). There was no significant difference in the fluorescence in the PLM between wild type and *tiar-2(tm2923)* suggesting that *tiar-2* acts through this stem-loop structure in the PLM (Figure 3.7B).

We also examined the single-copy reporters of *cebp-1* 3'UTR in the *tiar-2(tm2923)* background. These analyses were in the nerve ring, examining a different neuronal subset than the mechanosensory neurons. The cebp-1 3'UTR reporter shows an increase in *tiar-2(tm2923)* confirming our previous results that *tiar-2* regulates *cebp-1*'s 3'UTR in the nervous system (Figure 3.8). Interestingly, *tiar-2* acts similarly to *rpm-1* as the reporter with the deletion of 339-438bp fails to increase in either the *tiar-2(tm2923)* or *rpm-1(lf)* background (Figure 2. 10A, 3.8). This result indicates that these two regulating factors may regulate *cebp-1* 's 3'UTR in the same *cis* elements.

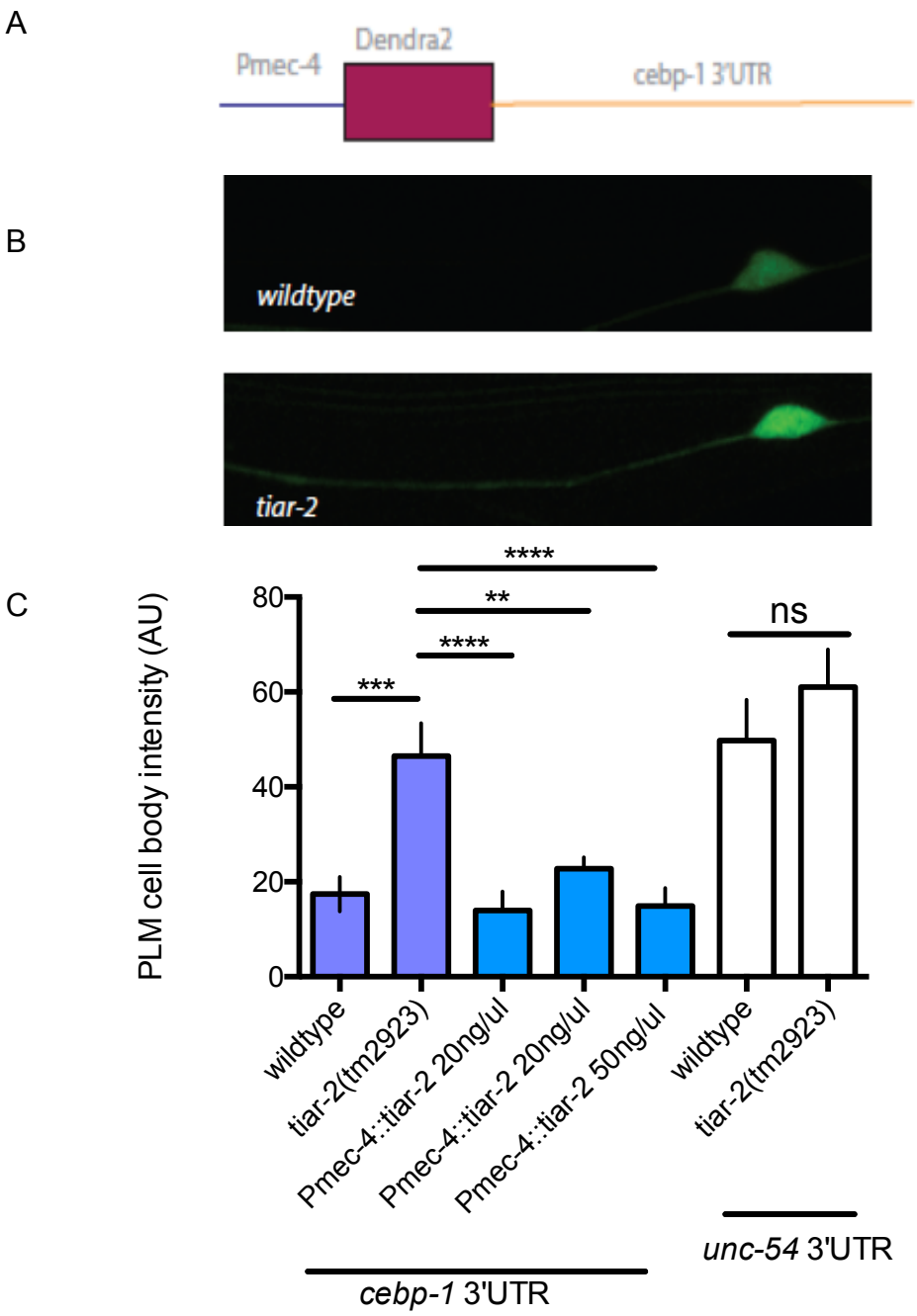


Figure 3.5: *tiar-2* regulates *cebp-1* through its 3'UTR A) Diagram of 3'UTR reporter in mechanosensory neurons B) Z-stack images of reporter in wild type and *tiar-2(tm2923)* in one-day young adult animals using the same conditions C) quantification of fluorescent signal in PLM cell body in different mutant backgrounds. Statistical test for reporter with *cebp-1* 3'UTR is one-way ANOVA with Tukey's test for multiple comparisons. For the reporter with *unc-54* 3'UTR, a unpaired t-test was the statistical test used

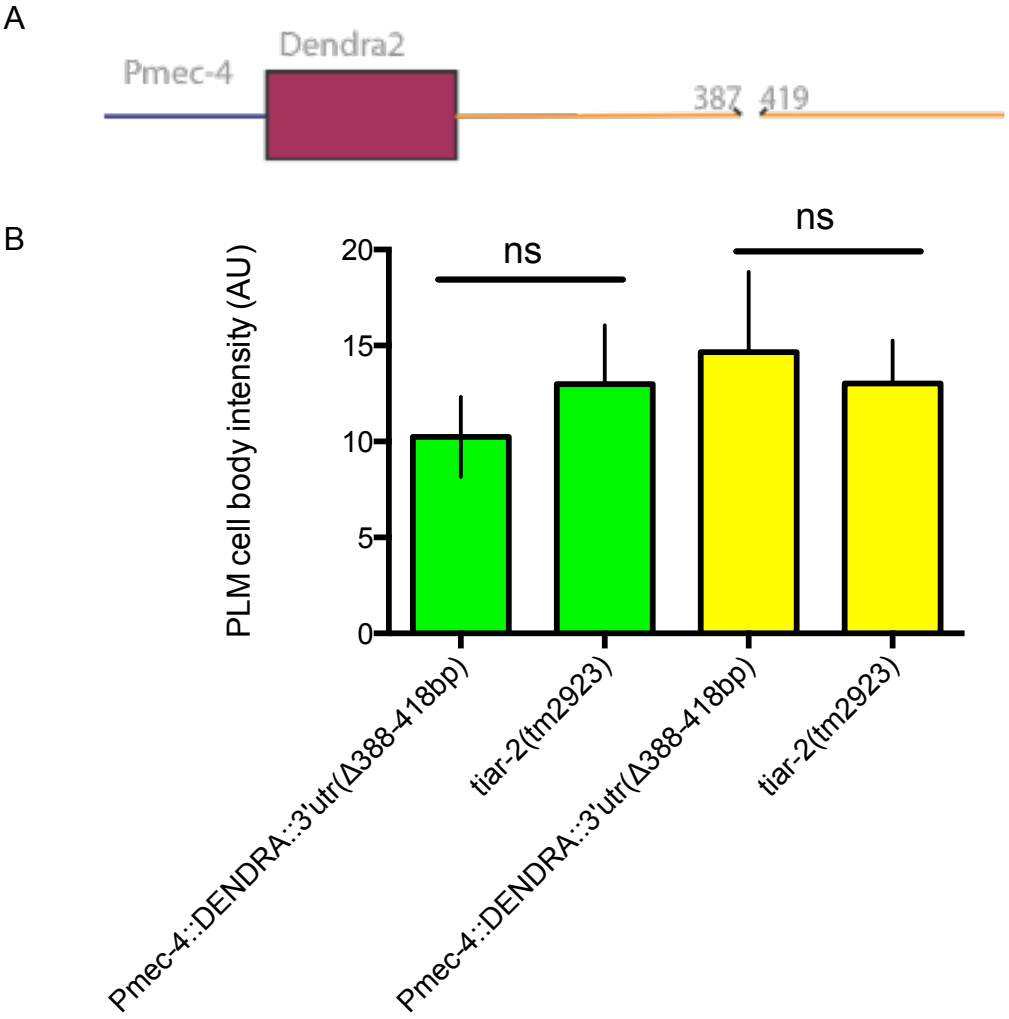


Figure 3.6: *tiar-2* may interact with *cebp-1* mRNA through stem-loop structure A) diagram of stem-loop deleted reporter in mechanosensory neurons B) quantification of GFP in PLM cell body in wild type and *tiar-2(tm2923)* background. Statistical test used is unpaired t-test.

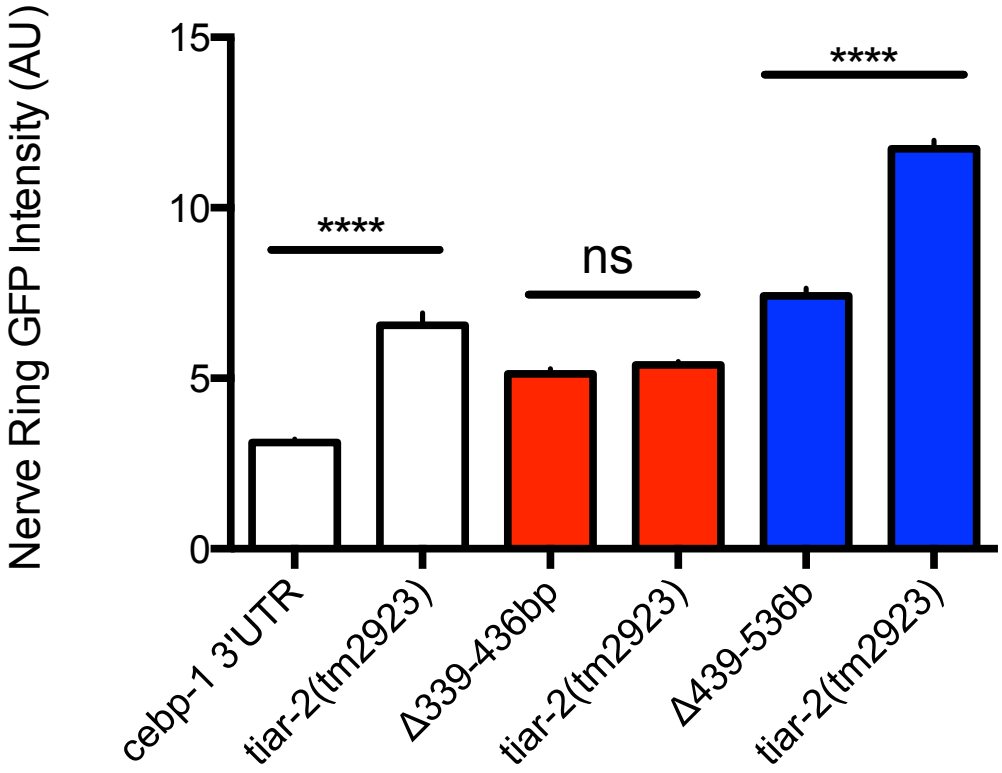


Figure 3.7: *tiar-2(tm2923)* regulates *cebp-1* 3'UTR *cis* elements 339-438bp in nerve ring. *tiar-2(tm2923)* shows increase of the *cebp-1* 3'UTR reporter and 439-536bp deletion, but does not show a difference with the 230-358bp reporter compared to wild type. The colors indicate the different reporters in different mutant backgrounds. For example, the full 3'UTR reporter in wild type and different backgrounds is in white. Statistical test used is the unpaired t-test.

CHAPTER 3.4 – *TIAR-2* IS EXPRESSED IN CYTOPLASM AND INHIBITS REGENERATION IN THE PLM

To address how TIAR-2 functions, we next examined its expression by constructing a transcriptional reporter consisting of *tiar-2*'s promoter tagged to GFP and a minigene reporter (Figure 3.9). The promoter consisted of 524bp upstream of the start site of the first exon. This transcriptional reporter showed very low expression that occasionally was detected in a pair of neurons in the head and sheath cells (Figure 3.10A). The minigene reporter consists of *tiar*-2's promoter with genomic DNA from exon one to four, cDNA for exon 5 and 6, followed by genomic DNA from the intron after exon 6 to the end of exon 7. In contrast to the transcriptional reporter, this reporter showed expression in a variety of tissues, including neurons and the intestine (Figure 3.10B). Neurons in the head and the tail were labeled and showed cytosolic expression (Figure 3.10B). This increased expression from the minigene reporter suggests elements within *tiar-2* coding sequence are critical for its expression.

Previous work has shown that *cebp-1* is required for regeneration(94). Here we find that *tiar-2* represses *cebp-1* reporter expression in touch neurons. We next examined if *tiar-2* affected axon regeneration in the PLM neuron and found that the *tiar-2(tm2923)* enhanced regeneration(Figure 3.11A,B). Expressing *tiar-2* cDNA in the mechanosensory neurons was able to rescue this phenotype, showing *tiar-2* inhibits regeneration cell autonomously (Figure 3.11B). The other two TIA-1/TIAR homologs, *tiar-1* and *tiar-3*, did not differ from

wild type, indicating this repression of regeneration was specific to *tiar-2* (data not shown).

We examined if the enhanced regeneration in the *tiar-2* mutant depended on *cebp-1* by testing the double mutant of *tiar-2(lf); cebp-1(lf)* and found that *cebp-1(lf)* suppressed the increased regeneration (Figure 3.11B).

tiar-2 is localized cytosolically in the mechanosensory neurons (Figure 3.12), suggesting it would be able to respond quickly to stimuli such as nerve injury. We examined if this localization changes after axotomy by tagging *tiar-2* with GFP in the mechanosensory neurons and imaging these neurons at certain time points after axotomy (Figure 3.13A,B). Preliminary data showed that before injury, few TIAR-2 labeled puncta were present in the axon (Figure 3.13A). We found increased green puncta in the proximal axon 1 hour after axotomy as well as faint green puncta along the length of axon (Figure 3.13B), suggesting *tiar-2* responds to the injury signal and is involved in the downstream signaling pathways in response to stress.

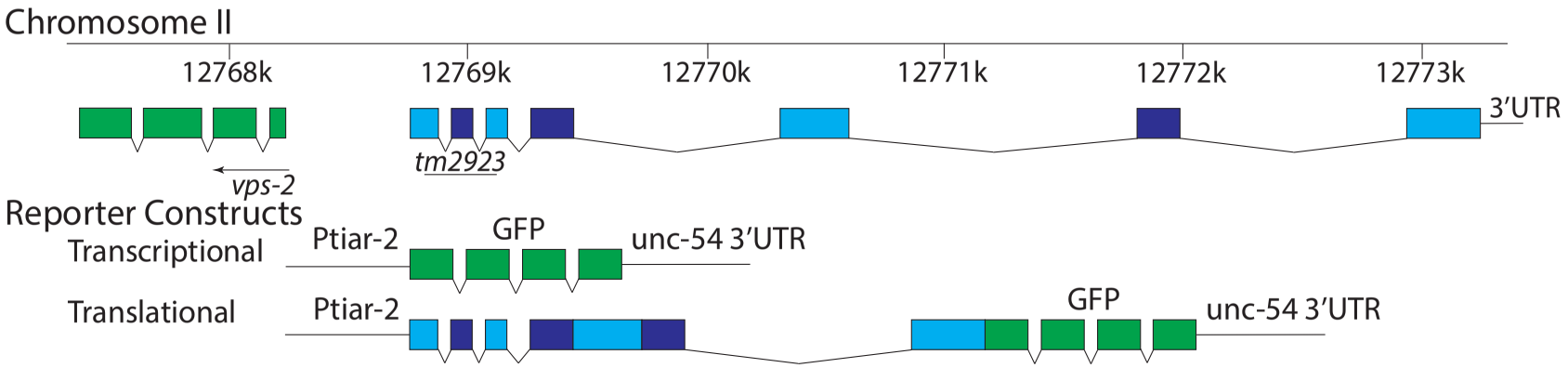


Figure 3.8: Genetic locus and transcriptional and translational construct reporters for *tiar-2*. Exons for *tiar-2* are in alternating blue and purple colors. Deletion of *tm2923* is illustrated.

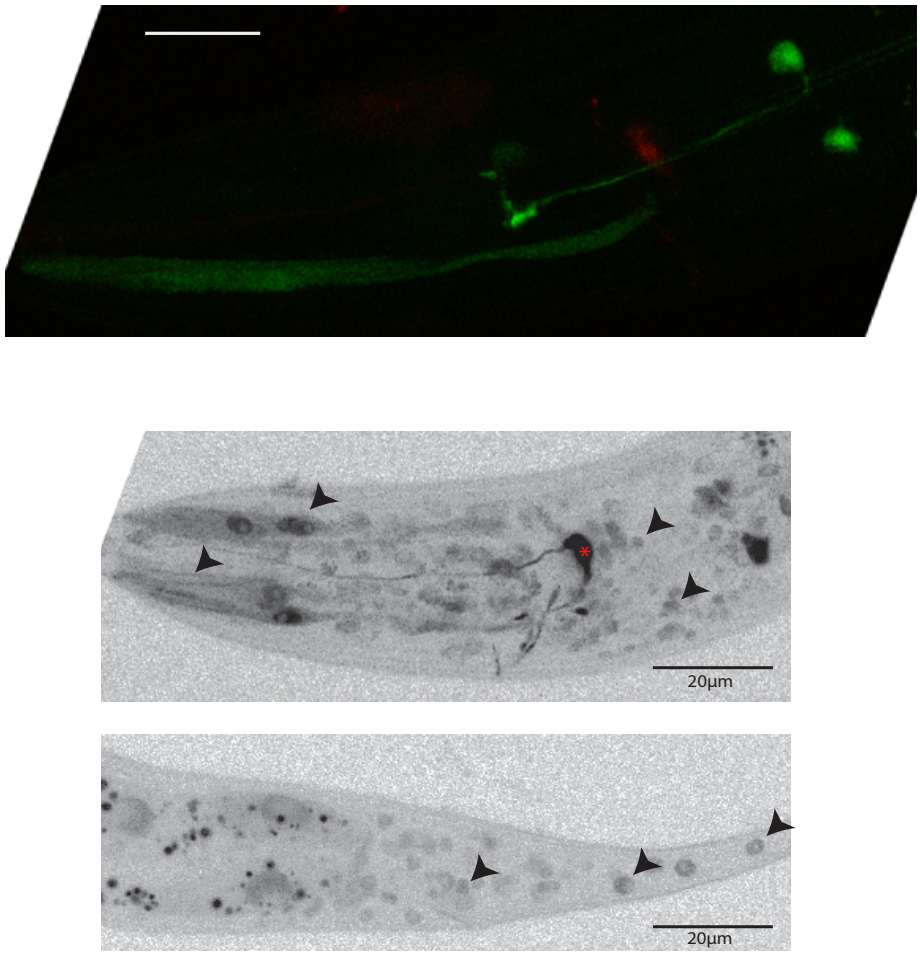


Figure 3.9: *tiar-2* is expressed cytosolically in different tissues A) sample image of transcriptional reporter in head of L4 stage animal. B) Z-stack images of translational reporter in head and tail of L4 stage animal. Arrowheads denote GFP signal in cells in the head and tail of animal. Scale bars represent 20µm.

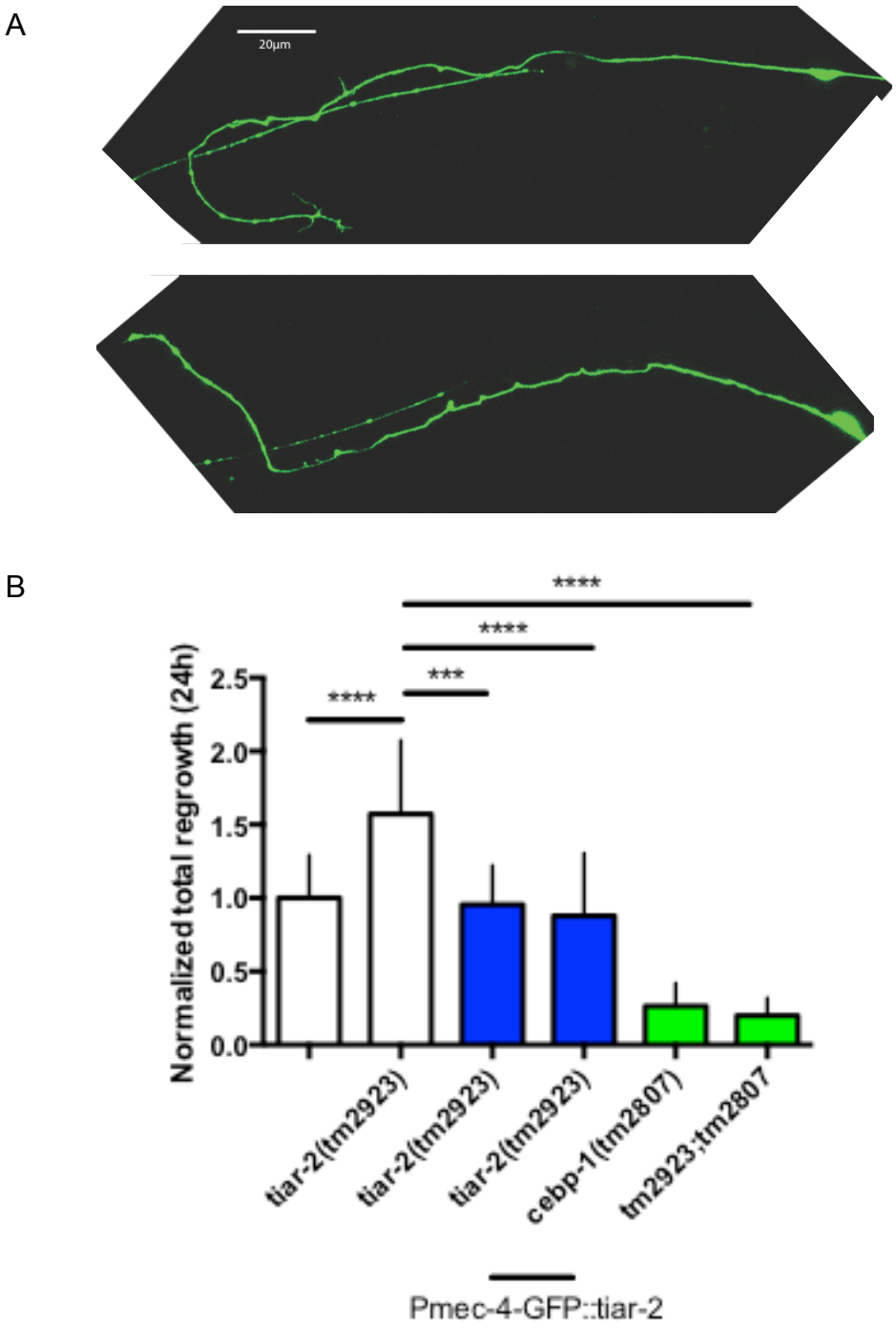


Figure 3.10: *tiar-2(tm2923)* enhances PLM regeneration A)sample images of regenerating axons of *tiar-2(tm2923)* 24hours after axotomy B) quantification of normalized regrowth in different mutant backgrounds. *tiar-2(tm2923)* phenotype is rescued by *tiar-2* cDNA expressed in mechanosensory neurons as well as suppressed by *cebp-1(lf)*. One way ANOVA was used for statistical analysis.

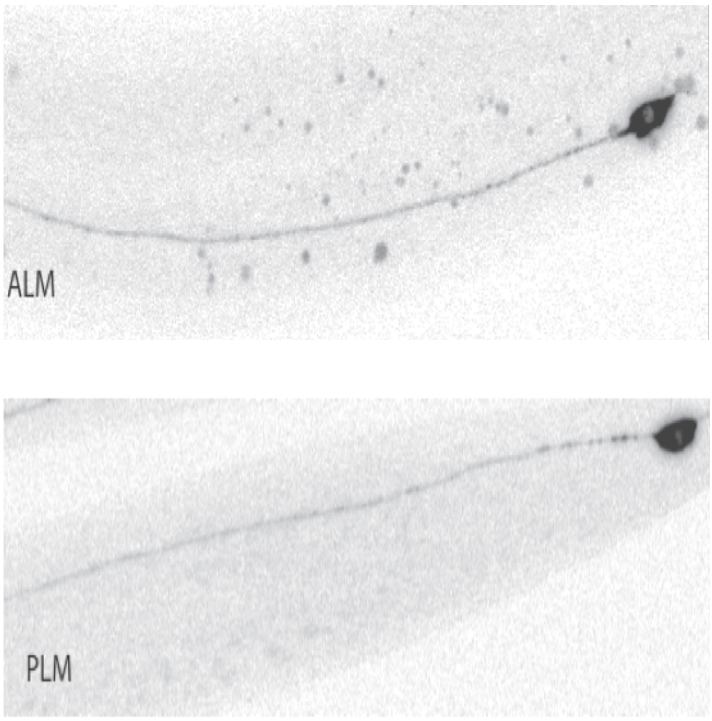
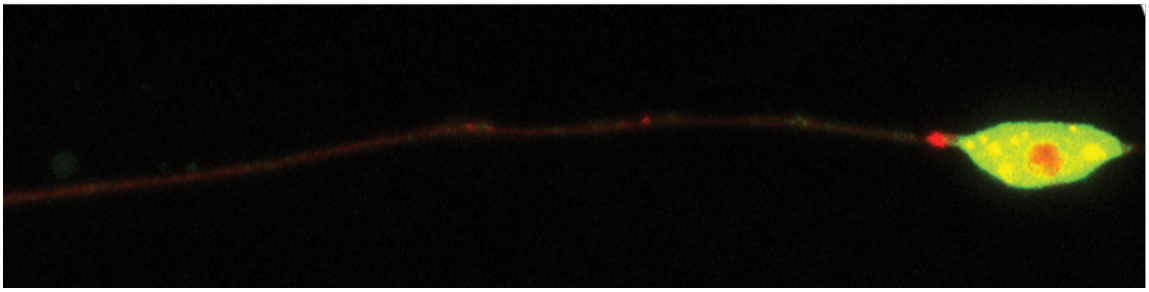


Figure 3.11: *tiar-2* is expressed cytosolically in the ALM and PLM. L4 animals are expressing a Pmec-4::tiar-2(cDNA)-GFP construct.

A



B

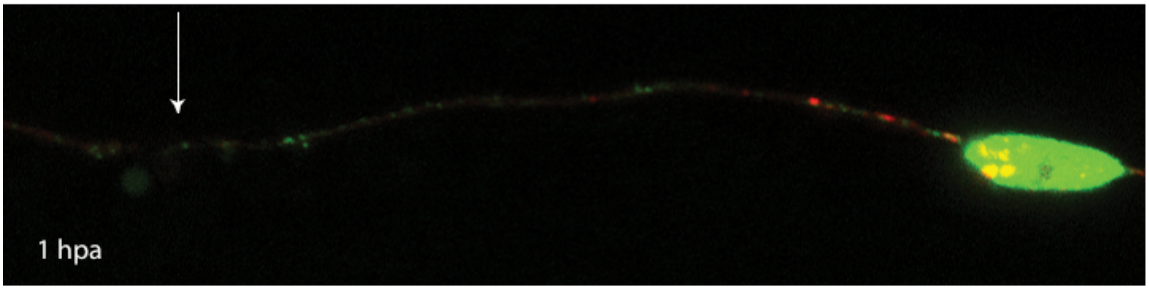


Figure 3.12: *tiar-2* changes localization after injury A) images of *tiar-2* localization in mechanosensory neurons before injury B) *tiar-2* localization 1 hour post axotomy. Arrow denotes cut site. Pmec-4::mcherry labels the mechanosensory neurons and TIAR-2 is labled with GFP.

CHAPTER 3.5 – TIAR-2 ROLE IN SYNAPTIC DEVELOPMENT

Genes involved in regulating *cebp-1* have previously been found to affect synaptic development (60, 94). We examined if *tiar-2* affected synaptic formation in the motor neurons by using a reporter labeling the presynaptic protein synaptobrevin-1. Compared to wild type, *tiar-2(tm2923)* has a mild decrease in number of synapses along the dorsal nerve cord (Figure 3.14A,B). The synapses also appeared to be smaller in size, as well as dimmer in fluorescence compared to the control strain (Figure 3.14A).

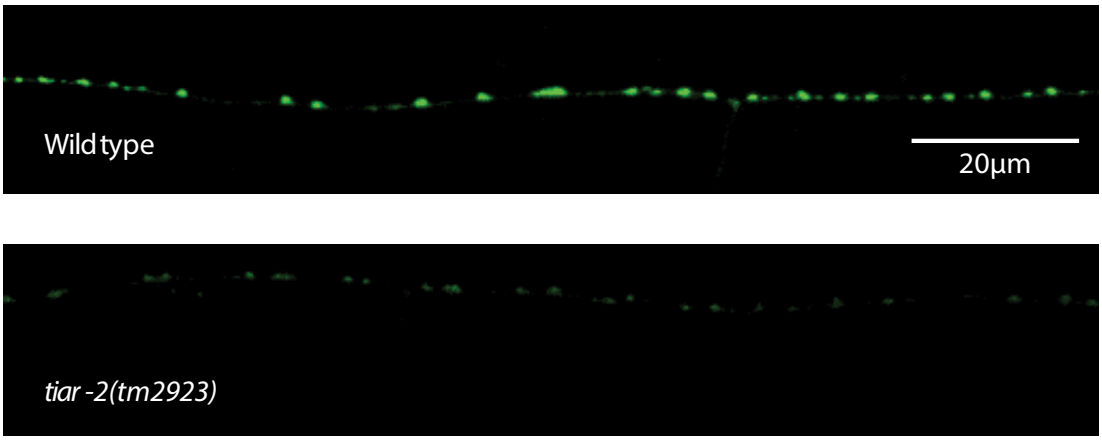
In addition to the motor neurons, *cebp-1* is known to regulate the development of the mechanosensory neurons. In wild type, the PLM extends a process anteriority from the cell body that terminates before the ALM and has a synaptic branch to the ventral nerve cord. In *rpm-1(lf)*, the PLM displays an abnormal trajectory and is missing the synaptic branch. *cebp-1* was found to suppress these phenotypes (94). We examined if *tiar-2(tm2923)* had a developmental phenotype in these neurons. *tiar-2*, by itself, does not show an *rpm-1(lf)*-like phenotype for mechanosensory development (Figure 3.16) . However, the posterior process of the PLM is overextended in the *tiar-2(tm2923)* background, compared to wild type (Figure 3.17A). Additionally we looked at the *tiar-2(lf)*; *rpm-1(lf)* double mutant and found a complex relationship. While it appeared that the *tiar-2* enhanced *rpm-1*'s overextension defects of the PLM, the double mutant also partially suppressed the loss of the synaptic branch to the ventral nerve cord (Figure 3.16). Furthermore, the double mutant

suppressed *tiar-2*'s posterior process extension phenotype. *cebp-1* suppressed the phenotypes of the *tiar-2(lf); rpm-1(lf)*, suggesting that *cebp-1* was the common downstream target for both genes in the PLM (Figure 3.16).

CHAPTER 3.6 – *TIAR-2* REGULATED BY *RPM-1* AND *DLK-1* PATHWAY

We had originally hypothesized an RBP would act downstream of *rpm-1* to regulate *cebp-1*. To examine if *rpm-1* could regulate *tiar-2* transcriptionally we ran qRT-PCR for *tiar-2* in *rpm-1(lf)* samples and found very low levels of *tiar-2* in *rpm-1(lf)* using two different primer sets, suggesting *rpm-1* functions upstream of *tiar-2* (Figure 3.14). Taken together, these data suggest *rpm-1* can regulate *tiar-2* expression.

We examined if *dlk-1(lf)* also affected *tiar-2*'s regulation of *cebp-1* in the mechanosensory neurons. The *rpm-1(lf); dlk-1(lf)* suppressed the increase in fluorescence in the PLM, similar to previous studies showing *dlk-1* acts downstream of *rpm-1*. In the *tiar-2(lf)*; *dlk-1(lf)*, the PLM fluorescence was also decreased (Figure 3.5C), suggesting that *tiar-2* acts through the DLK-1 pathway to regulate *cebp-1*.



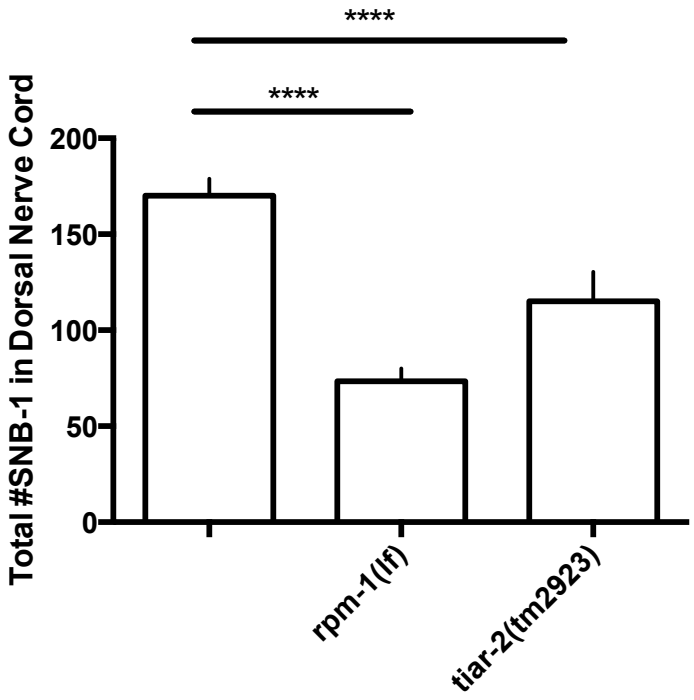


Figure 3.13: *tiar-2* affects motor neuron synaptic development A) sample images of ventral nerve cords labeled with synaptobrevin tagged GFP in wild type and *tiar-2(tm2923)* backgrounds B) quantification of synaptic puncta along dorsal nerve cord in different mutant backgrounds, showing a decrease in both *rpm-1(lf)* and *tiar-2(tm2923)* compared to control.

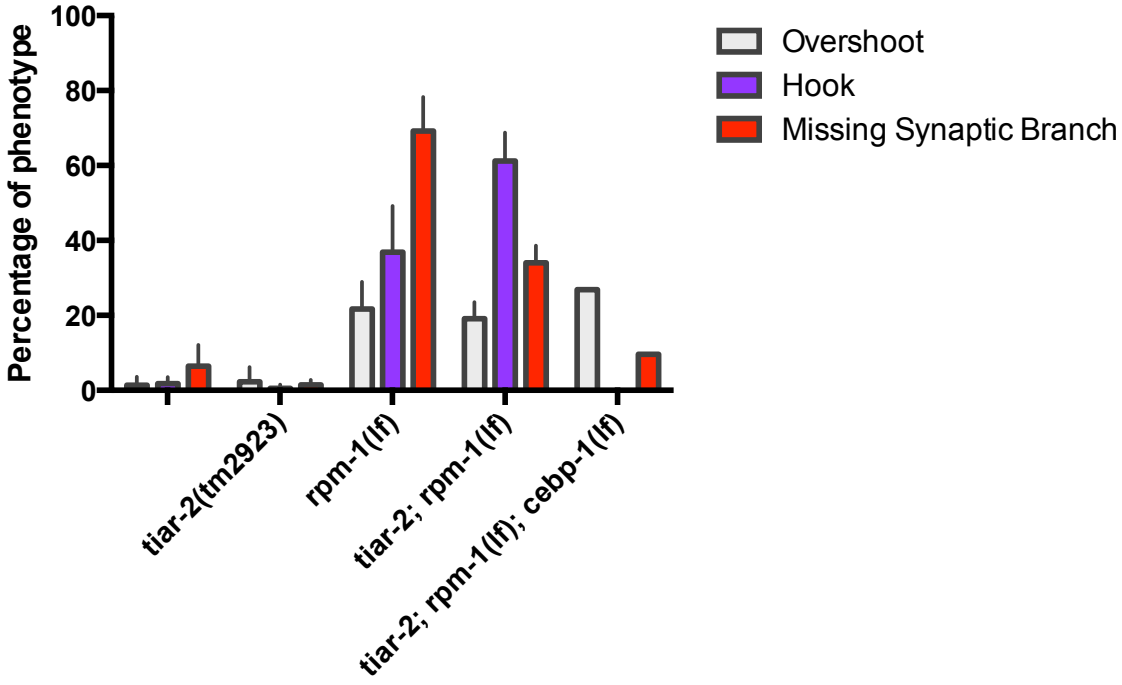
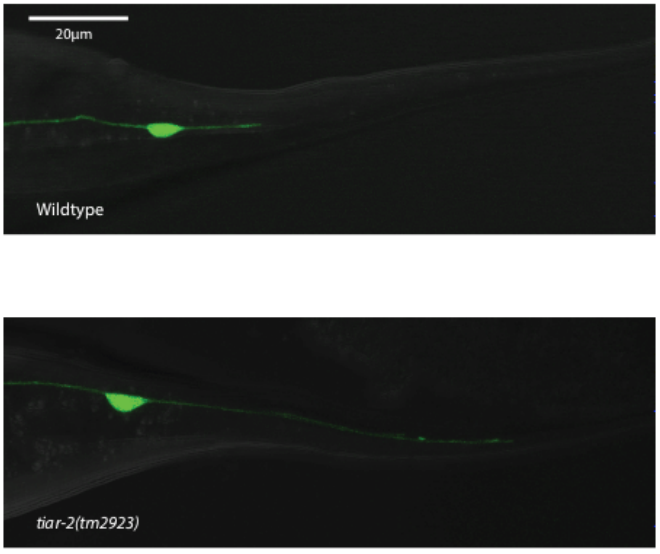


Figure 3.14: *tiar-2* does not have a *rpm-1*- like phenotype in the PLM. 3 phenotypes were scored – overshoot, hook, and absence of the PLM synaptic branch to the nerve cord. *tiar-2* appears to enhance the percentage of hooking phenotype of the PLM, but suppress the percentage of loss of synaptic branch.

A



B

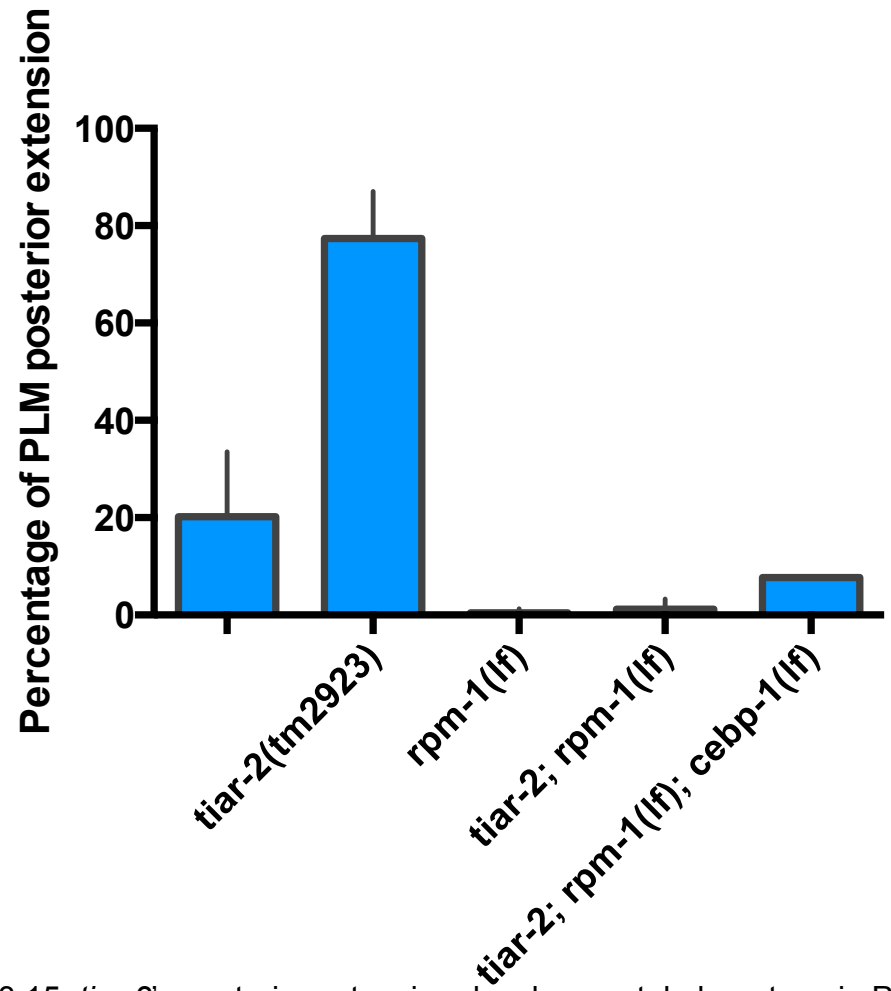


Figure 3.15: *tiar-2*'s posterior extension developmental phenotype in PLM A)sample images of wild type and *tiar-2(tm2923)* of posterior extension pheonotype B) quantification of PLM posterior extension developmental penotype among different strains.

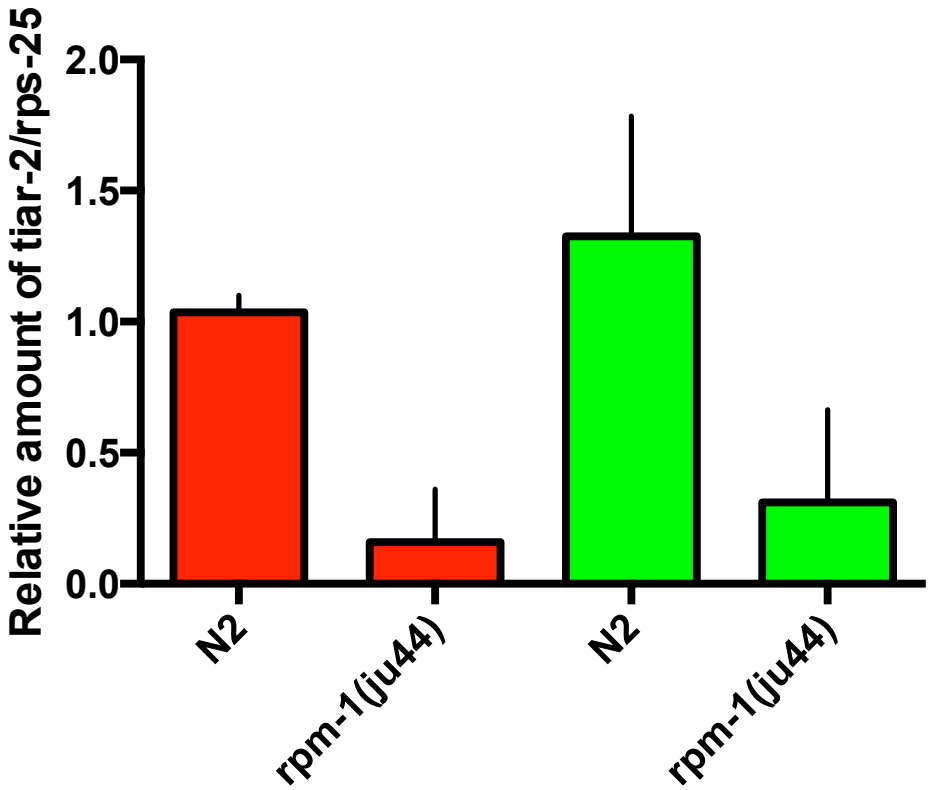


Figure 3.16: *rpm-1* positively regulates *tiar-2* transcriptionally. Using two primer sets, qRT-PCR in *rpm-1(lf)* showed decrease *tiar-2* transcripts relative to a control gene *rps-25*.

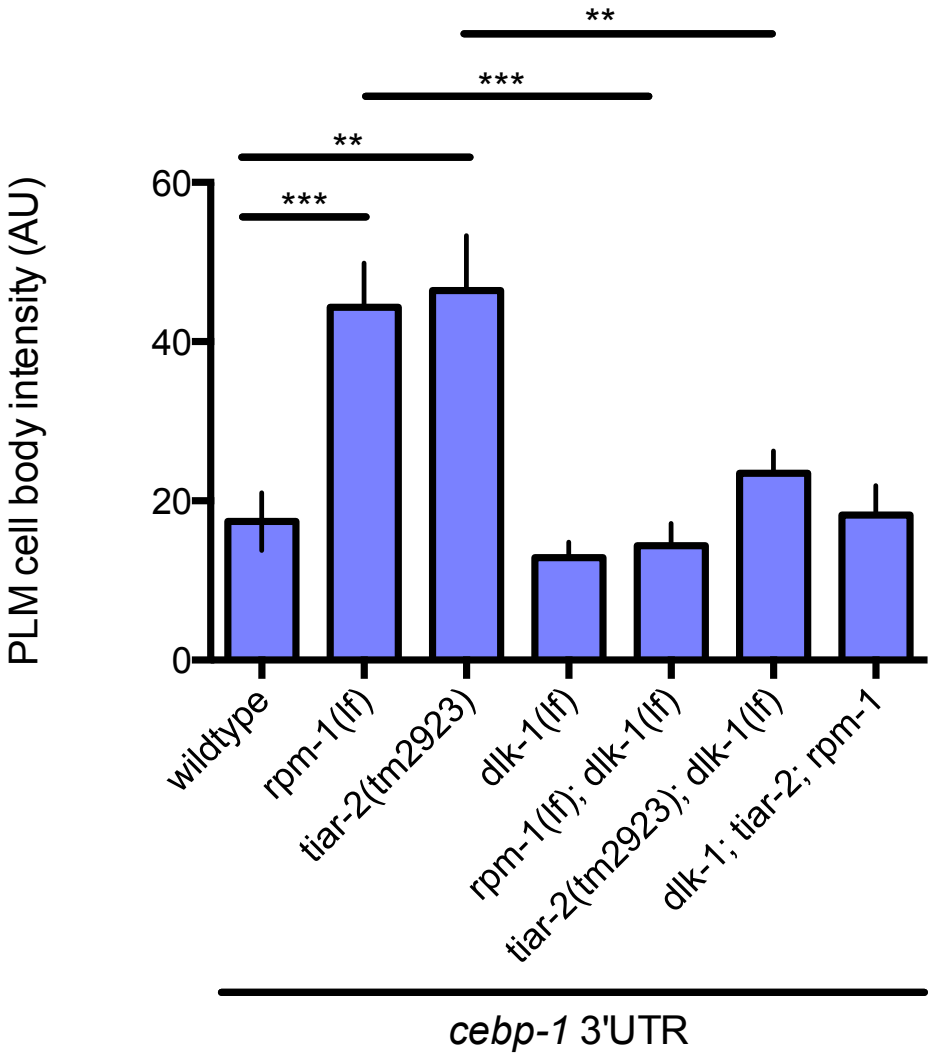


Figure 3.17: *dlk-1* acts downstream of *tiar-2*'s regulation of *cebp-1* through *cebp-1*'s 3'UTR in the PLM. Quantification of fluorescent protein reporter tagged to *cebp-1*'s 3'UTR in the PLM in different mutant backgrounds. The same data for *tiar-2* alone was shown in Figure 3.5. One way ANOVA with Tukey's test for multiple comparisons was used for statistical analysis.

CHAPTER 3.7 – *NIPI-3* REGULATES *CEBP-1*, POSSIBLY IN OTHER TISSUES

In our search for regulators of *cebp-1*, we began to analyze a gene *nipi-3*, based off the results of a collaborator. *nipi-3* is the *C. elegans* homolog of the Tribbles-like kinase found to function in innate immunity (114). Interestingly, a yeast 2 hybrid assay identified *nipi-3* as a binding partner to *cebp-1* as well as an upregulation of *cebp-1* mRNA in a *nipi-3* mutant (data not shown) Experiments in *Drosophilia* found the homolog of *nipi-3* regulated a homolog of C/EBP (115), suggesting functional conservation of this interaction.

To further examine the interaction between *nipi-3* and *cebp-1*, we conducted experiments on an available mutant *fr4* for *nipi-3*. We examined if *nipi-3(fr4)* had any neuronal phenotype during development, similar to *rpm-1*. Using a marker for a presynatpic protein we found that *nipi-3(fr4)* does not differ from wild type in motor neuron synapse formation (Figure 3.19).

Additionally, *nipi-3(fr4)* did not have a developmental phenotype in the mechanosensory neurons (Figure 3.20). *nipi-3(fr4)* also did not enhance *rpm-1*'s phenotype in the PLM (Figure 3.20), suggesting the gene did not play a role in the nervous system similar to this other regulator of *cebp-1*.

However, one important caveat is that the nature of the mutation *nipi-3(fr4)* is unknown. Whether we are studying a true loss of function allele or a different type of allele could affect our interpretation of the data and thus more experiments are required to understand if *nipi-3* plays a role in the neurons.

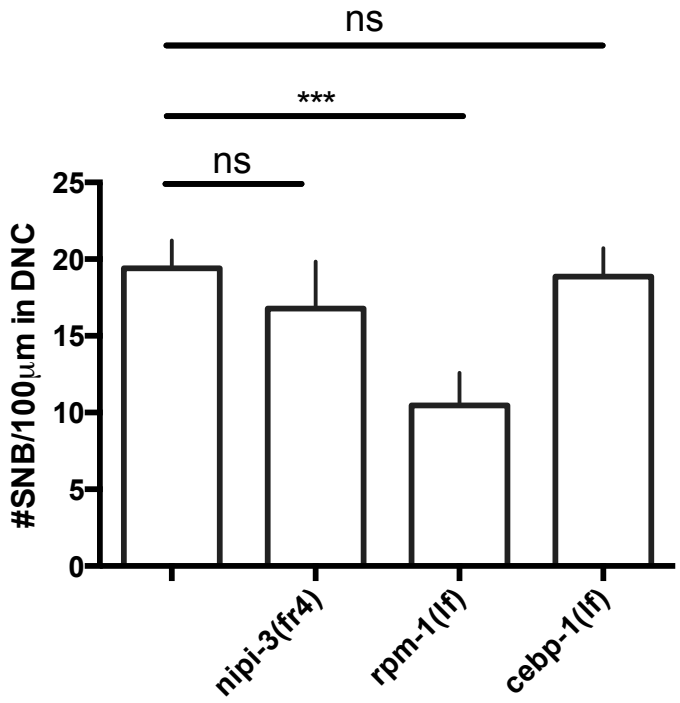


Figure 3.18: *nipi-3(fr4)* does not display a presynaptic developmental phenotype. The number of synaptic puncta in the dorsal nerve cord were counted by using *juIs1*, a fluorescent marker for synaptobrevin. Animals were analyzed as one day young adults immobilized in levamiosole under a compound scope. One way ANOVA was the statistical test used.

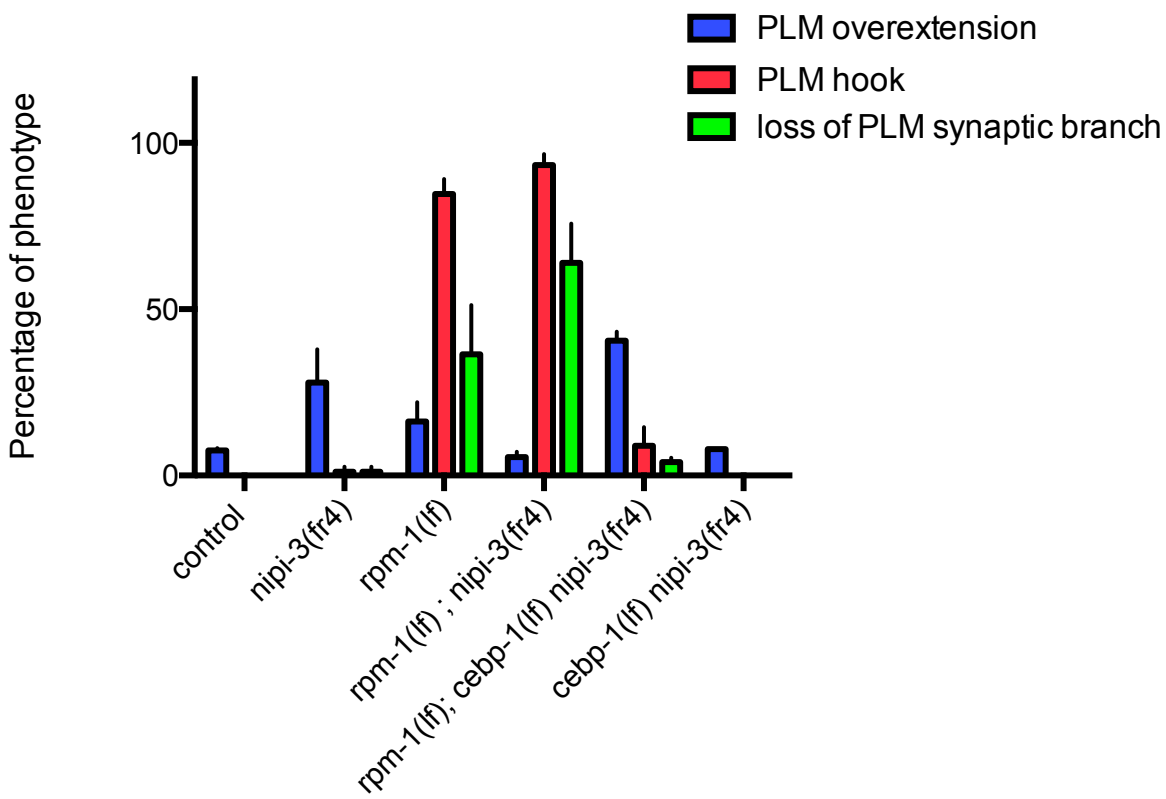


Figure 3.20: *nipi-3(fr4)* does not have a developmental phenotype in the PLM. Compared to control animals, *nipi-3(fr4)* does not display abnormal morphology of the PLM. In conjunction with other mutations, *nipi-3(fr4)* does not enhance any phenotype.

CHAPTER 3.8 – DISCUSSION

The TIA-1/TIAR family of RBPs have been examined for a variety of roles in mRNA regulation, mostly through its translational repression of transcripts (116). However, previous studies have not detailed if this family has a role in the nervous system. Here we report that one of the *C. elegans* homologs of this protein family, *tiar-2*, has roles in the developmental and adult nervous system.

We identified *tiar-2* through a screen for RBPs involved in axon regeneration and one of its downstream target, *cebp-1*, a transcription factor also important in the nervous system. *tiar-2* appears to regulate *cebp-1* as *cebp-1* mRNA was increased in the *tiar-2* mutant (Figure 3.4). However, this family of RBPs has primarily been studied for its role in translational repression. This experiment does not rule out *tiar-2*'s role as a repressor of translation as we did not examine the effect of a transcription inhibitor on *cebp-1* mRNA stability in the *tiar-2* mutant. Thus while we may have showed a novel role in mRNA stability for a member of the TIA-1/TIAR family, we haven't completely ruled out the mechanism of translation repression.

We find that *tiar-2* regulates *cebp-1* through its 3'UTR as reporters with *cebp-1*'s 3'UTR in the nervous system are increased in the *tiar-2* mutant background compared to wild type (Figure 3.5B,C, Figure 3.8). Interestingly, we find that *tiar-2* may interact with *cebp-1*'s 3'UTR through the stem-loop discussed in Chapter 2 that regulates *cebp-1*'s reporter translation (Figure 3.7B), suggesting that this stem-loop can mediate both *tiar-2*'s regulation as well as *rpm-1'*s of *cebp-1*. This result makes us speculate that the stem-loop could

mediate interaction between large protein complexes, including *rpm-1* and *tiar-2*, to tightly regulate *cebp-1* levels but further work needs to address this possibility.

Our results suggest a novel function for *tiar-2* in the nervous system during development and adult stages. *tiar-2* appears to be expressed in the nervous system and functions cell-autonomously in axon regeneration (Figure 3.10, 3.11). We observed that *tiar-2* changes it localization in response to axon injury (Figure 3.13), making it possible for *tiar-2* to respond quickly to a stimulus such as injury and controlling the localization of mRNA it is bound to, as well as the stability, decay, and translation of the same mRNAs.

tiar-2 also appears to affect development as the mutant in the motor neurons and mechanosensory neuron shows phenotypes that differ from wild type (Figure 3.14, 3.16). The number of synaptic puncta in the animals are slightly lower than control and display smaller puncta as well, indicating *tiar-2* might have a role during development.

Interestingly, we find that *rpm-1* regulates levels of *tiar-2* (Figure 3.17), suggesting that *rpm-1* could signal *tiar-2* to bind and regulate *cebp-1* and this interaction goes through *dlk-1* (Figure 3.18). However, our results from the phenotype in the mechanosensory neurons indicate the relationship is not as straight forward (Figure 3.15). It is possible that *tiar-2*'s other mRNA targets also affect its neuronal phenotype, thus complicating the quantification of the PLM phenotype. While further studies need to examine *tiar-2*'s movement, as well as mRNAs it directly associates with, these results overall suggest *tiar-2* regulates

cebp-1, during development and adult stages, which may contribute to its role in the nervous system.

We also examined the *C. elegans* homolog of the Tribbles-like kinase for a possible interaction with *cebp-1*. Our results show that *nipi-3* may not have a function in the nervous system, at least in regards to phenotypes associated with misregulation of *cebp-1*. However, the mutation we based our studies may not be a loss of function allele. Furthermore, *nipi-3* may regulate *cebp-1* in other tissues as both are expressed in the epidermis.

Trans factors with differential expression patterns could control *cebp-1* expression. It is tempting to describe a model where *rpm-1* and *tiar-2* regulate *cebp-1* in the neurons, while *nipi-3* may regulate *cebp-1* in the epidermis but more experiments will need to be done to completely understand the mechanisms controlling *cebp-1* in different tissues in a spatial and temporal manner.

CHAPTER 3.9 – MATERIALS AND METHODS

We maintained *C. elegans* strains on NGM plates at 20-25°C as previously described (108).The mutations and transgenes we used are listed in Table 3.1.

Table 3.1: List of strains with genotypes and transgenes used in this study.

Strain Name	Genotype	Transgene #
CZ20395	*tiar-2(tm2923) II*	
CZ19566	*Pmec-4::dendra-3'utr(cebp-1)*	*juEx5896*
CZ20723	*tiar-2(tm2923) II ; Pmec-4::dendra::3'utr(cebp-1)*	*juEx5896*
CZ19807	*rpm-1(ju23) V; Pmec-4::dendra::3'utr(cebp-1)*	*juEx5896*
CZ21601	*tiar-2(tm2923); juEx5896(Pmec-4::dendra::3'utr(cebp-1) juEx6543 (Pmec-4::tiar-2(cDNA)*	*juEx5896* and *juEx6543*
CZ21603	*tiar-2(tm2923); Pmec-4::dendra::3'utr(cebp-1) Pmec-4::tiar-2(cDNA)*	*juEx5896* and *juEx6544*
CZ21604	*tiar-2(tm2923); Pmec-4::dendra::3'utr(cebp-1) Pmec-4::tiar-2(cDNA)*	*juEx5896* and *juEx6545*
CZ21600	*dlk-1(tm4024); tiar-2(tm2923);Pmec-4::dendra-3'utr(cebp-1)*	*juEx5896*
CZ21599	*dlk-1(tm4024); rpm-1(ju23); Pmec-4::dendra-3'utr(cebp-1)*	*juEx5896*
CZ20724	*tiar-2(tm2923);rpm-1(ju23); Pmec-4::dendra-3'utr(cebp-1)*	*juEx5896*
CZ21601	*dlk-1(tm4024); tiar-2(tm2923);rpm-1(ju23); Pmec-4::dendra-3'utr(cebp-1)*	*juEx5896*
CZ20399	*dlk-1(tm4024); Pmec-4::dendra-3'utr(cebp-1)*	*juEx5896*
CZ19568	*Pmec-4::dendra-3'utr(unc-54)*	*juEx5898*
CZ20725	*tiar-2(tm2923) II; Pmec-4::dendra-3'utr(unc-54)*	*juEx5898*
CZ20726	*rpm-1(ju23) V; Pmec-4::dendra-3'utr(unc-54)*	*juEx5898*
CZ20727	*tiar-2(tm2923)II; rpm-1(ju23) V; Pmec-4::dendra-3'utr(unc-54)*	*juEx5898*

Table 3.1: List of strains with genotypes and transgenes used in this study, Continued.

Strain Name	Genotype	Transgene #
CZ21671	*Pmec-4::dendra::3'utr(cebp-1 del 388-418bp)*	*juEx6570*
CZ21672	*Pmec-4::dendra::3'utr(cebp-1 del 388-418bp)*	*juEx6571*
CZ21675	*tiar-2(tm2923); Pmec-4::dendra::3'utr(cebp-1 del 388-418bp)*	*juEx6570*
CZ21676	*tiar-2(tm2923); Pmec-4::dendra::3'utr(cebp-1 del 388-418bp)*	*juEx6571*
CZ21673	*rpm-1(ju23); Pmec-4::dendra::3'utr(cebp-1 del 388-418bp)*	*juEx6570*
CZ21674	*rpm-1(ju23); Pmec-4::dendra::3'utr(cebp-1 del 388-418bp)*	*juEx6571*
CZ18841	*Prgef-1::GFP::3'utr(cebp-1) line 1 II; unc-119(ed9) III*	*juSi136*
CZ18848	*Prgef-1::GFP::3'utr(cebp-1) line 1 II; rpm-1(ju44) V*	*juSi136*
CZ21605	*tiar-2(tm2923) Prgef-1::GFP::3'utr(cebp-1) line 1 II*	*juSi136*
CZ20715	*Prgef-1::GFP::3'utr(del 339-438bp) II; unc-119(ed3) III;*	*juSi177*
CZ20721	*Prgef-1::GFP::3'utr(del 339-438bp) II; unc-119(ed3) III; rpm-1(ju44)V*	*juSi177*
CZ21606	*tiar-2(tm2923) Prgef-1::GFP::3'utr(del 339-438bp) line 1 II*	*juSi177*
CZ20717	*Prgef-1::GFP::3'utr(del 439-536) line 1 II; unc-119(ed3) III*	*juSi182*
CZ20722	*Prgef-1::GFP::3'utr(del 439-536) line 1 II; unc-119(ed3) III; rpm-1(ju44)V*	*juSi182*
CZ21607	*tiar-2(tm2923) Prgef-1::GFP::3'utr(del 439-536) line 1 II; unc-119(ed3) III*	*juSi182*
	Ptiar-2::GFP	
CZ21566	*Ptiar-2::tiar-2(minigene)::GFP::3'utr(unc-54)*	*juEx6535*
CZ19839	*mec-4-GFP; tiar-2(tm2923)*	*zdIs5*

Table 3.1: List of strains with genotypes and transgenes used in this study, Continued.

Strain Name	Genotype	Transgene #
CZ10175	*mec-4-GFP*	*zdIs5*
CZ20396	*mec-4-GFP I ; tiar-2(tm2923) II ; cebp-1(tm2807) X*	*zdIs5*
CZ18809	*mec-4-GFP; cebp-1(tm2807) X*	*zdIs5*
CZ21076	*mec-4-GFP I ; tiar-2(tm2923) II ; Pmec-4-GFP::tiar-2(cDNA)(juEx6348)*	*juEx6348*
CZ21077	*mec-4-GFP I ; tiar-2(tm2923) II ; Pmec-4-GFP::tiar-2(cDNA)*	*zdIs5* and *juEx6349*
CZ21557	*Pmec-4-GFP::tiar-2(cDNA)*	*juEx6526*
CZ21558	*Pmec-4-GFP::tiar-2(cDNA)*	*juEx6527*
CZ21569	*Pmec-4-mcherry; Pmec-4-GFP::tiar-2(cDNA)*	*juIs252* and *juEx6528*
CZ333	*Punc-25-SNB::GFP IV*	*juIs1*
CZ20728	*Punc-25-SNB::GFP IV ; tiar-2(tm2923) II*	*juIs1*
CZ445	*Punc-25-SNB::GFP IV; rpm-1(ju44) V*	*juIs1*
CZ7097	*mec-4-GFP I; rpm-1(ju44) V*	*zdIs5*
CZ20397	*mec-4-GFP I ; tiar-2(tm2923) II ; rpm-1(ju44ts) V*	*zdIs5*
CZ20398	*mec-4-GFP I ; tiar-2(tm2923) II ; rpm-1(ju44ts) V ; cebp-1(tm2807) X*	*zdIs5*
CZ18845	*Punc-25-SNB::GFP IV; nipi-3(fr4)*	*juIs1*
CZ19122	*Pmec-7-GFP II; nipi-3(fr4) X*	*muIs32*
CZ19142	*Pmec-7-GFP II; rpm-1(ju44) V; nipi-3(fr4) X*	*muIs32*
CZ19143	*Pmec-7-GFP II; rpm-1(ju44) V; nipi-3(fr4) cebp-1(tm2807) X*	*muIs32*
CZ19144	*Pmec-7-GFP II; nipi-3(fr4) cebp-1(tm2807) X*	*muIs32*

Extrachromosomal transgenes were generated by injecting different concentrations of the construct with the co-injection marker Pgcy-8::tagRFP into the *C. elegans* gonad. Lines were formed and analyzed. Plasmids constructed and used are described in Table 3.2.

Table 3.2: Plasmid construct numbers and descriptions

pCZGY#	Construct
2698	PCR8::tiar-2(cDNA)
2699	*tiar-2* minigene (cDNA and genomic)
2700	*Ptiar-2-GFP*
2702	*Pmec-4::tiar-2(cDNA)*
2701	*Pmec-4-GFP-tiar-2(cDNA)*

Fluorescence Microscopy

Fluorescence reporters in live worms were scored using the Zeiss LSM710 microscope. Confocal z-stack images were taken on the LSM710. For quantification of touch neuron morphology (using *zdIs5)* we examined at least 100 one-day old young adult worms, under the Zeiss Axioplan2 Microscope. For quantification of touch neuron morphology we examined at least 100 one-day old young adult worms, under the Zeiss Axioplan2 Microscope. For quantification of GABAergic motor neurons synapses, we examined worms 4 hours after L4 stage, immobilized with 1mM Levamoisole dissolved in M9, under the Zeiss Axioplan2 Microscope.

Fluorescence intensity was measured using ImageJ (US NIH). Measurements for all images were subtracted for background intensity.

3'UTR *cebp-1* Reporter Fluorescence Quantification

All strains were cultured at 25°C. With the extrachromosomal array transgenes, we quantified GFP in the ventral nerve cord, posterior to the vulva. To enable visual comparison, we switched to use standard GFP with the single copy reporter since the expression of the reporter was low. This system involves injection of the reporter with *unc-119* into a strain with a null *unc-119* allele. This null allele may affect the expression of our reporters so we checked this possibility by comparing the full *cebp-1* 3'UTR reporter in the background of the *unc-119* null allele and wild type and found no difference in GFP expression. We examined GFP expression by measuring the fluorescence intensity in the nerve ring in young adult, as well as qRT-PCR for GFP.

mRNA analysis

We isolated total RNA from strains using a combined TRIzol/RNeasy Mini Kit (Invitrogen and Qiagen) protocol. Worms were synchronized by a bleaching protocol, grown in the same conditions and collected at the L4 stage. We used 1-2µg of RNA to reverse transcribe into cDNA using the SuperScript III® First Strand Synthesis System (Invitrogen) with an oligoDT primer. We measured levels of *cebp-1* using two primer sets YJ8984, YJ10370 and YJ10371, YJ8983. *tiar-2* levels were measured using two sets of primers YJ11404, YJ11405 and

YJ11406, YJ11407. *rps-25* was used as a control with primers YJ10368, YJ10369. Primer sequences are listed in Table 3.3.

Table 3.3: Primers and sequences used for qRT-PCR

Gene	YJ#	Sequence
cebp-1	8984	R: TCCTTCGCAAGACAAGACTCTCTTA
	10370	L: CGTCAAGATCGTGGAGCAC
cebp-1	10371	R: GCACGACAAGATGAAGAGG
	8983	L: CATCGGGCCTTTATTCCTGAG
rps-25	10368	R: CTCTACAAGGAGGTCATCACC
	10369	L: GACCTGTCCGTGATGATGAACG
tiar-2	11404	R : CGCGATAACAATACGAACAAGG
	14405	L : CCATGCTCCATTCATCTCATCTA
tiar-2	11406	R : CGGGCGATTGTACAGATGAATA
	11407	L : CTCGGATGGCTTTCCAGAAT

Laser Axotomy

PLM axons were cut on anesthetized L4 larvae worms on the near-infrared Ti-Sapphire laser (KMLabs) as previously described (Wu et al.). Worms were placed in 1% 1-phenoxy-2-propanol dissolved in M9, recovered in M9 solution after axotomy and analyzed 24 hours after axotomy for regrowth length.

Chapter 3 of this dissertation is from a paper in preparation. Sharifnia P, Andrusiak M, Wu Z, Jin Y. The role of *tiar-2* in the nervous system. The dissertation author was the primary investigator and author of the paper

REFERENCES

1. Crick F. Central dogma of molecular biology. Nature. 1970;227(5258):561-3. PubMed PMID: 4913914.

2. Garneau NL, Wilusz J, Wilusz CJ. The highways and byways of mRNA decay. Nature reviews Molecular cell biology. 2007;8(2):113-26. doi: 10.1038/nrm2104. PubMed PMID: 17245413.

3. Licatalosi DD, Darnell RB. RNA processing and its regulation: global insights into biological networks. Nature reviews Genetics. 2010;11(1):75-87. doi: 10.1038/nrg2673. PubMed PMID: 20019688; PubMed Central PMCID: PMC3229837.

4. Steward O, Levy WB. Preferential localization of polyribosomes under the base of dendritic spines in granule cells of the dentate gyrus. The Journal of neuroscience : the official journal of the Society for Neuroscience. 1982;2(3):284-91. PubMed PMID: 7062109.

5. Jansen RP. mRNA localization: message on the move. Nature reviews Molecular cell biology. 2001;2(4):247-56. doi: 10.1038/35067016. PubMed PMID: 11283722.

6. Lee MH, Schedl T. RNA-binding proteins. WormBook : the online review of C elegans biology. 2006:1-13. doi: 10.1895/wormbook.1.79.1. PubMed PMID: 18050487.

7. Colombrita C, Silani V, Ratti A. ELAV proteins along evolution: back to the nucleus? Molecular and cellular neurosciences. 2013;56:447-55. doi: 10.1016/j.mcn.2013.02.003. PubMed PMID: 23439364.

8. Dasgupta T, Ladd AN. The importance of CELF control: molecular and biological roles of the CUG-BP, Elav-like family of RNA-binding proteins. Wiley interdisciplinary reviews RNA. 2012;3(1):104-21. doi: 10.1002/wrna.107. PubMed PMID: 22180311; PubMed Central PMCID: PMC3243963.

9. Huang V, Li LC. Demystifying the nuclear function of Argonaute proteins. RNA biology. 2014;11(1):18-24. doi: 10.4161/rna.27604. PubMed PMID: 24384674; PubMed Central PMCID: PMC3929419.

10. Modic M, Ule J, Sibley CR. CLIPing the brain: studies of protein-RNA interactions important for neurodegenerative disorders. Molecular and cellular neurosciences. 2013;56:429-35. doi: 10.1016/j.mcn.2013.04.002. PubMed PMID: 23583633; PubMed Central PMCID: PMC3793874.

11. MacNicol MC, Cragle CE, MacNicol AM. Context-dependent regulation of Musashi-mediated mRNA translation and cell cycle regulation. Cell cycle. 2011;10(1):39-44. PubMed PMID: 21191181; PubMed Central PMCID: PMC3048072.

12. Quenault T, Lithgow T, Traven A. PUF proteins: repression, activation and mRNA localization. Trends in cell biology. 2011;21(2):104-12. doi: 10.1016/j.tcb.2010.09.013. PubMed PMID: 21115348.

13. Fire A, Xu S, Montgomery MK, Kostas SA, Driver SE, Mello CC. Potent and specific genetic interference by double-stranded RNA in Caenorhabditis elegans. Nature. 1998;391(6669):806-11. doi: 10.1038/35888. PubMed PMID: 9486653.

14. Lagos-Quintana M, Rauhut R, Lendeckel W, Tuschl T. Identification of novel genes coding for small expressed RNAs. Science. 2001;294(5543):853-8. doi: 10.1126/science.1064921. PubMed PMID: 11679670.

15. Lau NC, Lim LP, Weinstein EG, Bartel DP. An abundant class of tiny RNAs with probable regulatory roles in Caenorhabditis elegans. Science. 2001;294(5543):858-62. doi: 10.1126/science.1065062. PubMed PMID: 11679671.

16. Lee RC, Ambros V. An extensive class of small RNAs in Caenorhabditis elegans. Science. 2001;294(5543):862-4. doi: 10.1126/science.1065329. PubMed PMID: 11679672.

17. Chang S, Johnston RJ, Jr., Frokjaer-Jensen C, Lockery S, Hobert O. MicroRNAs act sequentially and asymmetrically to control chemosensory laterality in the nematode. Nature. 2004;430(7001):785-9. doi: 10.1038/nature02752. PubMed PMID: 15306811.

18. Johnston RJ, Hobert O. A microRNA controlling left/right neuronal asymmetry in Caenorhabditis elegans. Nature. 2003;426(6968):845-9. doi: 10.1038/nature02255. PubMed PMID: 14685240.

19. Gerstein MB, Lu ZJ, Van Nostrand EL, Cheng C, Arshinoff BI, Liu T, Yip KY, Robilotto R, Rechtsteiner A, Ikegami K, Alves P, Chateigner A, Perry M, Morris M, Auerbach RK, Feng X, Leng J, Vielle A, Niu W, Rhrissorrakrai K, Agarwal A, Alexander RP, Barber G, Brdlik CM, Brennan J, Brouillet JJ, Carr A, Cheung MS, Clawson H, Contrino S, Dannenberg LO, Dernburg AF, Desai A, Dick L, Dose AC, Du J, Egelhofer T, Ercan S, Euskirchen G, Ewing B, Feingold EA, Gassmann R, Good PJ, Green P, Gullier F, Gutwein M, Guyer MS, Habegger L, Han T, Henikoff JG, Henz SR, Hinrichs A, Holster H, Hyman T, Iniguez AL, Janette J, Jensen M, Kato M, Kent WJ, Kephart E, Khivansara V,

Khurana E, Kim JK, Kolasinska-Zwierz P, Lai EC, Latorre I, Leahey A, Lewis S, Lloyd P, Lochovsky L, Lowdon RF, Lubling Y, Lyne R, MacCoss M, Mackowiak SD, Mangone M, McKay S, Mecenas D, Merrihew G, Miller DM, 3rd, Muroyama A, Murray JI, Ooi SL, Pham H, Phippen T, Preston EA, Rajewsky N, Ratsch G, Rosenbaum H, Rozowsky J, Rutherford K, Ruzanov P, Sarov M, Sasidharan R, Sboner A, Scheid P, Segal E, Shin H, Shou C, Slack FJ, Slightam C, Smith R, Spencer WC, Stinson EO, Taing S, Takasaki T, Vafeados D, Voronina K, Wang G, Washington NL, Whittle CM, Wu B, Yan KK, Zeller G, Zha Z, Zhong M, Zhou X, mod EC, Ahringer J, Strome S, Gunsalus KC, Micklem G, Liu XS, Reinke V, Kim SK, Hillier LW, Henikoff S, Piano F, Snyder M, Stein L, Lieb JD, Waterston RH. Integrative analysis of the Caenorhabditis elegans genome by the modENCODE project. Science. 2010;330(6012):1775-87. doi: 10.1126/science.1196914. PubMed PMID: 21177976; PubMed Central PMCID: PMC3142569.

20. Ramani AK, Calarco JA, Pan Q, Mavandadi S, Wang Y, Nelson AC, Lee LJ, Morris Q, Blencowe BJ, Zhen M, Fraser AG. Genome-wide analysis of alternative splicing in Caenorhabditis elegans. Genome research. 2011;21(2):342-8. doi: 10.1101/gr.114645.110. PubMed PMID: 21177968; PubMed Central PMCID: PMC3032936.

21. Jan CH, Friedman RC, Ruby JG, Bartel DP. Formation, regulation and evolution of Caenorhabditis elegans 3'UTRs. Nature. 2011;469(7328):97-101. doi: 10.1038/nature09616. PubMed PMID: 21085120; PubMed Central PMCID: PMC3057491.

22. Mangone M, Manoharan AP, Thierry-Mieg D, Thierry-Mieg J, Han T, Mackowiak SD, Mis E, Zegar C, Gutwein MR, Khivansara V, Attie O, Chen K, Salehi-Ashtiani K, Vidal M, Harkins TT, Bouffard P, Suzuki Y, Sugano S, Kohara Y, Rajewsky N, Piano F, Gunsalus KC, Kim JK. The landscape of C. elegans 3'UTRs. Science. 2010;329(5990):432-5. doi: 10.1126/science.1191244. PubMed PMID: 20522740; PubMed Central PMCID: PMC3142571.

23. Grishok A, Pasquinelli AE, Conte D, Li N, Parrish S, Ha I, Baillie DL, Fire A, Ruvkun G, Mello CC. Genes and mechanisms related to RNA interference regulate expression of the small temporal RNAs that control C. elegans developmental timing. Cell. 2001;106(1):23-34. PubMed PMID: 11461699.

24. Zhang L, Ding L, Cheung TH, Dong MQ, Chen J, Sewell AK, Liu X, Yates JR, 3rd, Han M. Systematic identification of C. elegans miRISC proteins, miRNAs, and mRNA targets by their interactions with GW182 proteins AIN-1 and AIN-2. Molecular cell. 2007;28(4):598-613. doi: 10.1016/j.molcel.2007.09.014. PubMed PMID: 18042455; PubMed Central PMCID: PMC2186060.

25. Zisoulis DG, Lovci MT, Wilbert ML, Hutt KR, Liang TY, Pasquinelli AE, Yeo GW. Comprehensive discovery of endogenous Argonaute binding sites in Caenorhabditis elegans. Nature structural & molecular biology. 2010;17(2):173-9. doi: 10.1038/nsmb.1745. PubMed PMID: 20062054; PubMed Central PMCID: PMC2834287.

26. Bagga S, Bracht J, Hunter S, Massirer K, Holtz J, Eachus R, Pasquinelli AE. Regulation by let-7 and lin-4 miRNAs results in target mRNA degradation. Cell. 2005;122(4):553-63. doi: 10.1016/j.cell.2005.07.031. PubMed PMID: 16122423.

27. Kudlow BA, Zhang L, Han M. Systematic analysis of tissue-restricted miRISCs reveals a broad role for microRNAs in suppressing basal activity of the C. elegans pathogen response. Molecular cell. 2012;46(4):530-41. doi: 10.1016/j.molcel.2012.03.011. PubMed PMID: 22503424; PubMed Central PMCID: PMC3365535.

28. Than MT, Kudlow BA, Han M. Functional analysis of neuronal microRNAs in Caenorhabditis elegans dauer formation by combinational genetics and Neuronal miRISC immunoprecipitation. PLoS genetics. 2013;9(6):e1003592. doi: 10.1371/journal.pgen.1003592. PubMed PMID: 23818874; PubMed Central PMCID: PMC3688502.

29. Eulalio A, Huntzinger E, Izaurralde E. GW182 interaction with Argonaute is essential for miRNA-mediated translational repression and mRNA decay. Nature structural & molecular biology. 2008;15(4):346-53. doi: 10.1038/nsmb.1405. PubMed PMID: 18345015.

30. Ding L, Spencer A, Morita K, Han M. The developmental timing regulator AIN-1 interacts with miRISCs and may target the argonaute protein ALG-1 to cytoplasmic P bodies in C. elegans. Molecular cell. 2005;19(4):437-47. doi: 10.1016/j.molcel.2005.07.013. PubMed PMID: 16109369.

31. Martinez NJ, Ow MC, Reece-Hoyes JS, Barrasa MI, Ambros VR, Walhout AJ. Genome-scale spatiotemporal analysis of Caenorhabditis elegans microRNA promoter activity. Genome research. 2008;18(12):2005-15. doi: 10.1101/gr.083055.108. PubMed PMID: 18981266; PubMed Central PMCID: PMC2593583.

32. Kuroyanagi H, Watanabe Y, Suzuki Y, Hagiwara M. Position-dependent and neuron-specific splicing regulation by the CELF family RNA-binding protein UNC-75 in Caenorhabditis elegans. Nucleic acids research. 2013;41(7):4015-25. doi: 10.1093/nar/gkt097. PubMed PMID: 23416545; PubMed Central PMCID: PMC3627589.

33. Norris AD, Gao S, Norris ML, Ray D, Ramani AK, Fraser AG, Morris Q, Hughes TR, Zhen M, Calarco JA. A pair of RNA-binding proteins controls networks of splicing events contributing to specialization of neural cell types. Molecular cell. 2014;54(6):946-59. doi: 10.1016/j.molcel.2014.05.004. PubMed PMID: 24910101; PubMed Central PMCID: PMC4096705.

34. Burghes AH, Beattie CE. Spinal muscular atrophy: why do low levels of survival motor neuron protein make motor neurons sick? Nature reviews Neuroscience. 2009;10(8):597-609. doi: 10.1038/nrn2670. PubMed PMID: 19584893; PubMed Central PMCID: PMC2853768.

35. Chalfie M, Sulston J. Developmental genetics of the mechanosensory neurons of Caenorhabditis elegans. Developmental biology. 1981;82(2):358-70. PubMed PMID: 7227647.

36. Lundquist EA, Herman RK, Rogalski TM, Mullen GP, Moerman DG, Shaw JE. The mec-8 gene of C. elegans encodes a protein with two RNA recognition motifs and regulates alternative splicing of unc-52 transcripts. Development. 1996;122(5):1601-10. PubMed PMID: 8625846.

37. Spike CA, Davies AG, Shaw JE, Herman RK. MEC-8 regulates alternative splicing of unc-52 transcripts in C. elegans hypodermal cells. Development. 2002;129(21):4999-5008. PubMed PMID: 12397108.

38. Gilchrist EJ, Moerman DG. Mutations in the sup-38 gene of Caenorhabditis elegans suppress muscle-attachment defects in unc-52 mutants. Genetics. 1992;132(2):431-42. PubMed PMID: 1427037; PubMed Central PMCID: PMC1205147.

39. Lundquist EA, Herman RK. The mec-8 gene of Caenorhabditis elegans affects muscle and sensory neuron function and interacts with three other genes: unc-52, smu-1 and smu-2. Genetics. 1994;138(1):83-101. PubMed PMID: 8001796; PubMed Central PMCID: PMC1206141.

40. Calixto A, Ma C, Chalfie M. Conditional gene expression and RNAi using MEC-8-dependent splicing in C. elegans. Nature methods. 2010;7(5):407-11. doi: 10.1038/nmeth.1445. PubMed PMID: 20364149; PubMed Central PMCID: PMC2862115.

41. Goodman MB, Ernstrom GG, Chelur DS, O'Hagan R, Yao CA, Chalfie M. MEC-2 regulates C. elegans DEG/ENaC channels needed for mechanosensation. Nature. 2002;415(6875):1039-42. doi: 10.1038/4151039a. PubMed PMID: 11875573.

42. Loria PM, Duke A, Rand JB, Hobert O. Two neuronal, nuclear-localized RNA binding proteins involved in synaptic transmission. Current biology : CB. 2003;13(15):1317-23. PubMed PMID: 12906792.

43. Rand JB. Acetylcholine. WormBook : the online review of C elegans biology. 2007:1-21. doi: 10.1895/wormbook.1.131.1. PubMed PMID: 18050502.

44. Kuroyanagi H, Watanabe Y, Hagiwara M. CELF family RNA-binding protein UNC-75 regulates two sets of mutually exclusive exons of the unc-32 gene in neuron-specific manners in Caenorhabditis elegans. PLoS genetics. 2013;9(2):e1003337. doi: 10.1371/journal.pgen.1003337. PubMed PMID: 23468662; PubMed Central PMCID: PMC3585155.

45. Pujol N, Bonnerot C, Ewbank JJ, Kohara Y, Thierry-Mieg D. The Caenorhabditis elegans unc-32 gene encodes alternative forms of a vacuolar ATPase a subunit. The Journal of biological chemistry. 2001;276(15):11913-21. doi: 10.1074/jbc.M009451200. PubMed PMID: 11110798.

46. Campos AR, Grossman D, White K. Mutant alleles at the locus elav in Drosophila melanogaster lead to nervous system defects. A developmental-genetic analysis. Journal of neurogenetics. 1985;2(3):197-218. PubMed PMID: 3926976.

47. Graus F, Elkon KB, Cordon-Cardo C, Posner JB. Sensory neuronopathy and small cell lung cancer. Antineuronal antibody that also reacts with the tumor. The American journal of medicine. 1986;80(1):45-52. PubMed PMID: 2417479.

48. Szabo A, Dalmau J, Manley G, Rosenfeld M, Wong E, Henson J, Posner JB, Furneaux HM. HuD, a paraneoplastic encephalomyelitis antigen, contains RNA-binding domains and is homologous to Elav and Sex-lethal. Cell. 1991;67(2):325-33. PubMed PMID: 1655278.

49. Bassani S, Folci A, Zapata J, Passafaro M. AMPAR trafficking in synapse maturation and plasticity. Cellular and molecular life sciences : CMLS. 2013;70(23):4411-30. doi: 10.1007/s00018-013-1309-1. PubMed PMID: 23475111.

50. Mellem JE, Brockie PJ, Zheng Y, Madsen DM, Maricq AV. Decoding of polymodal sensory stimuli by postsynaptic glutamate receptors in C. elegans. Neuron. 2002;36(5):933-44. PubMed PMID: 12467596.

51. Juo P, Kaplan JM. The anaphase-promoting complex regulates the abundance of GLR-1 glutamate receptors in the ventral nerve cord of C. elegans. Current biology : CB. 2004;14(22):2057-62. doi: 10.1016/j.cub.2004.11.010. PubMed PMID: 15556870.

52. Brockie PJ, Madsen DM, Zheng Y, Mellem J, Maricq AV. Differential expression of glutamate receptor subunits in the nervous system of Caenorhabditis elegans and their regulation by the homeodomain protein UNC-42. The Journal of neuroscience : the official journal of the Society for Neuroscience. 2001;21(5):1510-22. PubMed PMID: 11222641.

53. Wang GJ, Kang L, Kim JE, Maro GS, Xu XZ, Shen K. GRLD-1 regulates cell-wide abundance of glutamate receptor through post-transcriptional regulation. Nature neuroscience. 2010;13(12):1489-95. doi: 10.1038/nn.2667. PubMed PMID: 21037582; PubMed Central PMCID: PMC3087617.

54. Konieczny P, Stepniak-Konieczna E, Sobczak K. MBNL proteins and their target RNAs, interaction and splicing regulation. Nucleic acids research. 2015;42(17):10873-87. doi: 10.1093/nar/gku767. PubMed PMID: 25183524.

55. Begemann G, Paricio N, Artero R, Kiss I, Perez-Alonso M, Mlodzik M. muscleblind, a gene required for photoreceptor differentiation in Drosophila, encodes novel nuclear Cys3His-type zinc-finger-containing proteins. Development. 1997;124(21):4321-31. PubMed PMID: 9334280.

56. Spilker KA, Wang GJ, Tugizova MS, Shen K. Caenorhabditis elegans Muscleblind homolog mbl-1 functions in neurons to regulate synapse formation. Neural development. 2012;7:7. doi: 10.1186/1749-8104-7-7. PubMed PMID: 22314215; PubMed Central PMCID: PMC3353867.

57. Noma K, Goncharov A, Jin Y. Systematic Analyses of rpm-1 Suppressors Reveal Roles for ESS-2 in mRNA Splicing in Caenorhabditis elegans. Genetics. 2014. doi: 10.1534/genetics.114.167841. PubMed PMID: 25194163.

58. Schaefer AM, Hadwiger GD, Nonet ML. rpm-1, a conserved neuronal gene that regulates targeting and synaptogenesis in C. elegans. Neuron. 2000;26(2):345-56. PubMed PMID: 10839354.

59. Zhen M, Huang X, Bamber B, Jin Y. Regulation of presynaptic terminal organization by C. elegans RPM-1, a putative guanine nucleotide exchanger with a RING-H2 finger domain. Neuron. 2000;26(2):331-43. PubMed PMID: 10839353.

60. Nakata K, Abrams B, Grill B, Goncharov A, Huang X, Chisholm AD, Jin Y. Regulation of a DLK-1 and p38 MAP kinase pathway by the ubiquitin ligase RPM-1 is required for presynaptic development. Cell. 2005;120(3):407-20. doi: 10.1016/j.cell.2004.12.017. PubMed PMID: 15707898.

61. Hegele A, Kamburov A, Grossmann A, Sourlis C, Wowro S, Weimann M, Will CL, Pena V, Luhrmann R, Stelzl U. Dynamic protein-protein interaction

wiring of the human spliceosome. Molecular cell. 2012;45(4):567-80. doi: 10.1016/j.molcel.2011.12.034. PubMed PMID: 22365833.

62. Aroian RV, Levy AD, Koga M, Ohshima Y, Kramer JM, Sternberg PW. Splicing in Caenorhabditis elegans does not require an AG at the 3' splice acceptor site. Molecular and cellular biology. 1993;13(1):626-37. PubMed PMID: 8417357; PubMed Central PMCID: PMC358941.

63. Zhen M, Jin Y. The liprin protein SYD-2 regulates the differentiation of presynaptic termini in C. elegans. Nature. 1999;401(6751):371-5. doi: 10.1038/43886. PubMed PMID: 10517634.

64. Wang Y, Gracheva EO, Richmond J, Kawano T, Couto JM, Calarco JA, Vijayaratnam V, Jin Y, Zhen M. The C2H2 zinc-finger protein SYD-9 is a putative posttranscriptional regulator for synaptic transmission. Proceedings of the National Academy of Sciences of the United States of America. 2006;103(27):10450-5. doi: 10.1073/pnas.0602073103. PubMed PMID: 16803962; PubMed Central PMCID: PMC1502478.

65. Razin SV, Borunova VV, Maksimenko OG, Kantidze OL. Cys2His2 zinc finger protein family: classification, functions, and major members. Biochemistry Biokhimiia. 2012;77(3):217-26. doi: 10.1134/S0006297912030017. PubMed PMID: 22803940.

66. Grondin B, Cote F, Bazinet M, Vincent M, Aubry M. Direct interaction of the KRAB/Cys2-His2 zinc finger protein ZNF74 with a hyperphosphorylated form of the RNA polymerase II largest subunit. The Journal of biological chemistry. 1997;272(44):27877-85. PubMed PMID: 9346935.

67. Kim SC, Kim YS, Jetten AM. Kruppel-like zinc finger protein Gli-similar 2 (Glis2) represses transcription through interaction with C-terminal binding protein 1 (CtBP1). Nucleic acids research. 2005;33(21):6805-15. doi: 10.1093/nar/gki985. PubMed PMID: 16326862; PubMed Central PMCID: PMC1301595.

68. Van Epps H, Dai Y, Qi Y, Goncharov A, Jin Y. Nuclear pre-mRNA 3'-end processing regulates synapse and axon development in C. elegans. Development. 2010;137(13):2237-50. doi: 10.1242/dev.049692. PubMed PMID: 20530551; PubMed Central PMCID: PMC2882140.

69. Bargmann CI, Hartwieg E, Horvitz HR. Odorant-selective genes and neurons mediate olfaction in C. elegans. Cell. 1993;74(3):515-27. PubMed PMID: 8348618.

70. L'Etoile ND, Coburn CM, Eastham J, Kistler A, Gallegos G, Bargmann CI. The cyclic GMP-dependent protein kinase EGL-4 regulates olfactory adaptation in C. elegans. Neuron. 2002;36(6):1079-89. PubMed PMID: 12495623.

71. Kaye JA, Rose NC, Goldsworthy B, Goga A, L'Etoile ND. A 3'UTR pumilio-binding element directs translational activation in olfactory sensory neurons. Neuron. 2009;61(1):57-70. doi: 10.1016/j.neuron.2008.11.012. PubMed PMID: 19146813.

72. Wharton RP, Struhl G. RNA regulatory elements mediate control of Drosophila body pattern by the posterior morphogen nanos. Cell. 1991;67(5):955-67. PubMed PMID: 1720354.

73. Miller MA, Olivas WM. Roles of Puf proteins in mRNA degradation and translation. Wiley interdisciplinary reviews RNA. 2011;2(4):471-92. doi: 10.1002/wrna.69. PubMed PMID: 21957038.

74. Juang BT, Gu C, Starnes L, Palladino F, Goga A, Kennedy S, L'Etoile ND. Endogenous nuclear RNAi mediates behavioral adaptation to odor. Cell. 2013;154(5):1010-22. doi: 10.1016/j.cell.2013.08.006. PubMed PMID: 23993094.

75. L'Etoile ND, Bargmann CI. Olfaction and odor discrimination are mediated by the C. elegans guanylyl cyclase ODR-1. Neuron. 2000;25(3):575-86. PubMed PMID: 10774726.

76. Yu S, Avery L, Baude E, Garbers DL. Guanylyl cyclase expression in specific sensory neurons: a new family of chemosensory receptors. Proceedings of the National Academy of Sciences of the United States of America. 1997;94(7):3384-7. PubMed PMID: 9096403; PubMed Central PMCID: PMC20379.

77. Gu W, Shirayama M, Conte D, Jr., Vasale J, Batista PJ, Claycomb JM, Moresco JJ, Youngman EM, Keys J, Stoltz MJ, Chen CC, Chaves DA, Duan S, Kasschau KD, Fahlgren N, Yates JR, 3rd, Mitani S, Carrington JC, Mello CC. Distinct argonaute-mediated 22G-RNA pathways direct genome surveillance in the C. elegans germline. Molecular cell. 2009;36(2):231-44. doi: 10.1016/j.molcel.2009.09.020. PubMed PMID: 19800275; PubMed Central PMCID: PMC2776052.

78. Studencka M, Wesolowski R, Opitz L, Salinas-Riester G, Wisniewski JR, Jedrusik-Bode M. Transcriptional repression of Hox genes by C. elegans HP1/HPL and H1/HIS-24. PLoS genetics. 2012;8(9):e1002940. doi: 10.1371/journal.pgen.1002940. PubMed PMID: 23028351; PubMed Central PMCID: PMC3441639.

79. Hadziselimovic N, Vukojevic V, Peter F, Milnik A, Fastenrath M, Fenyves BG, Hieber P, Demougin P, Vogler C, de Quervain DJ, Papassotiropoulos A, Stetak A. Forgetting is regulated via Musashi-mediated translational control of the Arp2/3 complex. Cell. 2014;156(6):1153-66. doi: 10.1016/j.cell.2014.01.054. PubMed PMID: 24630719.

80. Yoda A, Sawa H, Okano H. MSI-1, a neural RNA-binding protein, is involved in male mating behaviour in Caenorhabditis elegans. Genes to cells : devoted to molecular & cellular mechanisms. 2000;5(11):885-95. PubMed PMID: 11122376.

81. White JG, Albertson DG, Anness MA. Connectivity changes in a class of motoneurone during the development of a nematode. Nature. 1978;271(5647):764-6. PubMed PMID: 625347.

82. Hallam SJ, Jin Y. lin-14 regulates the timing of synaptic remodelling in Caenorhabditis elegans. Nature. 1998;395(6697):78-82. doi: 10.1038/25757. PubMed PMID: 9738501.

83. Thompson-Peer KL, Bai J, Hu Z, Kaplan JM. HBL-1 patterns synaptic remodeling in C. elegans. Neuron. 2012;73(3):453-65. doi: 10.1016/j.neuron.2011.11.025. PubMed PMID: 22325199; PubMed Central PMCID: PMC3278716.

84. Lee RC, Feinbaum RL, Ambros V. The C. elegans heterochronic gene lin-4 encodes small RNAs with antisense complementarity to lin-14. Cell. 1993;75(5):843-54. PubMed PMID: 8252621.

85. Wightman B, Ha I, Ruvkun G. Posttranscriptional regulation of the heterochronic gene lin-14 by lin-4 mediates temporal pattern formation in C. elegans. Cell. 1993;75(5):855-62. PubMed PMID: 8252622.

86. Prasad BC, Ye B, Zackhary R, Schrader K, Seydoux G, Reed RR. unc-3, a gene required for axonal guidance in Caenorhabditis elegans, encodes a member of the O/E family of transcription factors. Development. 1998;125(8):1561-8. PubMed PMID: 9502737.

87. Simon DJ, Madison JM, Conery AL, Thompson-Peer KL, Soskis M, Ruvkun GB, Kaplan JM, Kim JK. The microRNA miR-1 regulates a MEF-2-dependent retrograde signal at neuromuscular junctions. Cell. 2008;133(5):903-15. doi: 10.1016/j.cell.2008.04.035. PubMed PMID: 18510933; PubMed Central PMCID: PMC2553566.

88. Hu Z, Hom S, Kudze T, Tong XJ, Choi S, Aramuni G, Zhang W, Kaplan JM. Neurexin and neuroligin mediate retrograde synaptic inhibition in C.

elegans. Science. 2012;337(6097):980-4. doi: 10.1126/science.1224896. PubMed PMID: 22859820; PubMed Central PMCID: PMC3791080.
89. Andreassi C, Riccio A. To localize or not to localize: mRNA fate is in 3'UTR ends. Trends in cell biology. 2009;19(9):465-74. doi: 10.1016/j.tcb.2009.06.001. PubMed PMID: 19716303.

90. Liu CM, Wang RY, Saijilafu, Jiao ZX, Zhang BY, Zhou FQ. MicroRNA-138 and SIRT1 form a mutual negative feedback loop to regulate mammalian axon regeneration. Genes & development. 2013;27(13):1473-83. doi: 10.1101/gad.209619.112. PubMed PMID: 23796896; PubMed Central PMCID: PMC3713428.

91. Williams AH, Valdez G, Moresi V, Qi X, McAnally J, Elliott JL, Bassel-Duby R, Sanes JR, Olson EN. MicroRNA-206 delays ALS progression and promotes regeneration of neuromuscular synapses in mice. Science. 2009;326(5959):1549-54. doi: 10.1126/science.1181046. PubMed PMID: 20007902; PubMed Central PMCID: PMC2796560.

92. Zou Y, Chiu H, Zinovyeva A, Ambros V, Chuang CF, Chang C. Developmental decline in neuronal regeneration by the progressive change of two intrinsic timers. Science. 2013;340(6130):372-6. Epub 2013/04/20. doi: 340/6130/372 [pii]
10.1126/science.1231321. PubMed PMID: 23599497.

93. Chen L, Wang Z, Ghosh-Roy A, Hubert T, Yan D, O'Rourke S, Bowerman B, Wu Z, Jin Y, Chisholm AD. Axon regeneration pathways identified by systematic genetic screening in C. elegans. Neuron. 2011;71(6):1043-57. doi: 10.1016/j.neuron.2011.07.009. PubMed PMID: 21943602; PubMed Central PMCID: PMC3183436.

94. Yan D, Wu Z, Chisholm AD, Jin Y. The DLK-1 kinase promotes mRNA stability and local translation in C. elegans synapses and axon regeneration. Cell. 2009;138(5):1005-18. doi: 10.1016/j.cell.2009.06.023. PubMed PMID: 19737525; PubMed Central PMCID: PMC2772821.

95. Meer EJ, Wang DO, Kim S, Barr I, Guo F, Martin KC. Identification of a cis-acting element that localizes mRNA to synapses. Proceedings of the National Academy of Sciences of the United States of America. 2012;109(12):4639-44. doi: 10.1073/pnas.1116269109. PubMed PMID: 22383561; PubMed Central PMCID: PMC3311331.

96. Mignone F, Gissi C, Liuni S, Pesole G. Untranslated regions of mRNAs. Genome biology. 2002;3(3):REVIEWS0004. PubMed PMID: 11897027; PubMed Central PMCID: PMC139023.

97. Li B, Si J, DeWille JW. Ultraviolet radiation (UVR) activates p38 MAP kinase and induces post-transcriptional stabilization of the C/EBPdelta mRNA in G0 growth arrested mammary epithelial cells. Journal of cellular biochemistry. 2008;103(5):1657-69. doi: 10.1002/jcb.21554. PubMed PMID: 17902160.

98. Frand AR, Russel S, Ruvkun G. Functional genomic analysis of C. elegans molting. PLoS biology. 2005;3(10):e312. doi: 10.1371/journal.pbio.0030312. PubMed PMID: 16122351; PubMed Central PMCID: PMC1233573.

99. Li X, Zhao X, Fang Y, Jiang X, Duong T, Fan C, Huang CC, Kain SR. Generation of destabilized green fluorescent protein as a transcription reporter. The Journal of biological chemistry. 1998;273(52):34970-5. PubMed PMID: 9857028.

100. Frokjaer-Jensen C, Davis MW, Hopkins CE, Newman BJ, Thummel JM, Olesen SP, Grunnet M, Jorgensen EM. Single-copy insertion of transgenes in Caenorhabditis elegans. Nat Genet. 2008;40(11):1375-83. Epub 2008/10/28. doi: ng.248 [pii]10.1038/ng.248. PubMed PMID: 18953339; PubMed Central PMCID: PMC2749959.

101. Wan Y, Kertesz M, Spitale RC, Segal E, Chang HY. Understanding the transcriptome through RNA structure. Nature reviews Genetics. 2011;12(9):641-55. doi: 10.1038/nrg3049. PubMed PMID: 21850044; PubMed Central PMCID: PMC3858389.

102. Rabani M, Kertesz M, Segal E. Computational prediction of RNA structural motifs involved in posttranscriptional regulatory processes. Proceedings of the National Academy of Sciences of the United States of America. 2008;105(39):14885-90. doi: 10.1073/pnas.0803169105. PubMed PMID: 18815376; PubMed Central PMCID: PMC2567462.

103. Hofacker IL, Fontana W, Stadler PF, Bonhoeffer LS, Tacker M, Schuster P. Fast folding and comparison of RNA secondary structures. Monatsh Chem. 1994;125(2):167-88. doi: 10.1007/BF00818163.

104. McCaskill JS. The equilibrium partition function and base pair binding probabilities for RNA secondary structure. Biopolymers. 1990;29(6-7):1105-19. doi: 10.1002/bip.360290621. PubMed PMID: 1695107.

105. Zuker M, Stiegler P. Optimal computer folding of large RNA sequences using thermodynamics and auxiliary information. Nucleic acids research. 1981;9(1):133-48. PubMed PMID: 6163133; PubMed Central PMCID: PMC326673.

106. Ramji DP, Foka P. CCAAT/enhancer-binding proteins: structure, function and regulation. Biochem J. 2002;365(Pt 3):561-75. Epub 2002/05/15. doi: 10.1042/BJ20020508 BJ20020508 [pii]. PubMed PMID: 12006103; PubMed Central PMCID: PMC1222736.

107. Lopez de Heredia L, Magoulas C. Lack of the transcription factor C/EBPdelta impairs the intrinsic capacity of peripheral neurons for regeneration. Experimental neurology. 2013;239:148-57. doi: 10.1016/j.expneurol.2012.10.012. PubMed PMID: 23099414.

108. Brenner S. The genetics of Caenorhabditis elegans. Genetics. 1974;77(1):71-94. PubMed PMID: 4366476; PubMed Central PMCID: PMC1213120.

109. Kawakami A, Tian Q, Duan X, Streuli M, Schlossman SF, Anderson P. Identification and functional characterization of a TIA-1-related nucleolysin. Proceedings of the National Academy of Sciences of the United States of America. 1992;89(18):8681-5. PubMed PMID: 1326761; PubMed Central PMCID: PMC49984.

110. Tian Q, Streuli M, Saito H, Schlossman SF, Anderson P. A polyadenylate binding protein localized to the granules of cytolytic lymphocytes induces DNA fragmentation in target cells. Cell. 1991;67(3):629-39. PubMed PMID: 1934064.

111. Kim HS, Kuwano Y, Zhan M, Pullmann R, Jr., Mazan-Mamczarz K, Li H, Kedersha N, Anderson P, Wilce MC, Gorospe M, Wilce JA. Elucidation of a C-rich signature motif in target mRNAs of RNA-binding protein TIAR. Molecular and cellular biology. 2007;27(19):6806-17. doi: 10.1128/MCB.01036-07. PubMed PMID: 17682065; PubMed Central PMCID: PMC2099219.

112. Piecyk M, Wax S, Beck AR, Kedersha N, Gupta M, Maritim B, Chen S, Gueydan C, Kruys V, Streuli M, Anderson P. TIA-1 is a translational silencer that selectively regulates the expression of TNF-alpha. The EMBO journal. 2000;19(15):4154-63. doi: 10.1093/emboj/19.15.4154. PubMed PMID: 10921895; PubMed Central PMCID: PMC306595.

113. Zhu H, Hinman MN, Hasman RA, Mehta P, Lou H. Regulation of neuron-specific alternative splicing of neurofibromatosis type 1 pre-mRNA. Molecular and cellular biology. 2008;28(4):1240-51. doi: 10.1128/MCB.01509-07. PubMed PMID: 18086893; PubMed Central PMCID: PMC2258745.

114. Pujol N, Cypowyj S, Ziegler K, Millet A, Astrain A, Goncharov A, Jin Y, Chisholm AD, Ewbank JJ. Distinct innate immune responses to infection and wounding in the C. elegans epidermis. Current biology : CB. 2008;18(7):481-9. Epub 2008/04/09. doi: S0960-9822(08)00361-8 [pii]

10.1016/j.cub.2008.02.079. PubMed PMID: 18394898; PubMed Central PMCID: PMC2394561.

115. Masoner V, Das R, Pence L, Anand G, LaFerriere H, Zars T, Bouyain S, Dobens LL. The kinase domain of Drosophila Tribbles is required for turnover of fly C/EBP during cell migration. Developmental biology. 2013;375(1):33-44. doi: 10.1016/j.ydbio.2012.12.016. PubMed PMID: 23305818.

116. Mazan-Mamczarz K, Lal A, Martindale JL, Kawai T, Gorospe M. Translational repression by RNA-binding protein TIAR. Molecular and cellular biology. 2006;26(7):2716-27. doi: 10.1128/MCB.26.7.2716-2727.2006. PubMed PMID: 16537914; PubMed Central PMCID: PMC1430315.